

K-104(2)

UCRL-16898

FALL 1966

# SEMIANNUAL REPORT BIOLOGY and MEDICINE

GPO PRICE \$ \_\_\_\_\_

CFSTI PRICE(S) \$ \_\_\_\_\_

Hard copy (HC) 3.00

Microfiche (MF) 1.95

# 653 July 65

FACILITY FORM 602

N67 15941	N67 15956
(ACCESSION NUMBER)	(THRU)
161	1
(PAGES)	(CODE)
CR-81246	04
(NASA CR OR TMX OR AD NUMBER)	(CATEGORY)

DONNER LABORATORY  
and DONNER PAVILION

## LEGAL NOTICE

This report was prepared as an account of Government sponsored work. Neither the United States, nor the Commission, nor any person acting on behalf of the Commission:

A. Makes any warranty or representation, express or implied, with respect to the accuracy, completeness, or usefulness of the information contained in this report, or that the use of any information, apparatus, method, or process disclosed in this report may not infringe privately owned rights; or

B. Assumes any liabilities with respect to the use of, or for damages resulting from the use of any information, apparatus, method, or process disclosed in this report.

As used in the above, "person acting on behalf of the Commission" includes any employee or contractor of the Commission to the extent that such employee or contractor prepares, handles or distributes, or provides access to, any information pursuant to his employment or contract with the Commission.

**DONNER LABORATORY AND DONNER PAVILION**

**LAWRENCE RADIATION LABORATORY – UNIVERSITY OF CALIFORNIA  
BERKELEY, CALIFORNIA**

**SEMIANNUAL REPORT — BIOLOGY AND MEDICINE**

**FALL 1966**

**John H. Lawrence, M.D., Editor  
Tove Neville, Associate Editor**



## Foreword

The biomedical program in the Donner Laboratory of the Lawrence Radiation Laboratory traces its beginning to the first biomedical investigations carried out in 1935 with heavy particles and artificially produced radioisotopes from the then newly developed cyclotron. These studies soon indicated to us the importance of this growing field of research in biology and medicine.

One of the first persons to recognize this was Mr. William H. Donner who attended a seminar in New Haven where some of the early work was presented. He visited Berkeley and shortly afterwards, in 1940, provided funds for the construction of Donner Laboratory, which was dedicated to "the application of physics, chemistry, and the natural sciences to biology and medicine." This concept of an interdisciplinary approach, originally established as the basic pattern for research carried out in the Laboratory, continues to be our philosophy.

In the present issue, the paper by Landaw and Winchell, taken from a Ph. D. Thesis, demonstrates how metabolism of heme and heme enzymes can be traced by monitoring the breath for labeled carbon dioxide. This work has many implications and applications in basic research and in space physiology. The article by Loughman, Winchell, Raju and Lawrence illustrates our continuing interest in the development of new radiation knowledge for potential application in the therapy of human neoplasias. Negative pion beams may have important therapeutic implications, since it has been shown that there is a significant cytogenetic difference in biological effectiveness at the end of the pi meson's range in tissue, this effect resulting from the ionization caused by the secondaries produced when the pi meson is captured in tissue.

Aspects of cellular kinetics of a variety of blood cells are discussed in several papers. In Schooley's study important evidence is presented that erythropoietin produces its effects by acting upon the progeny of stem cells rather than upon stem cells themselves.



## TABLE OF CONTENTS

Endogenous Production of $^{14}\text{Co}$ : an <u>in vivo</u> Technique for the Study of Heme Catabolism STEPHEN A. LANDAW AND H. SAUL WINCHELL	1	✓
A Significant Difference in Mammalian-Cell Polyploidy Induction Between Plateau and "Star" Regions of a Negative Pion Beam WILLIAM D. LOUGHMAN, H. SAUL WINCHELL, MUDUNDI R. RAJU AND JOHN H. LAWRENCE	11	✓
Biological Specialization in Megakaryocytes and Platelets JEAN-MICHEL PAULUS	14	✓
The Effect of Erythropoietin on the Growth and Development of Spleen Colony-Forming Cells JOHN C. SCHOOLEY	22	✓
Influence of Severe Hypoxia on Human Erythropoietin WILLIAM E. SIRI	42	✓
Studies on the Thymus and the Recirculating Lymphocyte Pool JOHN C. SCHOOLEY AND MARVIN M. SHREWSBURY	53	✓
Serum-Lipoprotein Distribution and Protein Analysis by Refractometry FRANK T. LINDGREN, NORMAN K. FREEMAN, ROBERT D. WILLS, ALICIA M. EWING AND LIN C. JENSEN	64	✓
Studies on Deficient Mammalian Cells Isolated from X-Irradiation Cultures PAUL W. TODD	72	✓
Fluctuations of Energy Loss by Heavy Charged Particles in Thin Absorbers HOWARD D. MACCABEE, MUDUNDI R. RAJU AND CORNELIUS A. TOBIAS	82	✓
Secondary-Electron Distribution for Heavy Ions NOBUO ODA AND JOHN T. LYMAN	87	✓
The Interpretation of Microbial Inactivation and Recovery Phenomena ROBERT H. HAYNES	97	✓
Inactivation of Phage $\alpha$ by Single-Strand Breakage DAVID FREIFELDER	117	✓
Replication of DNA During F' Lac Transfer DAVID FREIFELDER	123	✓
Pleiotropy and Polymorphism JACK LESTER KING	128	✓
Increase in Plasma Growth Hormone Level in the Monkey Following the Administration of Sheep Hypothalamic Extracts JOSEPH F. GARCIA AND IRVING I. GESCHWIND	130	✓
Staff Publications	137	

# Endogenous Production of $^{14}\text{CO}$ : An in vivo Technique for the Study of Heme Catabolism

Stephen A. Landaw and H. Saul Winchell

N67 15942

In the late 1940's, Sjöstrand demonstrated the presence of carbon monoxide in the expired air of the normal, nonsmoking man (1). By in vivo and in vitro techniques he was able to show that this carbon monoxide was produced during the catabolism of heme, the important prosthetic group of hemoglobin, in the ratio of one mole of carbon monoxide per mole of heme catabolized. Later, Ludwig, Blakemore and Drabkin (2, 3) showed that the  $\alpha$ -methene bridge carbon of heme was the direct source of this carbon monoxide.

It has been established that the metabolic precursor of the four methene bridge carbon atoms of heme is the methylene (number 2 carbon) carbon of glycine (4), and several investigators have been able to recover carbon 14-labelled carbon monoxide in the expired air of mammals, including man, following injection of glycine-2- $^{14}\text{C}$  (2, 3, 5, 6). Since it has been adequately demonstrated that endogenously produced carbon monoxide can be detected and/or recovered with efficiencies approaching 100% in man (7), other mammals (8) and in vitro systems (9), it was expected that an isotopic technique using the above findings would allow quantitative, continuous, in vivo study of heme catabolism by measuring the rate of production of  $^{14}\text{CO}$  following the injection of glycine-2- $^{14}\text{C}$ .

## METHODS AND INSTRUMENTATION

**STANDARDIZATION OF RADIOACTIVE GASES** Standard tanks of  $^{14}\text{CO}$  and  $^{14}\text{CO}_2$  were obtained by adding the labelled gases (New England Nuclear, Boston, Mass.) to a measured volume of air containing carrier CO and  $\text{CO}_2$ , respectively, in pressurized cylinders. Exact determination of the concentration of radioactive gas in the cylinders ( $\mu\text{Ci/liter}$ ) was simultaneously performed by two separate methods.

**Method I: Ionization-Chamber Standardization** The  $^{14}\text{CO}$  and  $^{14}\text{CO}_2$  standard gases were passed through a 22-liter ionization chamber operating at atmospheric pressure, with a collecting potential of 300 V. The signal from this chamber was then passed to a vibrating reed electrometer (Model 30, Applied Physics Corporation, Pasadena, Calif.) fitted with a  $10^{12}$  ohm precision resistor (Victoreen Company, Cleveland, Ohio). The resulting voltage was recorded on a recording potentiometer.

Tolbert (10) has shown that ionization chambers of this size have counting efficiencies for the beta particle of carbon 14 approaching 100%, with a very high stability over a period of months. He calculated a theoretical calibration constant of  $1.24 \times 10^{-4} \mu\text{Ci/mV}$  for a  $10^{12}$ -ohm resistor. A signal of 1 mV from a chamber of this size means that the total

Table 1. Calibration of the  $^{14}\text{CO}$  and  $^{14}\text{CO}_2$  standard gases

Table 1a

Ionization chamber calibration of the $^{14}\text{CO}$ and $^{14}\text{CO}_2$ standard gases		
Standard gas	Maximum net millivolts recorded	Calculated activity concentration ( $\mu\text{Ci/liter}$ )
(A) $^{14}\text{CO}_2$	9.80	$5.53 \times 10^{-4}$ (A)
(B) $^{14}\text{CO}$	137.00	$7.73 \times 10^{-3}$ (B)

Table 1b

Alkali absorption and liquid scintillation calibration of the $^{14}\text{CO}_2$ standard gas (A)		
Liters of standard $^{14}\text{CO}_2$ gas (A) passed through absorber solution	Net DPM absorbed	Calculated activity concentration ( $\mu\text{Ci/liter}$ )
15.00	17,620	$5.29 \times 10^{-4}$
16.00	19,600	$5.52 \times 10^{-4}$
17.00	20,310	$5.38 \times 10^{-4}$
Total: 48.00	57,530	$5.40 \times 10^{-4}$ (A)

activity within the chamber is  $1.24 \times 10^{-4} \mu\text{Ci}$ , with a concentration of activity of  $5.64 \times 10^{-5} \mu\text{Ci/liter}$ . The results obtained for the two standard gases are shown in Table 1a.

The method just outlined is subject to various errors, some of which are not easily ascertained. These include: error in the calibration of the precision resistor ( $\pm 2\%$ ), error of reading the potentiometer signal, changes in ambient temperature and atmospheric pressure, plus any deviation from ideality in the counting efficiency. In addition, the calculation of the calibration constant requires accurate values for the average energy of the carbon-14 beta particle and the average ionization potential for air. Thus, the values calculated in Table 1a are probably accurate only to within 5 to 10%.

**Method II:  $^{14}\text{CO}_2$  Absorption in Alkali and Liquid Scintillation Counting** The  $^{14}\text{CO}_2$  standard gas was studied by absorption of known volumes of the gas in an alkali solution, and was subsequently counted by liquid scintillation techniques. The method of Jeffay and Alvarez was used without modification (11). A measured amount of the  $^{14}\text{CO}_2$  standard gas was absorbed in 13 ml of a 1:2 (v/v) solution of ethanolamine in ethylene glycol monomethyl ether. Three milliliter aliquots of this absorber solution were added to 15 ml of a scintillator solution made of a 1:2 (v/v) solution of ethylene glycol monomethyl ether in toluene, containing 5.50 g per liter of 2, 5-diphenyloxazole (PPO, Scintillation Grade, Packard Instrument Company,

Downers Grove, Illinois). The resulting homogenous, colorless solution was then counted at 0°C in a Nuclear Chicago Model 725 Liquid Scintillation Counter. Internal standardization was achieved with a standard toluene- $^{14}\text{C}$  solution ( $3.83 \times 10^5$  dpm/ml, New England Nuclear, Boston, Mass.). Typical counting efficiencies (cpm/dpm) were in the range of 0.497 to 0.510. Background ranged from 34 to 43 cpm. Table 1b shows the results obtained using this method. Standard  $^{14}\text{CO}$  gas was found to be completely insoluble in the ethanolamine solution, and could not be standardized by this technique.

The sources of error are more precisely known in this method than in the ionization-chamber method. They include: Estimated volumetric errors (0.5%), error in internal standard (2.4% for 99.5% confidence) and flowmeter error (0.5%). The values calculated in Table 1b are probably accurate to within 3%.

The value obtained for the  $^{14}\text{CO}_2$  standard using the liquid-scintillation method agrees with the value determined by the ionization chamber method within 2.4%. The close agreement of the results from these two different techniques supports the accuracy of both methods, and allows one to assume that the  $^{14}\text{CO}$  standard activity is approximately that calculated from the ionization-chamber method alone. These two standard gases were then used to test the breath collection system shown in Fig. 1.

IN VIVO  $^{14}\text{CO}$  DETECTION SYSTEM (FIG. 1) The metabolism cage is made out of clear plastic, with a volume of approximately two liters. It can hold a 350- 450-g rat with ease, and allows freedom of motion for the animal. Air enters through an intake port in the top. An additional opening (not shown) can be used to monitor the pressure within the cage with a water-filled manometer. Air exiting from the cage is dried by passage through anhydrous  $\text{CaSO}_4$  (Drierite, Indicating, W. A. Hammond Drierite Company, Xenia, Ohio). The air then passes through a 22-liter ionization-chamber system as previously described under Method I. Air is continuously evacuated from the ionization chamber by means of a constant-flow diaphragm pump (N. V. Godart, Holland). The air is then passed through a sodalime cannister containing approximately 250 g of sodium calcium hydrate, and 100 g of Ascarite (Arthur H. Thomas Co., Philadelphia, Pennsylvania), which serves to remove the  $\text{CO}_2$  and  $^{14}\text{CO}_2$  from the air stream. Exhaustion of this cannister is detected by a color change in the Ascarite.

The air then passes through a cannister containing approximately 17 g of Hopcalite (Mine Safety Appliances Company, part No. 41566). Hopcalite is a trade name for a mixture of magnesium and copper oxides with other catalytic agents, and serves to oxidize CO to  $\text{CO}_2$  at low ambient temperatures (12). Care must be taken to insure that the air passing through the Hopcalite is completely dry in order to obtain maximum oxidative efficiency. The air is then bubbled through a coarse sintered-glass gas dispersion tube into the ethanolamine-ethylene glycol monomethyl ether solution previously described. The air exiting from the absorption tube is passed through a wet-test meter (American Meter Company, Albany, New York) for accurate determination of flow rates.

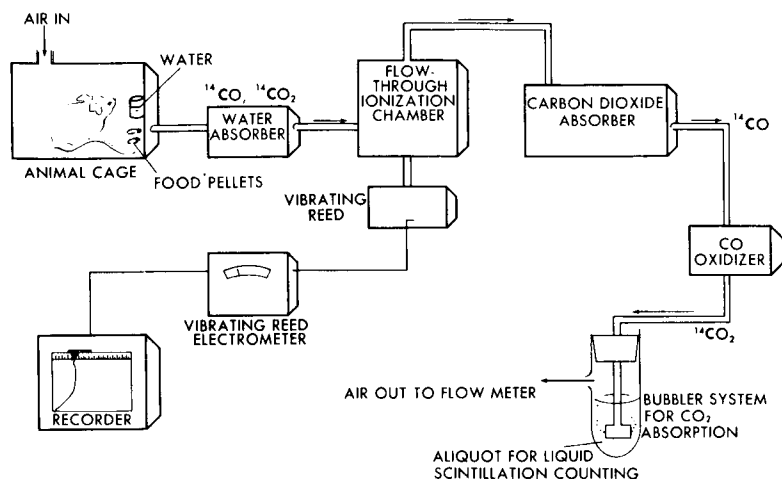
SIMULTANEOUS DETECTION OF  $^{14}\text{CO}$  AND  $^{14}\text{CO}_2$  COLLECTION SCHEME

Figure 1. In Vivo Breath Collection System  
Schematic representation of apparatus used to measure  $^{14}\text{CO}_2$  and  $^{14}\text{CO}$  production simultaneously and continuously in the intact rat. The radioactive gases present in the air stream are noted for three different portions of the apparatus. The separate components of the system are described in the text.

MUB-10650

Animals used for experimentation were male buffalo rats, weighing 340 to 370 g, corresponding to an age of approximately 3 to 4 months. Glycine-2- $^{14}\text{C}$  was purchased in multiple-dose vials containing 50  $\mu\text{Ci}/\text{ml}$  in sterile saline (New England Nuclear, Boston, Mass.). Fifty microcuries were injected intravenously into each animal under light ether anesthesia. The animal was placed inside the metabolism cage immediately thereafter and breath collection started within 1 min of the time of injection. The animals were fully reactive, and radioactivity of the expired air was noted via the ionization chamber readings 3 to 5 min after placing the animal in the metabolism cage. The flow pump was set to deliver a flow of approximately 0.35 to 0.50 liters/min. At these flow rates, the animals were apparently comfortable, and there was moderately vigorous bubbling in the gas absorber tube.

## TECHNIQUE ANALYSIS

**ABSORPTION EFFICIENCY OF ETHANOLAMINE ABSORBER FOR  $^{14}\text{CO}_2$**  For the first experiments, two or three gas absorber tubes were connected in series. However, it became apparent that no statistically significant activity over background was ever present in the second and third absorbers when there were at least 10 ml of absorber solution in the first tube. Therefore, all subsequent experiments were performed with a single collecting tube. From prior experimentation by Sjöstrand (8), and with an absorption capacity of the ethanolamine for  $\text{CO}_2$  on the order of 2.67 millimoles per milliliters, it was calculated that 10 ml of solution would be sufficient for the collection of all the endogenously produced carbon monoxide in a small rodent for a length of time exceeding one week, if all the carbon monoxide is oxidized to carbon dioxide by the Hopcalite. Ten milliliters were sufficient to trap all of the radioactivity contained in more than 50 liters of the  $^{14}\text{CO}$  and  $^{14}\text{CO}_2$  standard gases.

Evaporation of the absorber solution was noted to be approximately 0.5 ml/hr at a flow rate of 0.4 liters/min. Since ethanolamine is a known quencher of radiation in a liquid scintillation system (11) while the ethylene glycol monomethyl ether is not, unequal evaporation of the components of the absorber solution causes a change in counting efficiency. When

the change in counting efficiency caused by evaporation was measured, it amounted to less than 0.3% and was thus not corrected for.

For these experiments, enough absorber solution was used so that the final volume after evaporation was between 12 and 13 ml. Unused absorber solution was then added to make the final volume 13 ml. Thus, a 3-ml aliquot represented 3/13 of the total absorbed activity. These aliquots were counted in the system mentioned previously for at least 200 min, and, when necessary, for longer periods of time to insure a maximum of 1% counting error. After subtraction of background counts, the net cpm were converted to dpm with the use of an internal  $^{14}\text{C}$ -toluene standard, and this value was multiplied by the factor 13/3 to calculate the total absorbed activity. Production rates were stated as cpm/hr or  $\mu\text{Ci/hr}$ .

**OXIDATION EFFICIENCY OF HOPCALITE FOR  $^{14}\text{CO}$**  In order to test the oxidation efficiency of Hopcalite for  $^{14}\text{CO}$ , varying volumes and concentrations of the standard  $^{14}\text{CO}$  gas were passed through the entire system as shown in Fig. 1. Results are shown in Table 2. It is apparent that oxidation efficiency approaches 100% at the highest CO concentration (5,000 ppm). Unfortunately, in the procedure used to prepare the standards containing the smaller concentrations of CO, errors were introduced which led to lower actual concentrations of  $^{14}\text{CO}$  than that calculated on the basis of dilution alone. Thus, the oxidation efficiencies shown in Table 2 for gases containing 25 and 5 ppm are minimum values. Experiments are now in progress to determine the oxidation efficiencies at these low concentrations with more accuracy. These experiments have been repeatedly performed over a 12-month period, with reproducible results, so that the oxidation efficiency seems to be rather consistent.

**CARBON DIOXIDE ABSORPTION EFFICIENCY OF SODALIME ABSORBER** One of the important requirements of the system depicted in Fig. 1 is that the radioactive  $\text{CO}_2$  must be quantitatively trapped in the sodalime, so that remaining activity in the air stream is due to  $^{14}\text{CO}$  alone. To test this, varying volumes of standard  $^{14}\text{CO}_2$  gas were passed through the system. If the sodalime absorber were 100% efficient, no counts above background should be noted in the ethanolamine absorber. A second standard  $^{14}\text{CO}_2$  gas, with approximately  $7.5 \times 10^{-3} \mu\text{Ci/liter}$  was made in order to determine this efficiency more accurately. Twenty liters of this standard  $^{14}\text{CO}_2$  gas were passed through the system. If there were no absorption of the  $^{14}\text{CO}_2$  by the sodalime, there would have been 38,400 cpm in the ethanolamine absorber. However, only 0.50 net cpm over background were detected (with a standard deviation of 0.36 cpm). Thus, the sodalime absorber allows the passage of about 1 part in 75,000 of the  $^{14}\text{CO}_2$ . It will be seen in a later section that this very high efficiency is necessary for complete separation of  $^{14}\text{CO}$  from  $^{14}\text{CO}_2$  in the experimental animal.

**ANIMAL EXPERIMENTATION RESULTS** Figure 2 shows results obtained with the system described during the first five days after injection of 50  $\mu\text{Ci}$  of glycine-2- $^{14}\text{C}$  into a normal buffalo rat. Three important features are noted in this figure:

1. The excretion pattern of the total breath activity (ionization-chamber readings) is distinctly different from the curve describing the activity absorbed in the ethanolamine. We may then conclude that each of the patterns reflects the excretion rate of a different



Table 2. Hopcalite oxidation efficiency

Experiment number	CO concentration (PPM)	Calculated oxidation efficiency (%)**
1	5000	97.8
2	5000	97.8
3	5000	96.4
*4	25	88.7
*5	5	83.9

\*See text for discussion of errors

\*\*Oxidation efficiency expressed as % of previously calibrated  $^{14}\text{CO}$  Standard Gas (B) activity concentration of  $7.73 \times 10^{-3} \mu\text{Ci/liter}$ . (Table 1a)

radioactive substance, and that the activity present in the ethanolamine is not due to a constant or variable leak of a small fraction of the  $^{14}\text{CO}_2$  past the sodalime absorber.

2. The total breath activity ( $^{14}\text{CO}_2 + \text{"}^{14}\text{CO}\text{"}$ ) is  $10^3$  to  $10^4$  times that of the activity absorbed in the ethanolamine ( $\text{"}^{14}\text{CO}\text{"}$ ). Thus, the very high absorption efficiency of the sodalime absorber previously noted is needed to achieve the desired separation. It may then be concluded that the ionization chamber readings are essentially a measure of  $^{14}\text{CO}_2$  production rates, since the fraction of the total breath activity not caused by  $^{14}\text{CO}_2$  is so small.

3. At the times noted on Fig. 2, the sodalime absorber, water absorber, and cage were replaced, without any significant change in the curve of activity absorbed in the ethanolamine ( $\text{"}^{14}\text{CO}\text{"}$ ). One can thus conclude that no significant artifacts were due to contamination with volatile compounds from urine or feces (even though the urine and feces were found to be highly radioactive throughout this time period), or due to exhaustion of the sodalime and Drierite cannisters.

In order to estimate the magnitude of contamination of the  $\text{"}^{14}\text{CO}\text{"}$  with volatile compounds from urine, feces, and breath more precisely, three separate experiments were carried out. In the first, all the urine and feces excreted during the first 20 hr after injection of  $50 \mu\text{Ci}$  of glycine-2- $^{14}\text{C}$  into a normal buffalo rat were placed inside a metabolism cage attached to the breath collection system of Fig. 1. Air was passed over this material for 5 hr at the usual flow rate ( $0.4 \text{ l/min}$ ), and the activity absorbed in the ethanolamine was noted. In the second experiment,  $10 \mu\text{Ci}$  of glycine-2- $^{14}\text{C}$  were used in place of the urine and feces, while in the third experiment,  $2 \mu\text{Ci}$  of acetone-2- $^{14}\text{C}$  were used. The results showed that evaporation of glycine (as might occur after glycinuria in the animal following the injection of a large mass of glycine) cannot account for more than 0.2% of the  $\text{"}^{14}\text{CO}\text{"}$  production, while the contribution from other volatile compounds in the urine and feces is 0.7% or less. In the case of acetone, only 0.008% of the activity placed inside the metabolism cage was absorbed

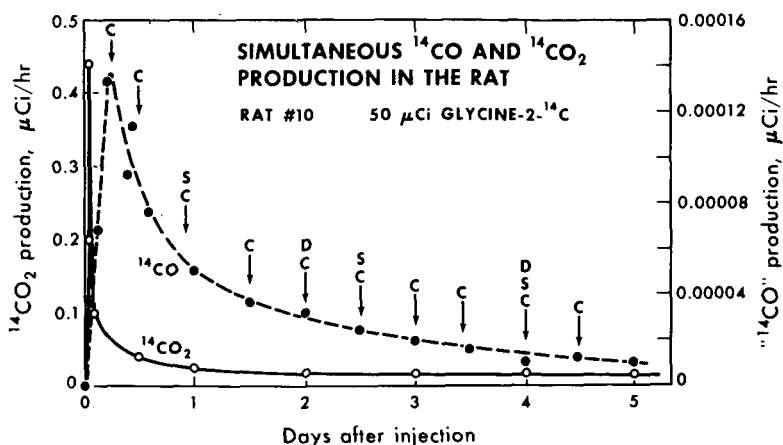
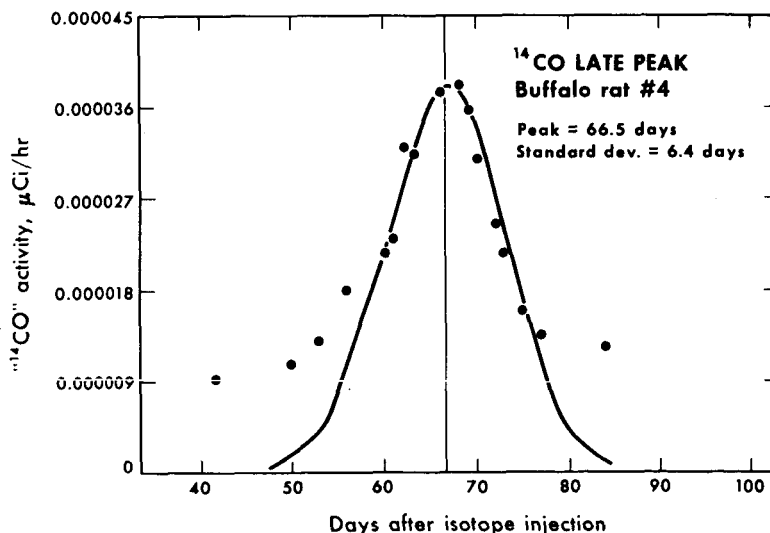


Figure 2. Simultaneous  $^{14}\text{CO}_2$  and  $^{14}\text{CO}$  Production in the Rat

The graph shows the rate of appearance of  $^{14}\text{CO}_2$  (open circles, left ordinate) and  $^{14}\text{CO}$  (closed circles, right ordinate) in the expired air of a normal rat following IV injection of 50  $\mu\text{Ci}$  of glycine-2- $^{14}\text{C}$ , as obtained by the apparatus shown in Fig. 1. The factor of 3,000 difference in the ordinate scales should be noted. Arrows refer to times when various components of the system were changed, as follows: C = Metabolism Cage, S = Soda-lime Cannister ( $\text{CO}_2$  absorber), D = Drierite cannister (water absorber). MUB-10649

Figure 3. "Late" Production of  $^{14}\text{CO}$  in a Normal Rat  
 The rate of appearance of  $^{14}\text{CO}$  in the expired air 40 to 90 days after administration of 50  $\mu\text{Ci}$  of glycine-2- $^{14}\text{C}$  to a normal rat is shown. Experimental points are indicated by closed circles. A "normal" or Gaussian curve is described by the heavy black line, having a mean of 66.5 days, and a standard deviation of 6.4 days. These values represent an *in vivo* estimation of the distribution of RBC life spans about the mean value for a normal rat. MUB-10648



in the ethanolamine. Thus it is unlikely that labelled acetone produced by a nonfasted animal can contribute significantly to the " $^{14}\text{CO}$ ".

Figure 3 shows the activity absorbed in the ethanolamine absorbers 30 to 90 days after injection of 50  $\mu\text{Ci}$  of glycine-2- $^{14}\text{C}$  intravenously into a normal buffalo rat. The points approximate a Gaussian distribution between 60 and 75 days, with a mean of 66.5 days, and a standard deviation of approximately 6.4 days. Since investigators in this laboratory, using independent techniques, have found a rat red-blood-cell life span on the order of 57 to 68 days (13, 14), it appears from this graph that the activity appearing in the ethanolamine is mirroring the senescence and destruction of the cohort of red blood cells produced at the time of injection of the labelled glycine.

## DISCUSSION

The functioning of this system depends upon four important assumptions. They are:

1. Respiratory  $^{14}\text{CO}_2$  can be completely absorbed in the sodalime cannister.
2. Breath activity remaining after  $^{14}\text{CO}_2$  absorption is due solely to endogenously produced  $^{14}\text{CO}$ .
3.  $^{14}\text{CO}$  can be quantitatively oxidized to  $^{14}\text{CO}_2$  by Hopcalite at ambient temperatures at the flow rates employed, and at the low concentrations present to mammalian breath.
4. The  $^{14}\text{CO}_2$  produced from the oxidation of  $^{14}\text{CO}$  can be quantitatively trapped in the ethanolamine solution, and counted with known efficiencies.

These points will be discussed individually:

1. Figure 2 shows that the activity in the respiratory  $^{14}\text{CO}_2$  is 1,000 to 10,000 times as great as that simultaneously present in the component absorbed by the ethanolamine (" $^{14}\text{CO}$ "). Eleven days after injection of the labelled glycine, the ratio of  $^{14}\text{CO}_2$  activity to " $^{14}\text{CO}$ " activity is approximately 800. The experiments with standard  $^{14}\text{CO}_2$  gases showed that the sodalime absorber allows passage of about 1 part in 75,000 of the  $^{14}\text{CO}_2$ . Thus, the efficiency of the sodalime cannisters is entirely sufficient for the desired separation.

2. Although it cannot be stated with absolute certainty from these experiments that the activity trapped in the ethanolamine is due solely to  $^{14}\text{CO}$  produced by the catabolism of heme in the experimental animals, several points of evidence exist which strongly suggest that it is indeed due almost entirely to this source. These points are:

(a) Only three types of carbon-containing compounds are present in the expired air to any significant degree:  $\text{CO}_2$ ,  $\text{CO}$ , and ketone bodies, all of which will be labelled with carbon 14 after injection of glycine-2- $^{14}\text{C}$ . Experiments showed that only 1 part in 75,000 of the  $^{14}\text{CO}_2$  escapes the sodalime absorber. Two of the ketone bodies, acetoacetic acid and beta hydroxy butyric acid, being acids, are likely to be absorbed by the sodalime with comparable efficiencies. It was also shown that only 1 part in 12,000 of acetone-2- $^{14}\text{C}$  added to the system is absorbed into the ethanolamine. Since the animals are not fasted during these experiments, it is unlikely that labelled ketone bodies exhaled by the animal can cause significant contamination of the " $^{14}\text{CO}$ ". Although recent studies of the atmosphere of closed systems have shown the presence of more than 50 carbon-containing compounds (15), separate experiments showed that contamination of the " $^{14}\text{CO}$ " by volatile  $^{14}\text{C}$ -containing compounds in the urine

and feces cannot exceed 0.7%, while the contribution from glycinuria with evaporation of glycine-2- $^{14}\text{C}$  cannot exceed 0.2%.

(b) Figure 3 shows that the production rate of the " $^{14}\text{CO}$ " in one normal rat follows a Gaussian distribution about a mean value of 66.5 days. This result is to be expected from destruction of labelled heme in the circulating red blood cells of the rat, with subsequent production of  $^{14}\text{CO}$ . Other experiments have shown that this peak production correlates well with the decrease in blood activity (16). This mean value also agrees well with estimates for the red-blood-cell life span of the rat, using other techniques.

(c) The amount of activity absorbed in ethanolamine during the first five days after injection of labelled glycine is equivalent to 15-30% of the activity incorporated into the  $\alpha$ -methene bridge carbon of heme of circulating red blood cells in the rat (17). This "early appearing" material thus correlates well (in time of appearance as well as quantitatively) with the production of "early labelled" bilirubin (18, 19) and stercobilin (20) in the rat, dog, and man. Since bilirubin, stercobilin, and CO are all breakdown products of heme, the correspondence is significant, although not conclusive.

(d) The magnitude of this "early appearing" material (" $^{14}\text{CO}$ ") was found to be increased when erythropoiesis was stimulated in the rat after phenylhydrazine treatment or phlebotomy, and was decreased when erythropoiesis was suppressed by hypertransfusion (16). These results agree well with the production rates of "early labelled" bilirubin in dogs with normal, increased, and decreased erythropoiesis (19).

3. The oxidation efficiency of Hopcalite was shown to be greater than 80% over the range of concentrations tested (Table 2). This range includes the CO concentrations normally found in small animals by Sjöstrand (8).

4. Numerous trials with 2 or more ethanolamine absorbers in series showed that all the activity was removed by the first absorber tube. The absorption capacity of the solution used is more than sufficient for 6-hr collections, the longest intervals routinely used.

The dose of 50  $\mu\text{Ci}$  was chosen so that the counting rate during the destruction of the labelled red blood cells would be at least twice the background counting rate. At the specific activities available (22 mCi/mM) 50  $\mu\text{Ci}$  means a dose of approximately 0.17 mg of glycine. Since it has been estimated that the turnover of glycine is approximately 27 mg per hour in a 350-g rat (21), this dose is probably still in the "tracer" range.

## SUMMARY

A method is presented for the separation, detection, and quantitation of endogenously produced carbon-14-labelled carbon monoxide in the rat, following injection of glycine-2- $^{14}\text{C}$ . In this method, respiratory  $^{14}\text{CO}_2$ , the only significant breath contaminant, is removed with a sodalime absorber. The remaining breath activity, due primarily, if not entirely, to  $^{14}\text{CO}$ , is oxidized to  $^{14}\text{CO}_2$  by Hopcalite, absorbed in an ethanolamine-containing solution, and counted by liquid scintillation. Standard  $^{14}\text{CO}$  and  $^{14}\text{CO}_2$  gases, as well as animal experimentation, confirm this method's ability to measure  $^{14}\text{CO}$  and  $^{14}\text{CO}_2$  production rates simultaneously, following a single injection of labelled glycine. Examples are given to show that this continuous, in vivo, and easily performed method can give important information

concerning heme catabolism. The technique should provide a unique source of information in the study of disease processes characterized by abnormal heme catabolism in man and other animals.

## ACKNOWLEDGMENTS

The authors wish to acknowledge the help of Dr. John H. Lawrence, without whose support and counsel these investigations could not have been performed.

## REFERENCES

1. Sjöstrand, T.; Scand. J. Lab. Clin. Invest. 1:201, 1949.
2. Ludwig, G. D.; Blakemore, W. S., and Drabkin, D. L.; Biochem. J. 66:38P, 1957.
3. Ludwig, G. D.; Blakemore, W. S., and Drabkin, D. L.; J. Clin. Invest. 36:912, 1957.
4. Wittenberg, J., and Shemin, D.; J. Biol. Chem. 185:103, 1950.
5. White, P.; Coburn, R. F.; Williams, W. J.; Goldwein, M. I.; Rother, M. L., and Shafer, B. C.; Blood 24:845, 1964.
6. Landaw, S. A., and Winchell, H. S.; Clin. Res. 14:141, 1966.
7. Coburn, R. F.; Williams, W. J., and Forster, R. E.; J. Clin. Invest. 43:1098, 1964.
8. Sjöstrand, T.; Acta Physiol. Scand. 26:338, 1952.
9. Sjöstrand, T.; Acta Physiol. Scand. 26:328, 1952.
10. Tolbert, B. M.; Lawrence Radiation Laboratory Report UCRL-3499, 1956.
11. Jeffay, H., and Alvarez, J.; Anal. Chem. 33:612, 1961.
12. Technical products release No. 1511. Mine Safety Appliances Company, Pittsburgh, Pa.
13. Berlin, N. I.; Van Dyke, D. C., and Lotz, C.; Proc. Soc. Exp. Biol. Med. 82:287, 1953.
14. Berlin, N. I.; Meyer, L. M., and Lazarus, M.; Am. J. Physiol. 165:565, 1951.
15. Toliver, W. H., and Morris, M. L.; Aerospace Med. 37:233, 1966.
16. Landaw, S. A., and Winchell, H. S.; Clin. Res. 14:319, 1966.
17. Landaw, S. A.; unpublished results.
18. Robinson, S. H.; Tsong, M.; Brown, B. W., and Schmid, R.; J. Lab. Clin. Med. 66:1015, 1965.
19. Israels, L. G.; Skanderbeg, J.; Guyda, H.; Zingg, W., and Zipursky, A.; Brit. J. Haemat. 9:50, 1963.
20. Gray, C. H.; Neuberger, A., and Sneath, P. H. A.; Biochem. J. 47:87, 1950.
21. Neuberger, A.; Biochem. J. 78:1, 1961.

# A Significant Difference in Mammalian-Cell Polyploidy Induction Between Plateau and "Star" Regions of a Negative Pion Beam

William D. Loughman, H. Saul Winchell,  
Mudundi R. Raju and John H. Lawrence

N67 15943

A preliminary report (1) has shown that plateau and "star" (or peak) regions of negative pion beams differ in their capacity to induce polyploidy and other effects on mammalian cells in vivo. Although the experiment described, as well as a subsequent experiment (2), demonstrated this difference, the results were not considered significant. This report describes further work in which a statistically significant difference between the effects of the two beam regions is demonstrated.

As in the two preceding experiments, LAF<sub>1</sub> mice with the A-2 lymphoma as an ascites tumor were irradiated in a negative pion beam from the 184-inch cyclotron. Dosimetric techniques and beam characteristics have been described previously (3, 4). Mice in the plateau portion of the beam (about 60% pions) received an average dose of about 230 rads. Mice in the peak region of the beam (30-40% pions) received about 350 rads. On the third and fourth days following irradiation, ascites cells were removed from the mice and prepared for chromosome examination. 4,000 metaphase cells from each mouse were scored as essentially diploid or as polyploid. The results are summarized in Fig. 1. In each case the incidence of polyploidy among irradiated cells was increased over control values. Significantly higher values were seen in cells irradiated in the beam's peak region than in cells irradiated in the plateau region.

The total peak/plateau ratio is 3.52. The ratio on a per rad basis is about 2.1. If the RBE (relative biological effectiveness) of muons and electrons (present as beam contaminants) is considered to be 1, their contribution to the effects can be estimated and subtracted from the total. This leads to an estimate of negative pion effects only, giving a peak/plateau ratio per rad of pions of about 4.7. These latter figures must be regarded as approximate, since negative pion dosimetry in the peak region is inherently difficult and subject to large errors.

Ninety five percent confidence intervals are given in Fig. 1 for the combined data of each experimental class. The intervals do not overlap, and the data are therefore significant. The probability that the observed difference differs from an estimated homogeneous population standard deviation, due to chance alone, is less than  $10^{-5}$ .

Additional mammalian cell experiments with negative pion beams have been performed in this laboratory (5, 6). Survival of mice given irradiated lymphoma cells was increased over control values, with peak-irradiated cells giving longer survival times than plateau-irradiated



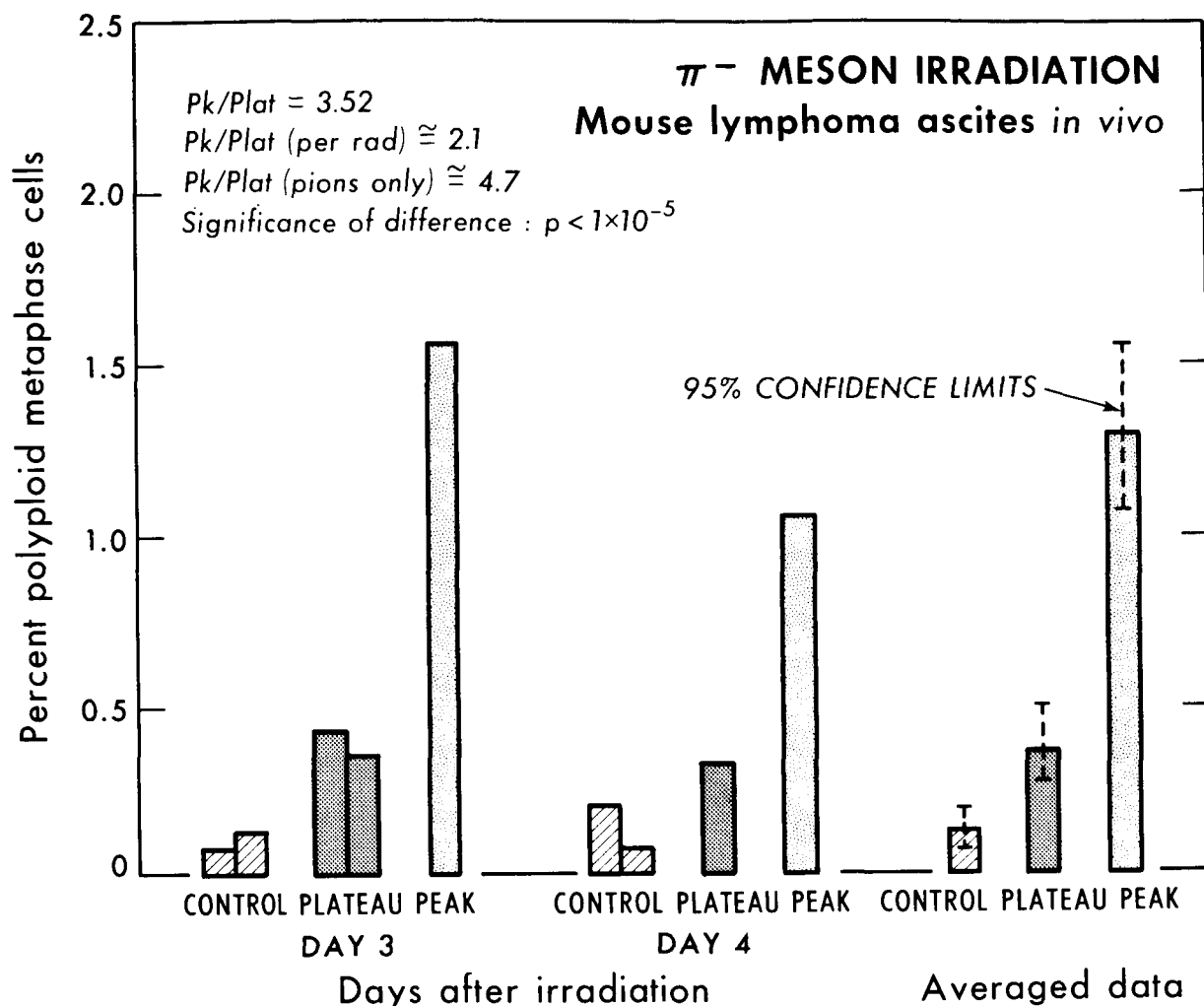


Figure 1. (MUB-12201)

cells. The results of both types of experiments confirm our previous results (1) and also the results of Richman *et al.* on plant material (7). All experiments indicate that negative pions in the peak ("star") region of the beam have a higher RBE than those in the plateau region.

## REFERENCES

1. Loughman, W. D.; Winchell, H. S.; Aceto, H., Jr.; Richman, C.; Raju, M. R., and Lawrence, J. H.; Semiannual Report, Donner Laboratory, Lawrence Radiation Laboratory, UCRL-16246: 100-102, 1965.
2. Loughman, W. D.; unpublished data.
3. Richman, C.; Aceto, H., Jr.; Raju, M. R.; Schwartz, B., and Weissbluth, M.; Semiannual Report, Donner Laboratory, Lawrence Radiation Laboratory, UCRL-11387: 114-126, 1964.
4. Raju, M. R.; Aceto, H., Jr., and Richman, C.; Nucl. Instr. Methods 37: 152-158, 1965.
5. Feola, J. M.; Richman, C.; Raju, M. R., and Lawrence, J. H.; Semiannual Report, Donner Laboratory, Lawrence Radiation Laboratory, UCRL-16613: 23-26, 1965.

6. Feola, J. M. ; personal communication.
7. Richman, S. P. ; Richman, C. ; Raju, M. R. , and Schwartz, B. ; Semiannual Report, Donner Laboratory, Lawrence Radiation Laboratory, UCRL-16613:15-22, 1965.

# Biological Specialization in Megakaryocytes and Platelets

N67 15944

Jean-Michel Paulus

In speaking of megakaryocytes Rhodin has stated: "Rarely does one find any single cell type that displays the great assortment of cell organelles and cell inclusions which the study of many cell types can bring together. In this regard the megakaryocyte is a unique case". (1). This statement can actually be applied to the thrombocytic series as a whole and is true not only at the submicroscopic level, but also at all levels of cellular organization. The properties of megakaryocytes and platelets might be considered to result mainly from a summation of the physiological activities of five cellular types, i. e. 1) a polyploid cell; 2) a glandular cell; 3) an enucleate element; 4) an endocytic cell; 5) a muscular cell.

## THE MEGAKARYOCYTE AS A POLYPOID CELL

The differentiation of a blast cell into a mature cell and the act of mitosis are closely related phenomena. Whereas it is in the few hours following a division that the intestinal crypt cell makes the crucial decision to reproduce itself exactly or to specialize (2), the megakaryoblast seems to make this choice in the course of mitosis itself (3). Kinoshita and Ohno found that in the case of the megakaryoblast a chromosome duplication without definitive cytodiastasis indicates that the cell is engaged in differentiation (3). This process is characterized by an inhibition of purely reproductive mitosis, and by a succession of four differentiation mitoses, which geometrically increase the ploidy up to the 32 N (4) or 64 N Value (5).

Certain other phenomena may also qualitatively demonstrate that a given cell has started to differentiate into a thrombopoietic one. Some early changes have been noted, but their relationship to the degree of polyploidy has not always been established, i. e. morphologic characteristics in phase contrast (6, 3) and electron microscopy (7), the presence of acetylcholinesterase (for some animal species) (8) or the presence of some platelet antigens (9). Conversely, the first appearance of the azurophilic granules occurs later. They become conspicuous only at the 8 N stage (3). None of these criteria, however, has the quantitative accuracy of the determination of the ploidy. Moreover, the latter has a special significance. It is known that polyploidy, common in plants, is normally associated both with differentiation and inhibition of reproductive mitosis (10, 11).

Polyploidy in megakaryocytes may have many additional consequences. Some of these consequences are morphological. For example, the large size of both nucleus and cell as well as the abnormal shape of the nucleus and perhaps the low normal number of megakaryocytes can be explained by their polyploidy. More important, however, may be the metabolic and genetic perturbations associated with a high chromosome number. As pointed out by

Frankhauser (12), the associated increase in cell size could influence the relationships between cytoplasm and nucleus and between cytoplasm and environment. Similarly, the increased amount of carotenoid pigment per gene, in the tetraploid yellow corn (13) as well as the abnormalities of development in triploid humans (14), show the possibility of a cumulative effect of excess genes. Finally polyploid cells are more susceptible to viral accumulation (15), a feature also demonstrated by megakaryocytes (16-18).

## THE MEGAKARYOCYTE AS A GLANDULAR CELL

The well-described process of partition and fragmentation of the megakaryocytic cytoplasm (19) has no other equivalent in the mammalian organism. This true apocrine secretion, as it is called by Porter and Bonneville (20), results in the birth of the fully autonomous, metabolically active platelets. It can be clearly distinguished from the five types of glandular secretion described by Kurosumi (21), in which are extruded only secretory products lacking cellular organization.

In the process of thrombopoiesis, the endoplasmic reticulum plays a special role. Whereas a part of the membranous cytoplasmic system is unstained by phosphotungstic acid and seems not to be involved in the demarcation of platelet territories, other components of this system which originate in the Golgi apparatus and are stained by phosphotungstic acid intervene in thrombopoiesis (22). They also may be considered endoplasmic reticulum. The coalescence of some of the phosphotungstic acid-stained vesicles gives rise to a network of "demarcation membranes" and prepares the liberation of the enclosed platelet territories (19, 22). This specialized part of the endoplasmic reticulum thus permits the segregation and the elimination of the secretory product. In the pancreas merocrine secretion, although the nature and destiny of the secretory product are quite different, the endoplasmic reticulum has a similar function (23).

Platelet extrusion, although still poorly understood, seems to be stimulated by platelet depletion in the blood (24) which suggests it to be a much more active process than was previously believed. In this regard, the following may be relevant: An ATPase enzyme has been found in the platelet membrane (25). Such an activity is present in many other cell membranes, resembling the nucleoside triphosphatase activity of actomyosin (26). It is also present in cell organelles associated with contraction, for instance the mitotic spindle (27). Furthermore, a contractile, actomyosin-like protein has been isolated from platelets (28). The platelet shedding could thus be a contractile phenomenon resulting in the separation of the partitioned platelet territories and in some way being stimulated by bleeding. Some *in vivo* observations of thrombopoiesis are in agreement with this hypothesis (29).

The final destiny of the megakaryocytes has been questioned. Some authors have observed that the nucleus of the megakaryocyte becomes pycnotic as thrombopoiesis occurs (3, 30), a fact that would suggest the death of these cells at this moment. Others consider the liberation of platelets as a cyclic phenomenon not necessarily fatal to the megakaryocytes (22). The possibility of obtaining 100% viable megakaryocytes from the rat bone marrow, after digestion by collagenase should be taken into account in this problem (31).

## THE PLATELET AS AN ENUCLEATE ELEMENT

The main cytological feature of the product secreted by the megakaryocyte - the blood platelet - is the absence of a nucleus. Among all mammalian "cell-like" elements this characteristic property is shared only by the reticulocyte and the erythrocyte. These cells however are highly specialized for a single protein, hemoglobin, and quickly lose their mitochondria (32). Thus the behavior of the platelet might best be compared (33) to that of other enucleate cells, such as surgically sectioned amoebae (32).

How much the absence of a nucleus may explain platelet metabolism as compared with the metabolism of a nucleate cell is difficult to estimate. One might hope to determine this relationship by studying platelets during their aging process, as has been done for the enucleated amoebae. However, normal circulating platelets are not suitable for such studies, since they are a heterogeneous mixture of elements of different ages. *In vitro* studies of the senescence effects are possible, but one must be careful in interpreting them, since isotopic (34) and electron-microscopic (35) experiments have proved that the use of chelating agents (essential to their preservation) is harmful to platelets.

Bearing in mind these reservations, one may compare the main features of platelet metabolism with those of the enucleated amoebae.

1. Unlike enucleated amoebae, the circulating thrombocyte degrades glucose mainly by glycolysis with 45% of the metabolized glucose being transformed into lactic acid (36). However, this metabolic sequence is highly susceptible to aging in an ACD medium (37). Furthermore, the glycolytic enzymes and ATP are protected by the addition of glutathione, nicotinamide and inosine (38). These facts strongly suggest an analogy between the glycolytic lesion occurring in senescent, enucleated amoebae and in senescent, *in vitro* preserved platelets.
2. Over a 21-day period the respiratory rate of platelets is unaffected by senescence (37). Enucleated amoebae display similar behavior.
3. As for enucleated amoebae, the incorporation of inorganic phosphate in energy-rich compounds is markedly time-dependent, and platelet  $P^{32}$  label falls to zero after a few days (39). Again, because of the possible influence of the EDTA plasma medium, the absence of a nuclear structure in the platelet cannot with certainty be considered responsible for the observed dysfunction.
4. Circulating platelets contain a low level of RNA (40) though young platelets are more basophilic than older ones, and reportedly contain ribosomes (41). These facts suggest an age-dependent decrease in RNA as in enucleated fragments. However, because of the progressive decrease in basophilia and in RNA synthesis during the megakaryocytic maturation (42), the nuclear deprivation cannot be considered as the sole factor for progressive depletion of RNA in platelets.

It may be concluded from this comparison that the biological importance of the absence of a nucleus in platelets cannot be clearly established.

## THE PLATELET AND MEGAKARYOCYTE AS ENDOCYTIC ELEMENTS

The well-known ability of platelets to clear the blood of foreign particles or of microorganisms results from two apparently distinct properties: 1) their adhesiveness and 2) their endocytic property. In adhesion, where a surface phenomenon plays the major role, loading of the platelets with particles or microorganisms leads to their agglutination. The platelets disappear from the circulating blood and are sequestered in the reticuloendothelial system from which they may subsequently be released (43). Another aspect of the adhesiveness of platelets is their ability to concentrate many of the coagulation factors in a so-called "atmosphère péri-plaquettaire (44)." Because of this property, they have been compared to sponges (45). In addition, the possibility of true endocytosis is clearly established by electron-microscopic pictures of "phagocytosis" (46) as well as by phase contrast studies of pinocytosis (47). Endocytic intervention may induce in vitro the liberation of ADP and the loss of the platelets granules (48) and in vivo a more prolonged thrombocytopenia (49). Recently, the immunological and collagen-induced destruction of platelets has been ascribed to the same process (48).

That these two different activities are in fact different steps of the same chain of reactions was already shown in 1927 by Roskam (44) who believed platelet adhesion was similar to the first phase of phagocytosis and that it depended on the modification of the microorganism and platelet surfaces by the medium. The suggestion of a selective inhibition of these different steps (adherence to the particle, phagocytosis, release of ADP with platelet agglutination) strengthens this interpretation (48).

Since the lysosomes are the cytoplasmic organelles involved in the process of digestion of exogenous material (50), their intervention in many of the aspects of platelet physiology and pathology has been suggested (51). The well-known tendency of the platelets to undergo a quick autolysis when preserved outside of the body further supports this hypothesis (52).

Two of the megakaryocyte and platelet organelles have some characteristics of lysosomes. First, granules contain acid phosphatase,  $\beta$  glucuronidase and cathepsin (53). They play a major role in platelet autolysis in EDTA (52) and are secreted into the surrounding medium during the course of viscous metamorphosis (54). However, their triple-layered structures (55) do not correspond with classical lysosomal morphology. Second, some of the vacuoles contain acid phosphatase activity (25). This common feature between granules and vacuoles is not surprising in the light of the ideas of Novikoff et al. (26, 56) who point out their common origin in the Golgi complex, as well as the formation of the lysosome membranes from the membranes of the Golgi apparatus. Moreover, in quite another respect these structures appear to have similar properties: in mice infected with the Gross leukemia virus, the virus particles bud only in the granules and vacuoles of megakaryocytes (16, 17).

## THE PLATELET AS A CONTRACTILE ELEMENT

The metabolic behavior of the circulating platelet is very similar to that of muscle. The high activities of the glycolytic enzymes, contrasting with the low activity of the hexosephosphate shunt, of the Krebs cycle and of the respiratory chain suggested this comparison to Waller et al. (36). It was further supported by Bettex-Galland and Lüscher's discovery



of a contractile protein in platelets, similar to actomyosin and endowed with an ATPase activity (28). Moreover, it can be shown that during the viscous metamorphosis (57, 58) or the qualitatively equivalent phenomenon of clot retraction (59), and during muscular contraction (60), the same sequence of reactions occurs. A modification of the permeability barrier allows the subsequent mobilization of Ca ions which initiates the contraction. A protein endowed with ATPase activity then contracts. During this process the consumption of ATP is great, and the intracellular level of ADP and phosphate has a tendency to rise. In anaerobic conditions such as those in which agglutinated platelets are found, this phenomenon stimulates glycolysis.

In spite of the similarities between the two contractile systems, two important differences in behavior exist: 1) In hemostasis, platelets first adhere to the collagen fibers of the conjunctive tissue of the ruptured vessel (61,62). This adhesion, together with the subsequently intervening thrombin, destroys the platelet organelles and releases ADP into the medium (63). Whereas in muscle an increase in ADP is prevented by the presence of the "high-energy phosphate buffering system" that regenerates the ATP, in platelets, this system is not so efficient. Perhaps the lack of phosphocreatin and the small concentration of creatin kinase (64) are among the reasons why a fast accumulation of ADP can occur. This nucleotide acts as the major thrombocyte agglutinating factor (63). Thus a triple biochemical specialization in platelets - i.e. their reaction with collagen and thrombin, their lack of an efficient ADP phosphorylating system and their aggregation ability under the influence of ADP - allows the assembly of a complex contractile system. In contrast, for muscle the contractile system is already completely preassembled. 2) Contrary to the muscular fiber, the contracted platelet aggregate is unable to relax. It is immobilized by the fibrin network and the platelets become altered. By coagulating fibrinogen, thrombin contributes to this immobilization. (In certain conditions, the clot will eventually be dissolved). Thrombin, like trypsin (57), is a powerful proteolytic enzyme that alters the permeability of platelets and releases not only ADP but also ATP (58, 63). In the case of muscle at least, ATP is an essential requirement for relaxation (65), and trypsin is known to inhibit the relaxation action of muscle vesicles (66). These facts suggest that the inability of the platelet aggregate to relax may depend upon the permeability, and coagulative, action of thrombin.

## CONCLUSION

Overall consideration of the five comparisons mentioned suggest the desirability of new and original studies of megakaryocytes and platelets. Unlike platelets, megakaryocytes have not been submitted to biochemical and cytological analysis. Progress in the direction of their isolation could contribute to the elucidation of some of the problems raised by this giant, multifunctional cell. Further information on this subject may be found in Marcus and Zucker's comprehensive review of platelet physiology, published posterior to the preparation of this manuscript (67).

## ACKNOWLEDGMENTS

I am grateful to Dr. Howard C. Mel and to Miss Nancyann Orth for their advice during the preparation of this manuscript.

## REFERENCES AND NOTES

1. Rhodin, J. A. G.: *An Atlas of Ultrastructure*, Philadelphia, Saunders, 1963.
2. Quastler, H., and Sherman, F. G.; *Exptl. Cell. Res.* 17:420, 1959.
3. Kinosita, R., and Ohno, S.; in *Blood Platelets*, Henry Ford Hosp. Symp., Boston, Little, Brown and Co., 1961, p. 611.
4. de Leval, M.; *Compt. Rend. Soc. Biol.* 158:2198, 1964.
5. Garcia, A. M.; *J. Cell. Biol.* 20:342, 1964.
6. Pisciotta, A. V.; Stefanini, M., and Dameshek, W.; *Blood* 8:703, 1953.
7. Sorenson, G. D.; *Am. J. Anat.* 106:27, 1960.
8. Zajicek, J.; *Acta Physiol. Scand.* 40:suppl. 138, 1957.
9. Humphrey, J. H.; *Nature* 176:38, 1955.
10. Torrey, J. G.; *Science* 128:1148, 1958.
11. Patau, K.; Das, N. K., and Skoog, F.; *Physiol. Plantarum* 10:949, 1957.
12. Fankhauser, G.; *Intern. Rev. Cytol.* 1:185, 1952.
13. Randolph, L. F., and Hand, D. B.; *J. Agr. Res.* 60:51, 1940.
14. Böök, J. A., and Santesson, B.; *Lancet* 1:858, 1960.
15. Puck, T. T., and Marcus, P. I.; *J. Exptl. Med.* 103:653, 1956.
16. de Harven, E., and Friend, C.; *J. Biophys. Biochem. Cytol.* 7:747, 1960.
17. Dalton, A. J.; Law, L. W.; Moloney, J. B., and Manaker, R. A.; *J. Nat. Cancer Inst.* 27:747, 1961.
18. Jerushalmy, Z.; Kaminski, E.; Kohn, A., and De Vries, A.; *Proc. Soc. Exptl. Biol. Med.* 114:687, 1963.
19. Yamada, E.; *Acta Anat.* 29:267, 1957.
20. Porter, K. R., and Bonneville, M. A.: *An Introduction to the Fine Structure of Cells and Tissues*, Philadelphia, Lea and Febiger, 1963.
21. Kurosumi, K.; *Intern. Rev. Cytol.* 11:1, 1961.
22. Gautier, A.; Jean, G.; Probst, M., and Falcão, L.; *Ultrastructure du mégakaryocyte et problèmes de plaquetogenèse. Arch. Ital. Anat. Istol. Patol.* 37:503, 1963.
23. Palade, G. E.; in *Electron Microscopy in Anatomy*, edited by J. D. Boyd, F. R. Johnson, and J. D. Lever, Baltimore, Williams and Williams Co., 1961, p. 176.
24. Matter, M.; Hartmann, J. R.; Kautz, J.; De Marsh, Q. B., and Finch, C. A.; *Blood* 15:174, 1960.
25. White, J. G.; Krivit, W., and Vernier, R. L.; *Blood* 25:604, 1965 (abstract).
26. Novikoff, A. B.; Essner, E.; Goldfischer, S., and Heus, M.; in *The Interpretation of Ultrastructure*, edited by R. J. C. Harris, New York, Academic Press, 1962, p. 199.
27. Mazia, D.; Chaffee, R. R., and Iverson, R. M.; *Proc. Nat. Acad. Sci.* 47:788, 1961.
28. Bettex-Galland, M., and Lüscher, E. F.; *Nature* 184:276, 1959.
29. Thiery, J. P., and Bessis, M.; *Rev. Hematol.* 11:162, 1956.
30. Bloom, W., and Fawcett, D. W.: *A Textbook of Histology*, Philadelphia, Saunders, 1962.
31. Paulus, J. M., and Mel, H. C.; *Viability studies on megakaryocytes in mechanically and enzymatically suspended bone marrow, in preparation.*
32. Brachet, J.; *Biochemical Cytology*, London, Pergamon Press, 1958.
33. Maupin, B.; *Les Plaquettes Sanguines de l'Homme*, Paris, Masson et Cie, 1959.
34. Aster, R. H., and Jandl, J. H.; *J. Clin. Invest.* 43:843, 1964.

35. Firkin, B. G.; O'Neill, B. J.; Dunstan, B., and Oldfield, R.; *Blood* 25:345, 1965.
36. Waller, H. D.; Löhr, G. W.; Grignagni, F., and Gross, R.; *Thromb. Diath. Haemorrhag.* 3:520, 1959.
37. Gross, R.; *Bibliotheca Haematol.* 9:92, 1959.
38. Gross, R.; Löhr, G. W., and Waller, H. D.; *Proc. Seventh Congress Europ., Soc. Haematol.*, New York, Karger, 1960, p. 686.
39. Rossi, E. C., and Grogan, N. J.; *Blood* 25:613, 1965.
40. Gude, W. D.; Upton, A. C., and Odell, T. T.; *Lab. Invest.* 5:348, 1956.
41. Feissly, R.; Gautier, A., and Marcovici, I.; *Rev. Hématol.* 12:397, 1957.
42. Datta, N.; Thorell, B., and Akerman, L.; *Acta Hematol.* 14:176, 1955.
43. Salvidio, E., and Crosby, W. H.; *J. Lab. Clin. Med.* 56:711, 1960.
44. Roskam, J.; *Physiologie Normale et Pathologique du Globulin*, Paris, Presses Universitaires de France, 1927.
45. Adelson, E.; Rheingold, J. J., and Crosby, W. H.; *Blood* 17:767, 1961.
46. David-Ferreira, J. F.; *Intern. Rev. Cytol.* 17:99, 1964.
47. Bessis, M., and Tabuis, J.; *Rev. Hématol.* 10:753, 1955.
48. Mustard, J. F.; Movat, H. Z.; Glynn, M. F., and Murphy, E. A.; *Can. Med. Assoc. J.* 92:362, 1965.
49. Tait, J., and Elvidge, A. R.; *J. Physiol.* 62:129, 1926.
50. de Duve, C.; in *Cellular Injury*, edited by A. V. S. de Reuck and J. Knight, Ciba Foundation Symposium, Boston, Little, Brown and Co., 1963, p. 369.
51. Firkin, B. G.; *Australasian Ann. Med.* 12:261, 1963.
52. Firkin, B. G.; O'Neill, B. J.; Dunstan, B., and Oldfield, R.; *Blood* 25:345, 1965.
53. Marcus, A. J.; *Thrombos. Diathes. Haemorrh. Suppl.* 17, 1965.
54. Hovig, T.; The ultrastructure of rabbit blood platelet aggregates. *Thromb. Diath. Haemorrhag.* 8:455, 1962.
55. Jean, G., and Racine, L.; in *Proc. Fifth. Int. Congr. Electr. Micr.*, New York, Academic Press, 1962.
56. Novikoff, A. B.; Essner, E., and Heus, M.; in *Proc. Fifth. Int. Congr. Electr. Micr.*, New York, Academic Press, 1962.
57. Grette, K.; *Acta Physiol. Scand.* 56:suppl. 195, 1962.
58. Bettex-Galland, M., and Lüscher, E. F.; *Thromb. Diath. Haemorrhag.* 4:178, 1960.
59. Lüscher, E. F., and Bettex-Galland, M.; *J. Physiologie* 53:145, 1961.
60. Distèche, A.; *Acad. Roy. Belg. Classe Sci. Mem.* 32, 1960.
61. Hugues, J.; *Compt. Rend. Soc. Biol.* 154:866, 1960.
62. Bounameaux, Y.; *Thromb. Diath. Haemorrhag.* 6:504, 1961.
63. Käser-Glanzmann, R., and Lüscher, E. F.; *Thromb. Diath. Haemorrhag.* 7:480, 1962.
64. Löhr, G. W.; Waller, H. D., and Gross, R.; *Deut. Med. Wochschr.* 86:897, 1961; 86:946, 1961.
65. Aubert, X.; in *Physiologie*, Vol. 2, edited by C. Kayser, Paris, Flammarion, 1963, p. 921.
66. Lorand, L.; in *Biochemistry of Muscle Contraction*, edited by J. Gergely, Boston, Little, Brown and Co., 1965, p. 253.

67. Marcus, A. J., and Zucker, M. B.: in Recent Biochemical Morphologic and Clinical Research, New York, Grune and Stratton, 1965.

The present address of Dr. Jean-Michel Paulus is Institut de Médecine, Département de Clinique et de Pathologie Médicales, Université de Liège, Belgium.

# The Effect of Erythropoietin on the Growth and Development of Spleen Colony-Forming Cells

N67 15945

John C. Schooley

The bone marrow, spleen, and fetal liver of the mouse contain cells which, upon transplantation into lethally irradiated hosts, settle down, proliferate, and form discrete nodules which are particularly obvious in the spleen (1-3). Cells capable of repopulating the hemopoietic tissues of irradiated mice and cells capable of forming spleen nodules are also found in the peripheral blood and peritoneal fluid (4-6). The splenic nodules, when first discernable, are composed primarily of primitive undifferentiated cells; mature cells obviously characteristic of the erythrocytic, granulocytic, and megakaryocytic series appear later. Becker *et al.* (7) observed that the same abnormal chromosome produced by irradiation of the donor bone marrow was found in the cells of any one individual spleen nodule. They concluded that "the general view that spleen colonies are clones is a most reasonable conclusion". Welshons' (8) failure to observe nodules having a mixed origin, following the transplantation of a suspension of bone-marrow cells derived from both normal and chromosome-marked donors, also supports the conclusion that the splenic nodules are clones, each derived from the proliferation of a single cell. The identity of the colony-forming cell or cells is unknown, but it appears reasonable to assume that it corresponds to the hemopoietic stem cell.

The mechanism regulating differentiation of stem cells into the various hemopoietic cell lines poses one of the basic problems of hematology. Considerable evidence indicates that erythropoiesis is normally regulated by a hormone, erythropoietin. This regulation appears to be achieved primarily by the action of the hormone upon some primitive cell that cannot, at least cytologically, be classified as an erythroid cell. It has been generally assumed that this primitive cell is the stem cell. Bruce and McCulloch (9) have studied the effects of prolonged exposure to hypoxia on the development of spleen colonies. They conclude that the colony-forming cell is not sensitive to erythropoietin, but that some early progeny of the colony-forming cell is responsive to the action of erythropoietin. In the present experiments, the progressive growth and development of spleen colonies have been studied in host animals, in which erythropoiesis has been modified by various procedures, such as the production of polycythemia, the injection of immune serum capable of neutralizing the biological activity of erythropoietin, or the injection of exogenous erythropoietin.

## METHODS

**PRODUCTION OF POLYCYTHEMIA** Mice were made polycythemic either by exposure to altitude followed by transfusion or by transfusion alone. Female BALB/c Cum mice were maintained at a simulated altitude of 18,000 ft ( $pO_2$  approximately 72 mm Hg) for

three weeks. The mice were subcutaneously injected with 1 mg iron dextran (Imferon) before being placed in an altitude chamber, following the recommendations of DeGowin *et al.* (10). Four days after the mice were removed from the altitude chamber they were injected intraperitoneally with 1 ml of packed isologous red blood cells. Two days after transfusion the mice were irradiated. Control mice were similarly injected with iron dextran and irradiated.

Female C<sub>3</sub>H/Cum mice weighing 19 to 25 g were hypertransfused with two daily intraperitoneal injections of 1 ml of isologous red blood cells. The red cells were obtained from donor mice by cardiac puncture and were washed three times with saline before injection. The buffy coat was removed after each washing. The final hematocrit of the red-cell suspension was about 80%. Recipient polycythemic mice were retransfused on the 4th day after transplantation with an intravenous injection of 1 ml of packed red blood cells. In some early experiments the red cells used for this last transfusion were taken from irradiated donors to prevent the transplantation of colony-forming cells in the transfusing blood. Experience demonstrated, however, that this procedure was unnecessary; washing of the red cells and removal of the buffy coat adequately removed the colony-forming cells in the transfusing blood. Only mice having hematocrits greater than 50% at the time of sacrifice were included in the experiments. Most animals had hematocrits of about 65%. Polycythemic mice of these strains have negligible 72-hr <sup>59</sup>Fe uptakes with these hematocrits.

**IRRADIATION** Mice were irradiated at 1.22 meters from a <sup>60</sup>Co source with a dose rate in air of 18.5 R/min, measured with a Victoreen condenser R-meter. Under these exposure conditions, the average tissue dose to the mouse was approximately 0.94 rad/R in air. The actual dose of irradiation varied between 872 and 960 R in the different experiments. However, in all experiments mice that received no bone-marrow or spleen cells were included as controls. After irradiation, groups of five mice were housed in sterilized cages and allowed to drink chlorinated water containing 0.5 to 1% terramycin. With these conditions of irradiation and care, generally less than 5% of the irradiated mice died within 10 days. The endogenous spleen-colony level was usually about one to two colonies per spleen.

**TRANSPLANTATION OF BONE-MARROW CELLS** Immediately after irradiation the various groups of mice were injected intravenously with 0.5 ml suspending medium containing 0.5 to  $1.0 \times 10^5$  viable bone-marrow cells obtained from the femurs and tibias of isologous donor mice. The total number of cells was counted using hemocytometers; counts were frequently checked with a Coulter Counter. The cell suspensions were prepared in either Tyrode's solution or Difco medium TC858. Viability of the cells was determined by the eosin dye exclusion method. Smears were made of the various donor cells; marrow from polycythemic donors contained only a few identifiable nucleated red cells. When transplants were prepared from different groups of donors, the recipients were injected in a random fashion in order to minimize errors due to death of colony-forming cells in the dilute solutions during the injection period.

The recipient groups of mice were sacrificed at various times after bone-marrow transplantation. Each experimental group generally contained at least 10 mice at the time of



sacrifice. Twenty-four hours before sacrifice the mice were injected intraperitoneally with 0.2 ml of saline containing 0.5  $\mu$ Ci of  $^{59}\text{Fe}$  as iron citrate (specific activity 10  $\mu\text{Ci}/\mu\text{g}$ ). Blood was taken by cardiac puncture from each mouse at the time of sacrifice, and the hematocrit and  $^{59}\text{Fe}$  content of a known amount of blood determined.

Whole blood was counted initially, but in later experiments the blood was washed with saline in order to remove any free plasma  $^{59}\text{Fe}$ . Immediately after the blood was taken, the spleen was removed and placed in a vial containing Bouin's fixative. The amount of  $^{59}\text{Fe}$  in each spleen was determined and the results expressed as the percent of the injected  $^{59}\text{Fe}$  per spleen. The  $^{59}\text{Fe}$  uptake of the blood was expressed either as the percent of injected  $^{59}\text{Fe}$  found per milliliter of packed red blood cells or the percent uptake of injected  $^{59}\text{Fe}$  in the estimated blood volume. The blood volume was assumed to be 7% of the body weight for polycythemic mice. In some experiments only the  $^{59}\text{Fe}$  uptake per milliliter of packed cells has been given since this value was calculated from actual measurements, whereas the  $^{59}\text{Fe}$  uptake in the blood volume was estimated on the basis of body weight, and blood-volume determinations of the heavily irradiated recipients were not made.

**COLONY COUNTS** The number of colonies in each spleen was counted, using a dissecting microscope. In most experiments the total colony count was subdivided into large, medium, and small colonies. Colonies with a diameter larger than 2 mm were considered large, colonies with a diameter of 1 to 2 mm, medium, and colonies with a diameter less than 1 mm, small. After being counted, they were embedded in paraffin, sectioned, and stained with hematoxylin and eosin. Some sections also were stained with Ralph's stain for hemoglobin, Mallory's triple stain, or Laidlaw's silver stain. In some experiments serial sections of 4  $\mu$  thickness were made of the spleens, and every 20th section was mounted. The outlines of these sections were traced on paper, utilizing a photographic enlarger as a slide projector. Each colony was then drawn within these outlines of the individual sections, and the type of hematopoietic colony was noted. The total number and types of individual colonies were then determined.

**ERYTHROPOIETIN AND ANTI-ERYTHROPOIETIN INJECTIONS** After transplantation of bone-marrow cells, different groups were injected with erythropoietin (ESF). Some groups were given erythropoietin daily, beginning immediately after transplantation; other groups did not receive erythropoietin until the 5th day after transplantation; and some groups did not receive erythropoietin until the 8th or 9th day after transplantation. Both sheep plasma erythropoietin (AL-0336, No. 103194A obtained from the Hematology Study Section of the National Institutes of Health) and human urinary erythropoietin were used. Some groups were injected daily or every other day after transplantation with 0.25 ml of immune serum obtained from rabbits immunized with human urinary erythropoietin. This serum, termed "anti-ESF", has been shown by appropriate methods (11) to neutralize the biological activity of erythropoietin: about 1.0 cobalt unit is neutralized by 0.04 ml of serum. Control groups of mice were injected with normal rabbit serum or serum obtained from rabbits immunized with normal human urinary proteins.

**TRANSPLANTATION OF SPLEEN CELLS** The fraction of colony-forming cells in the transplanted bone marrow which actually settles down in the spleen in normal and polycythemic mice was measured, using the procedure described by Siminovitch *et al.* (12). The growth curves of colony-forming cells in polycythemic mice and polycythemic mice receiving daily injections of 0.5 cobalt unit erythropoietin were measured, using the procedure described by McCulloch and Till (13). In these experiments  $2 \times 10^6$  viable bone-marrow cells were injected into irradiated mice, and at various times after transplantation the spleens were removed. A single cell suspension of the spleen was prepared by repeated injections of Medium 858 directly into the spleen. The spleen swells noticeably after each injection, and then collapses, discharging cells into the medium. Following this the remaining spleen was teased apart, injected several times through a 25-gauge and a 27-gauge needle, and finally filtered through a nylon gauze sack. Each suspension was made from at least four spleens, suitably diluted, and injected immediately into irradiated recipients. The total number of nucleated cells in the suspension was determined as above and smears were made. The colonies in the irradiated recipients were counted 10 days after transplantation.

**ASSAY FOR ERYTHROPOIETIN IN PLASMA OF HEAVILY IRRADIATED MICE** The erythropoietic activity in plasma obtained from groups of  $C_3H$  mice at 1, 3, 5 and 8 days after heavy irradiation was assayed in polycythemic  $C_3H$  mice. Donor mice were heavily irradiated, bled by cardiac puncture on the stated days after the irradiation, and the plasma collected. This plasma was used in the polycythemic mouse assay system for erythropoietin: five days after hypertransfusion groups of eight mice were injected intraperitoneally with 1 ml of the plasma to be tested. Fifty-six hours later  $^{59}Fe$  was injected intraperitoneally, and 72 hr after the iron injection the  $^{59}Fe$  uptake in a known volume of blood was measured. The results of the assay are expressed as percent of the injected dose of  $^{59}Fe$  in the calculated blood volume, which was assumed to be 7% of the body weight. It should be emphasized that the irradiated mice from which the plasma was obtained were older (nine months or more) than the recipients (two to four months) used in the transplantation studies; they were, however, healthy animals. Hematocrits were determined in the irradiated mice on the days plasma was collected, and hematocrits of other mice were taken at days 0, 9, 10, 11 and 14 after similar irradiation.

## RESULTS

**BONE-MARROW TRANSPLANTATION FROM NORMAL AND POLYCYTHEMIC MICE** Experimental procedures that increase or decrease erythropoiesis in normal and polycythemic mice were performed on irradiated BALB/c mice following the transplantation of  $10^5$  viable bone-marrow cells obtained from either normal or polycythemic donors. Polycythemia was induced in both donors and recipients by exposure to hypoxia, and animals were maintained polycythemic by transfusion. The  $^{59}Fe$  measurements and colony counts were performed 14 days after transplantation. The results are shown in Table 1. Bone marrow from the above polycythemic donors was transplanted in Groups IV through VII; the remaining groups were transplanted with marrow cells from normal donors. The recipients of Groups III and V through VII were polycythemic. The  $^{59}Fe$  uptake in the spleen and in the blood was markedly reduced by the injection of anti-erythropoietin. Nucleated erythroid cells were

Table 1. A comparison of the effect of the injection of erythropoietin and anti-erythropoietin on spleen colony formation and erythropoietic activity in the spleens and peripheral blood following the transplantation of normal or polycythemic bone-marrow cells into irradiated normal or polycythemic hosts. Animals were made polycythemic by exposure to hypoxia and maintained by hypertransfusion.

GROUP	DONOR BALB/C ♀ BONE MARROW CELLS	RECIPIENT IRRADIATED BALB/C ♀ MICE	TREATMENT	NO. OF MICE	NO. OF SPLEEN COLONIES	Fe <sup>59</sup> IN SPLEEN (%)	Fe <sup>59</sup> /ml PACKED RBC (%)	Fe <sup>59</sup> IN BLOOD VOLUME	HEMATOCRIT
I	NORMAL	NORMAL	-	15	CONFLUENT	3.41 ± 0.24	57.2 ± 2.3	29.7 ± 1.2	42.4 ± 0.8
II			ANTI- ERYTHRO- POIETIN	14	CONFLUENT	0.82 ± 0.7	2.17 ± 0.37	0.94 ± 0.16	32.8 ± 0.5
III		POLYCYTHEMIC	-	11	24.1 ± 1.4	1.23 ± 0.85	0.44 ± 0.06	0.31 ± 0.05	60.4 ± 2.4
IV	POLYCYTHEMIC	NORMAL	-	15	CONFLUENT	3.50 ± 0.36	62.9 ± 2.5	34.0 ± 1.4	41.9 ± 0.7
V		POLYCYTHEMIC	-	9	30.6 ± 1.5	1.19 ± 0.40	0.32 ± 0.04	0.26 ± 0.03	62.6 ± 2.4
VI			ESF FROM DAY 1	13	29.9 ± 2.6	4.61 ± 0.36	12.1 ± 1.3	10.3 ± 1.1	63.1 ± 0.4
VII			ESF FROM DAY 5	13	27.5 ± 2.0	3.73 ± 0.24	15.7 ± 2.0	13.5 ± 1.7	65.0 ± 1.3

virtually absent in the spleens of these mice. Colonies in the nonpolycythemic mice were confluent and could not be counted; however, the number of colonies in the polycythemic recipients could be counted satisfactorily. The number of colonies found in polycythemic mice transplanted with bone-marrow cells obtained from hypoxia-induced polycythemic donors (Group V) is significantly greater ( $P < 0.01$ ) than the number of colonies found when polycythemic mice received the same number of viable bone-marrow cells obtained from normal donors (Group III). This difference could be due to an actual increase in the numbers of colony-forming cells in the marrow or to a relative increase in their numbers because of a decrease in the number of nucleated erythroid cells in the transplanted marrow suspension. The injection of erythropoietin into the polycythemic recipients either from the day of transplantation or from the beginning of the 5th day after transplantation did not significantly increase or decrease the number of spleen colonies observed on the 14th day after transplantation, but did stimulate the colonies to become erythroid, i. e., the <sup>59</sup>Fe uptake in the spleen and blood was significantly higher than in the control polycythemic mice. Nucleated erythroid cells were only rarely seen in sections of the spleens of the uninjected polycythemic group but were very conspicuous in the spleens of the groups receiving erythropoietin. The labeled red cells found in the peripheral blood are presumably derived not only from erythroid colonies in the spleen but also from hematopoietic tissue that has settled down and proliferated in locations other than the spleen.

COMPARISON OF <sup>59</sup>Fe UPTAKE IN THE SPLEEN WITH NUMBER OF SPLEEN COLONIES The relationship between the number of colonies and the 24-hr uptake of <sup>59</sup>Fe in

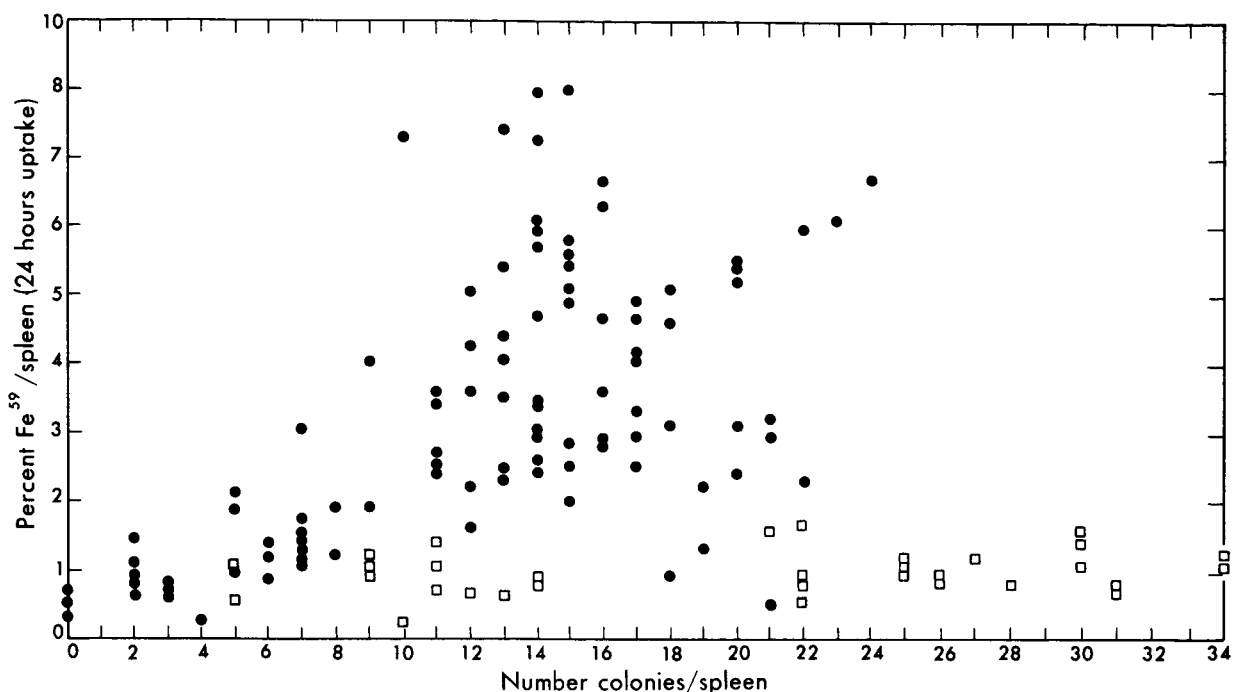


Figure 1. Relationship between the 24-hr  $^{59}\text{Fe}$  uptake in the spleen and the number of spleen colonies in irradiated normal (circles) and polycythemic mice (squares) transplanted with normal bone marrow. In this and all following figures and tables, the endogenous spleen colony level (generally 0-1 colony) has been subtracted. MUB-3204

the spleens of normal and hypertransfused recipient mice is shown in Fig. 1. These data comprise the results of several experiments in which recipient  $\text{C}_3\text{H}$  female mice were transplanted with variable numbers of isologous nucleated bone-marrow cells. It is evident that in the nonpolycythemic mice there is some correlation between the number of colonies and the  $^{59}\text{Fe}$  uptake in the spleen. In polycythemic mice such a correlation does not exist; even in mice whose spleens contain large numbers of colonies, very little  $^{59}\text{Fe}$  is taken up in the spleen. Similar results in normal and polycythemic mice have been observed when the iron uptake in the peripheral blood is compared to the number of spleen colonies.

**EFFECT OF ERYTHROPOIETIN AND ANTI-ERYTHROPOIETIN ON THE UPTAKE OF  $^{59}\text{Fe}$  IN THE PERIPHERAL BLOOD OF NORMAL MICE** The effect of daily injections of erythropoietin and anti-erythropoietin on the 24-hr uptake of  $^{59}\text{Fe}$  in peripheral blood in irradiated BALB/c mice nine and 14 days after transplantation with  $1 \times 10^5$  isologous bone-marrow cells obtained from normal donors is shown in Fig. 2. The 24-hr  $^{59}\text{Fe}$  uptake in the spleens of these mice was comparable to that seen in the peripheral blood. Erythropoiesis measured by this parameter was minimal nine days after transplantation, but by the 14th day considerable increase in the  $^{59}\text{Fe}$  uptake occurred in all groups, except the group of mice injected with anti-erythropoietin. On the ninth day nucleated erythroid cells were observed in the bone marrow of all the groups, except the group injected with anti-erythropoietin, even

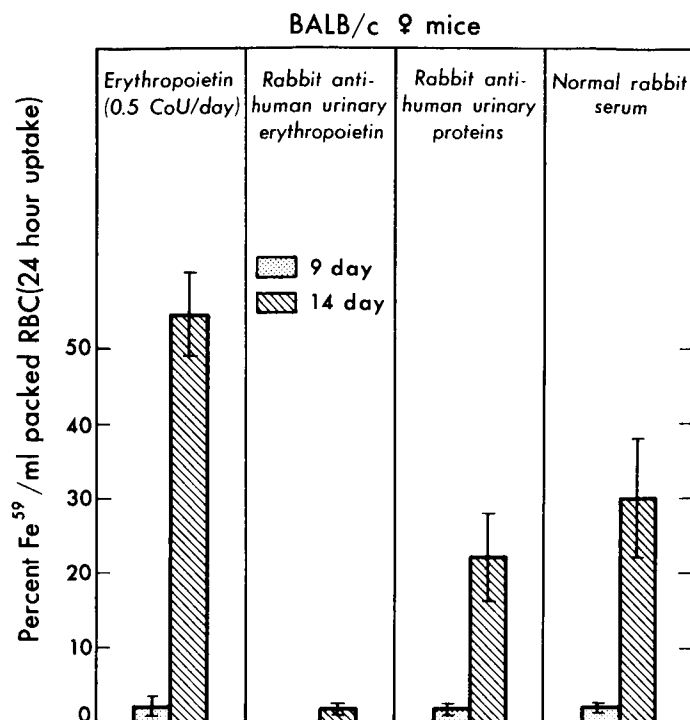
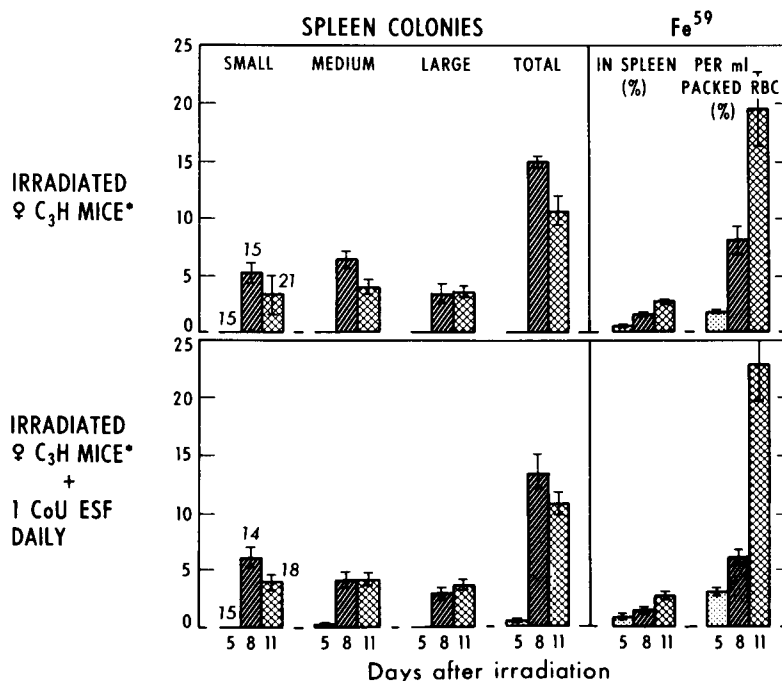


Figure 2. The effect of the daily injection of erythropoietin and anti-erythropoietin on the  $^{59}\text{Fe}$  uptake in the peripheral blood of heavily irradiated mice at 9 and 14 days after transplantation with  $1 \times 10^5$  bone-marrow cells. The effect of the daily injection of normal rabbit serum and rabbit anti-human urinary proteins is also shown. MUB-3203

Figure 3. A comparison of the progressive development of spleen colonies in terms of size and 24-hr  $^{59}\text{Fe}$  uptake in the spleen and peripheral blood of heavily irradiated normal mice with and without daily injections of 1.0 cobalt unit erythropoietin. The numbers over the small colony bars indicate the number of mice in each group. MUB-4426



\* All mice transplanted with  $6 \times 10^4$  viable bone marrow cells taken from ♀ C<sub>3</sub>H mice

though the  $^{59}\text{Fe}$  uptake in the spleen and blood was low. Although not shown in the figure, the total number of colonies observed in the spleens of these different experimental groups was not significantly different on the 9th or 14th day after transplantation.

**EFFECT OF ERYTHROPOIETIN ON IRRADIATED NORMAL MICE** The temporal effects of daily injections of one cobalt unit of sheep plasma erythropoietin on the development of spleen colonies in nonpolycythemic irradiated mice were studied after transplantation of  $6 \times 10^4$  bone-marrow cells. The results are shown in Fig. 3. The injection of exogenous erythropoietin had no significant effect on the size distribution or total numbers of spleen colonies, nor on the 24-hr  $^{59}\text{Fe}$  uptake in the spleen or peripheral blood. It seemed possible that the lack of effect of exogenous erythropoietin might be due to the dose administered; therefore, the experiment was repeated, injecting nine cobalt units of human erythropoietin daily after the transplantation of  $8 \times 10^4$  bone-marrow cells. The colonies were counted on the 8th day after transplantation. These results are in essential agreement with the previous experiment. There is, however, a slight increase in the number of large colonies, suggesting an increased erythropoietic activity.

#### ASSAY FOR ERYTHROPOIETIN IN PLASMA OF IRRADIATED NORMAL MICE

Figure 4 shows the results of the assay for erythropoietic activity in plasma obtained from groups of  $\text{C}_3\text{H}$  mice at 1, 3, 5 and 8 days after lethal irradiation, and the hematocrits of irradiated mice on different days after irradiation. A detectable amount of erythropoietin was present in the plasma within a day after irradiation. High levels of erythropoietin were evident by the 5th day after irradiation and reached the equivalent of about one cobalt unit per milliliter by the 8th day. The increasing levels of erythropoietin in the plasma appear to be reasonably correlated with a decrease in the hematocrits at later times after irradiation.

**EFFECT OF ERYTHROPOIETIN ON IRRADIATED POLYCYTHEMIC MICE** The effect of daily injections of one cobalt unit of erythropoietin on the temporal development of spleen colonies was reinvestigated using transfusion-induced polycythemic mice as recipients. The results are shown in Fig. 5. Erythropoiesis as measured by  $^{59}\text{Fe}$  uptake in the peripheral blood is insignificant in the hypertransfused recipients at 5, 8, and 11 days after bone-marrow transplantation, but in the hypertransfused recipients that received erythropoietin injections a significant  $^{59}\text{Fe}$  uptake was observed on the 14th day after transplantation. The total number of colonies in both groups of mice is not significantly different at any of the observed times. The distribution of colony sizes in the two experimental groups is somewhat different, however. Thus, on the 8th day after transplantation many more medium colonies are seen in the mice receiving erythropoietin than in those not receiving erythropoietin.

The cellular composition of the individual colonies in hypertransfused recipients receiving erythropoietin was compared to hypertransfused recipients receiving no erythropoietin injections. Serial sections of the spleens were made on the 14th day after transplantation. The results are shown in Table 2. The colonies were classified as erythroid, granulocytic, megakaryocytic, primitive, and mixed. The classification, except in the case of

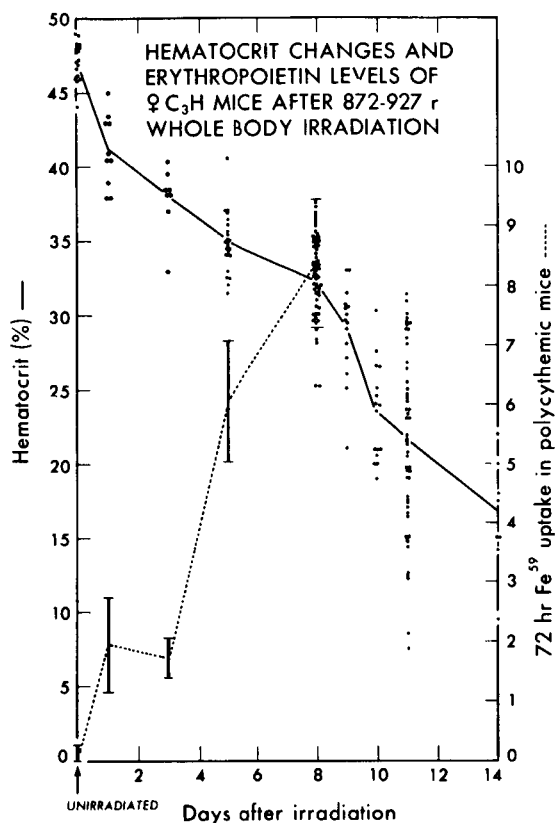
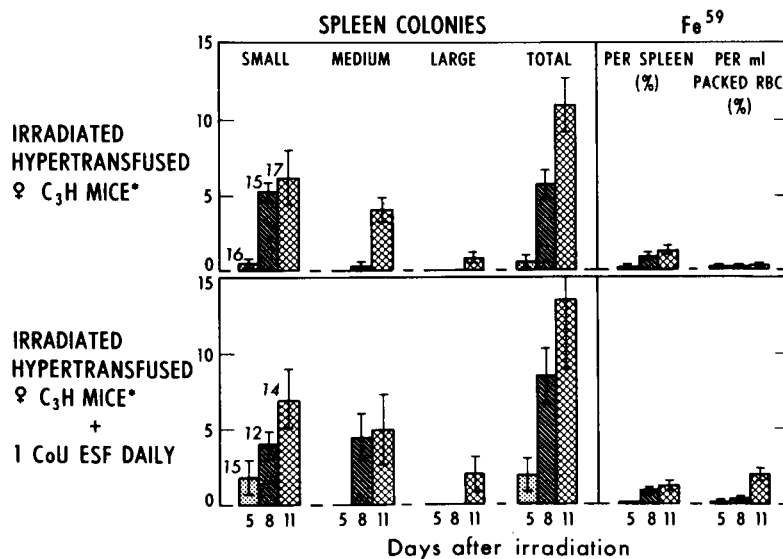


Figure 4. MUB-4231

Figure 5. A comparison of the progressive development of spleen colonies in terms of size and 24-hr  $^{59}\text{Fe}$  uptake in the spleen and peripheral blood of heavily irradiated polycythemic mice with and without daily injections of 1.0 cobalt unit erythropoietin. The numbers over the small colony bars indicate the number of mice in each group. MUB-4425



\* All mice transplanted with  $6 \times 10^4$  viable bone marrow cells taken from ♀ C<sub>3</sub>H mice

Table 2. Cellular composition of spleen colonies in hypertransfused recipients receiving erythropoietin.

	Erythroid	Granulocytic	Megakaryocytic	Primitive	Mixed	Total
Hypertransfused recipients	0	34	13	32	21	100
Hypertransfused recipients injected with erythropoietin	35	15	6	16	28	100

Table 3. A comparison of the effect of daily injections of 0.5 cobalt unit erythropoietin on spleen-colony formation and erythropoietic activity in the spleen and peripheral blood of lethally irradiated polycythemic mice 10 days following the transplantation of bone-marrow cells and of fetal liver cells in hypertransfused heavily irradiated C<sub>3</sub>H mice six to eight weeks old.

GROUP	C <sub>3</sub> H DONOR CELLS	TREATMENT	NO. OF MICE	NO. OF SPLEEN COLONIES	Fe <sup>59</sup> IN SPLEEN (%)	Fe <sup>59</sup> IN BLOOD VOLUME (%)	Fe <sup>59</sup> /ml PACKED RBC (%)
I	40×10 <sup>3</sup> BONE MARROW CELLS FROM 1 YR OLD ♀	NONE	14	6.57 ±0.54	1.05 ±0.08	0.05 ±0.01	0.05 ±0.01
II		0.5 Co UNIT ESF DAILY FROM DAY 0	16	20.5 ±1.31	1.98 ±0.11	0.62 ±0.07	0.65 ±0.07
III	40×10 <sup>3</sup> BONE MARROW CELLS FROM 6-8 WEEKS OLD HYPER TRANSFUSED ♀	NONE	19	5.45 ±0.66	1.04 ±0.04	0.05 ±0.00	0.05 ±0.00
IV		0.5 Co UNIT ESF DAILY FROM DAY 0	13	18.9 ±1.61	1.99 ±0.10	0.81 ±0.11	0.84 ±0.11
V	200×10 <sup>3</sup> LIVER CELLS FROM FETAL MICE	NONE	16	14.1 ±0.93	1.12 ±0.05	0.08 ±0.01	0.08 ±0.01
VI		0.5 Co UNIT ESF DAILY FROM DAY 0	17	21.3 ±0.97	3.68 ±0.27	3.69 ±0.41	3.86 ±0.43

primitive colonies, is based on the presence of relatively mature forms. The presence of immature forms of any of the other cell lines in a colony termed erythroid, granulocytic, or megakaryocytic is not necessarily excluded by this classification, since identification of such immature forms is not possible. The percentage of colonies classified as erythroid showed a marked increase in hypertransfused recipients injected with erythropoietin over uninjected controls, while the percentage of granulocytic, megakaryocytic, and primitive colonies decreased. It should be emphasized that all foci of hematopoietic cells seen on and within the spleen were classified as colonies in this particular experiment, and no attempt was made to



correlate the macroscopic colonies with the small microscopic foci of hematopoietic cells.

A preliminary report of these findings was presented at a recent conference (14). At this same conference similar studies were reported by Curry *et al.* (15) with almost opposite results. The effect of daily injections of erythropoietin on the development of spleen colonies in polycythemic mice was therefore reinvestigated. The results of three separate experiments are shown in Table 3. In contrast to the previous experiments and regardless of the source of donor marrow, a decided decrease in the total number of colonies was seen in hypertransfused mice that did not receive erythropoietin injections, when compared to the total number of colonies obtained when the same number of cells was transplanted into hypertransfused mice receiving daily injections of erythropoietin. The decrease observed between the erythropoietin-injected and noninjected polycythemic mice following transplantation of fetal liver cells was significant, but not as great as that observed when bone marrow from older donors or younger hypertransfused donors, was used.

**FRACTION OF TRANSPLANT SETTLING IN SPLEEN** The fraction of colony-forming cells in transplanted bone marrow which actually lodge in the spleen after intravenous injection into lethally irradiated transfusion-induced polycythemic and normal recipient mice was measured. A suspension of  $2 \times 10^6$  viable bone-marrow cells was injected intravenously. Since each  $6 \times 10^4$  viable cells contained  $12.6 \pm 1.04$  colony-forming cells, the two million transplanted cells contained a total of  $420 \pm 35$  colony-forming cells. Two hours later the spleens were removed and a single cell suspension prepared. A suitable dilution of this cell suspension, equivalent to 17.9% of the total spleen, was injected into other groups of normal lethally irradiated mice, and 10 days later the total number of spleen colonies was counted. A total of  $18.5 \pm 0.84$  and  $17.5 \pm 0.68$  colonies was produced by the spleen suspension taken from the polycythemic and normal mice respectively. Since this number of colonies was produced by 17.9% of the spleen, a total of  $18.5 \pm 0.84 \times \frac{100}{17.9}$  or  $103 \pm 4.7$  colonies were present in the total spleen taken from the polycythemic mice, and  $17.5 \pm 0.68 \times \frac{100}{17.9}$  or  $97.8 \pm 3.8$  colonies were present in the total spleen taken from the normal recipients. Therefore, 2 hr after lethal irradiation and transplantation of  $2 \times 10^6$  viable bone-marrow cells, the number of colony-forming cells that lodged in the spleen was not significantly different in normal and polycythemic mice. Since a total of 420 colony formers was injected into these mice, and an average of 100 colony formers was recovered in the spleen, the fraction of the injected colony formers that lodged in the spleen and could be recovered after 2 hr is  $100/420$  or 0.24. This is slightly higher than the value of 0.17 reported by Siminovitch *et al.* (12). These differences in the fraction of cells recovered in the spleen may be related to the strain of mouse used but are just as likely related to inherent variabilities in the technique itself, such as the efficiency of preparing the suspension of spleen cells, etc.

**EFFECT OF ERYTHROPOIETIN ON THE GROWTH OF COLONY-FORMING UNITS IN THE SPLEENS OF IRRADIATED POLYCYTHEMIC MICE** The number of colony formers that could be recovered from the spleens of transfusion-induced polycythemic mice after lethal irradiation and the transplantation of  $2 \times 10^6$  viable bone-marrow cells was measured during the first 10 days after transplantation, in order to obtain a curve showing the increase

in the number of colony-forming units as a function of time. The number of colony-forming units in the spleens of polycythemic mice receiving daily injections of erythropoietin was also measured. The results are shown in Fig. 6a.

The curves in Fig. 6a show that following an initial lag phase in the growth of colony formers after transplantation, the cells proliferate exponentially with a doubling time of about one day. The growth curves of colony formers in the polycythemic recipients with or without the daily injection of erythropoietin are almost identical to the curve reported by McCulloch and Till (13) for nonpolycythemic mice.

From the third day after transplantation there was consistently a greater number of colony formers in the spleens of polycythemic mice injected with erythropoietin than was observed in polycythemic mice receiving no injections, but this difference was not significant at the 95% confidence level except on the 6th day. At day 6 after transplantation the results of four separate experiments with a total of 280 mice have been plotted to confirm the statistical difference ( $P < 0.001$ ) in the total number of colonies between the two groups. Unplotted results of separate experiments for the other days again failed to demonstrate a significant difference between the number of colonies in polycythemic mice receiving erythropoietin and such mice not receiving erythropoietin.

**EFFECT OF ERYTHROPOIETIN ON THE CELLULAR CONTENT OF SPLEENS OF IRRADIATED POLYCYTHEMIC MICE** Figure 6b shows the total cells in the spleens of the irradiated mice that received the bone-marrow transplant plus erythropoietin, the bone-marrow transplant alone, or no erythropoietin or transplant. The total cell content of the spleen drops rapidly after irradiation. In polycythemic mice given erythropoietin an increase in the number of cells commences about the 4th day and increases very rapidly during the 5th and 6th days after transplantation. In polycythemic mice not receiving erythropoietin very little increase in the total cellularity of the spleen is evident until the 6th or 7th day after transplantation, following which it rises more slowly than with erythropoietin stimulation. The total cellularity of spleens from polycythemic mice receiving no bone-marrow cells remained low during the 10-day period. These changes in total cell count can be correlated with the presence of differentiated nucleated erythroid or granulocytic cells. Occasional immature erythroid cells are observed in smears made of cell suspensions from the spleens of polycythemic mice receiving erythropoietin on the 4th day after transplantation, and by the 6th day large numbers of erythroid cells at all stages of maturation are seen. Interestingly, on the 9th or 10th day fewer cells in the later stages of erythroid maturation are observed, whereas a relative increase in the number of proerythroblast and basophilic erythroblast stages occurs. This is presumably because the erythroid cells initially produced have matured and passed into the peripheral blood. Reticulocytes can be readily demonstrated in the peripheral blood at this time, when  $2 \times 10^6$  bone-marrow cells have been transplanted. An occasional immature granulocytic cell also can be seen in spleen smears by the 4th day after transplantation, but large numbers of such cells are not seen either in polycythemic mice or polycythemic mice receiving erythropoietin until the 7th day after transplantation. These findings indicate that the proliferation and maturation of erythroid cells are much more rapid

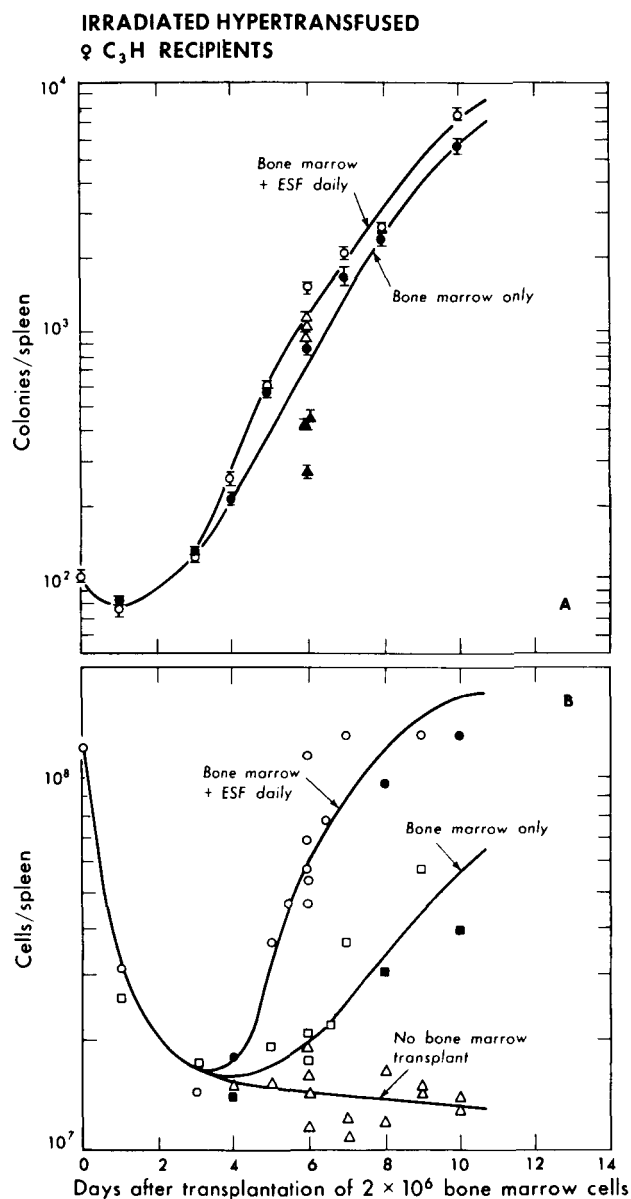


Figure 6. (a) Effect of erythropoietin on the number of colony-forming units as a function of time in the spleens of polycythemic mice that have been heavily irradiated and transfused with bone-marrow cells. The open circles and triangles indicate the total colony-forming units recovered from the spleens of polycythemic mice receiving daily injections of 0.5 cobalt unit erythropoietin (ESF) and the solid circles and triangles indicate the colony-forming units recovered in polycythemic mice receiving no erythropoietin. The values represented by solid circles or squares were determined in a different experiment at a different time from the values represented by the open figures. (b) Effect of erythropoietin on the total number of cells in the above mice. The circles indicate the total cells in the irradiated polycythemic mice which received the bone-marrow transplant and erythropoietin; the squares indicate the mice receiving only the bone marrow transplant; and the triangles those mice which received neither bone marrow nor erythropoietin.

MUB-6717

than that of granulocytic cells, and that most of the weight increase observed in spleens after irradiation and transplantation of bone marrow is primarily the result of the proliferation and maturation of erythroid cells. Thus, the spleens of the polycythemic mice during the 6th to 8th day after transplantation weighed about one-half as much or less than the spleens of polycythemic mice receiving erythropoietin after transplantation. If nucleated erythroid cells are excluded, the percentage of granulocytes seen in smears of the spleens of polycythemic mice is greater in mice not receiving erythropoietin than in mice injected with erythropoietin daily. This observation is consistent with that of the cellular composition of the individual colonies in the spleen and suggests increased granulocytopoietic activity in animals where erythropoiesis is suppressed.

## DISCUSSION

**EFFECT OF ERYTHROPOIETIN ON IRRADIATED NORMAL MICE** These experiments were designed to study the role of erythropoietin in the development of spleen colonies and the growth of colony-forming cells. The observations that either the production of polycythemia or the injection of immune serum capable of neutralizing the biological effects of erythropoietin prevented the development of colonies containing erythroid cells indicate that erythropoiesis in spleen colonies is regulated by the presence of erythropoietin produced by the host, as is erythropoiesis in the normal animal. The injection of exogenous erythropoietin into normal mice following lethal irradiation and bone-marrow transplantation had little effect on the development of spleen colonies or on the magnitude of the erythropoietic activity of the host. The observation that detectable levels of erythropoietin were present relatively soon after lethal irradiation suggests that the failure of exogenous erythropoietin to modify erythropoiesis in the lethally irradiated mouse is due to the fact that the mouse is already maximally stimulated by its own high levels of endogenous erythropoietin. This is in agreement with similar conclusions by Eskuche and Hodgson (16) and Hodgson (17) based on studies in the rat.

**EFFECT OF ERYTHROPOIETIN AND ANTI-ERYTHROPOIETIN ON THE UPTAKE OF  $^{59}\text{Fe}$  IN THE PERIPHERAL BLOOD OF NONPOLYCYTHEMIC MICE** It is apparent from Fig. 2 that the  $^{59}\text{Fe}$  uptake in the blood on the 14th day after irradiation and transplantation in mice injected with serum obtained from rabbits immunized with normal human urinary proteins, or with normal rabbit serum, was less than that observed in the mice injected with erythropoietin. It is also apparent from Fig. 3 that the daily injection of exogenous erythropoietin does not increase the  $^{59}\text{Fe}$  uptake above that seen without erythropoietin -- a result also observed in the experiment tabulated in Fig. 2 but not indicated in the figure. This suggests that in mice receiving injections of normal human urinary proteins or normal rabbit serum, erythropoiesis has been partially suppressed, as the iron uptake is markedly lower than in animals either receiving erythropoietin or saline uninjected. This may be related to the presence of some antibody capable of neutralizing erythropoietin in rabbits immunized with normal human urinary proteins, i. e., it is possible that normal human urinary proteins have a small amount of erythropoietin in them which stimulates the rabbit to make in low titer an antibody against erythropoietin. It is also possible that both normal serum and serum from

rabbits immunized with normal human urinary proteins may contain substances that compete with erythropoietin.

**EFFECT OF ERYTHROPOIETIN ON IRRADIATED POLYCYTHEMIC MICE** Studies of the effects of exogenous erythropoietin on the development of spleen colonies in polycythemic hosts have yielded equivocal results. In one experiment (Fig. 5) the presence of erythropoietin in polycythemic hosts did not alter the total number of colonies found in or on the spleen, following bone-marrow transplantation, compared to the total number of spleen colonies in polycythemic hosts, not injected with erythropoietin while in the other experiment (Table 3) significantly greater numbers of colonies were observed in polycythemic hosts receiving erythropoietin. The only obvious difference between the two experiments was that in the first the recipient mice received daily injections of 1.0 cobalt units of erythropoietin while in the second 0.5 cobalt unit of erythropoietin was injected daily. It is unlikely that the differences between the results of these experiments are related to this difference in the dose of erythropoietin administered. This question could not be further investigated, since a supply of sheep plasma erythropoietin was unavailable. The important conclusion from these experiments is that the injection of erythropoietin in either experiment did not decrease the number of spleen colonies as would be expected if erythropoietin acted directly on the colony-forming cell.

Careful examination of serial sections of the spleens from the hypertransfused groups showed accumulations of undifferentiated cells, too small to be visible as macroscopic colonies, under the splenic capsule. Mitotic figures were observed in these areas. Such accumulations were not observed in the erythropoietin-injected hypertransfused mice.

Clusters of erythroid cells (about  $3 \times 10^4$  cells) were often observed within larger accumulations of mature granulocytic cells in mice infected 8 or 9 days after transplantation and sectioned on the 10th. However, other granulocytic or mixed granulocytic-megakaryocytic colonies contained no obvious erythroid cells. Accumulations of erythroid cells were also observed beneath the capsules of spleens in which discrete granulocytic or megakaryocytic cells were not observed. These observations suggest that the differences between the results of these experiments may be related to the relative growth rates of the various types of differentiated colonies compared to undifferentiated colonies. Thus, slowly proliferating colonies comprised primarily of undifferentiated cells are not easily distinguished grossly on the spleen by the 10th day after transplantation, while colonies comprised predominantly of erythroid cells are easily recognized. These results also suggest that counting of visible colonies on the surface of the spleen in experiments with polycythemic mice may be a poor method for investigating the effects of erythropoietin on colony-forming cells.

**EFFECT OF ERYTHROPOIETIN ON INCREASE IN THE NUMBER OF COLONY-FORMING CELLS IN IRRADIATED POLYCYTHEMIC MICE** The results of the previous experiments suggest that erythropoietin does have definite effects on the development of erythroid colonies, but the effect of erythropoietin on the growth of colony-forming cells themselves cannot be studied adequately by counting the number of colonies grossly visible on the

surface of the spleen, particularly in polycythemic mice. The possibility of counting the total number of colonies within the spleen utilizing serial sections of the spleen was explored; however, this method appeared to have definite limitations. The boundaries between separate colonies are frequently poorly defined and without a complete reconstruction of the spleen individual small colonies may be missed. This could be of extreme importance in determining the presence of colonies comprised exclusively of colony-forming cells. Since the doubling time of colony-forming cells is about one day, a colony composed exclusively of colony formers, if derived from a single cell, would contain less than 1,000 cells after 10 days of growth. As stated earlier, small accumulations of proliferating cells were observed under the splenic capsule of polycythemic mice 10 days after transplantation. The presence of such accumulations within the splenic parenchyma is even more difficult to detect. For these reasons the growth curve of colony formers in polycythemic mice was determined for the 10-day period following transplantation and compared with a similar curve measured in polycythemic mice given daily injections of erythropoietin (Fig. 6). The overall doubling time of colony formers in the spleen of polycythemic mice was not influenced by the presence of erythropoietin. The observation that a greater number of colony formers were found in the spleen of the erythropoietin-injected mice on the 6th day after transplantation is probably significant, and is not related to the efficiency with which colony-forming cells were extracted from the larger spleens of the polycythemic mice injected with erythropoietin, since there was a similar difference in size between the two groups on the 7th and 8th days, and there was no significant difference in the number of spleen colonies produced. This observation suggests that the presence of erythropoietin does modify the life history of the colony-forming cells. It is possible that the generation time of colony formers in the mice receiving erythropoietin is more rapid than in the absence of erythropoietin.

The changes in the total number of cells in the spleen (Fig. 6b) following the transplantation of  $2 \times 10^6$  bone-marrow cells into polycythemic hosts injected daily with erythropoietin, compared to polycythemic mice receiving no erythropoietin, are of particular interest with regard to the question of whether erythropoietin acts on the colony-forming cells themselves. Between the 4th and 6th day after transplantation there is an increase of about  $30 \times 10^6$  nucleated cells in the polycythemic mice given erythropoietin, whereas there is only a slight increase in the number of nucleated cells in the spleens of the polycythemic mice receiving no erythropoietin. Differential counts of the nucleated cells in the erythropoietin-injected mice indicated that at least  $25 \times 10^6$  erythroid cells were produced in this two-day interval. What was the source of these erythroid cells? From the growth curve of colony formers (Fig. 6a) it is evident that by the 4th day after transplantation there are only about 250 colony formers in the spleen. Assuming that the colony formers settled outside of the spleen are proliferating at a rate similar to those in the spleen, one can calculate that only about 1,000 colony formers are present in the entire host animal. Even if a generation time of 8 hr is assumed for nucleated erythroid cells, and all the colony formers in the mouse migrated to the spleen, and they were all stimulated to differentiate into erythroid cells, it would be impossible to produce the  $25 \times 10^6$  nucleated erythroid cells in two days from the differentiation of the available colony-forming cells. It is obvious that if all the colony formers were stimulated to differentiate, the replication of colony formers themselves should either be abolished

or markedly inhibited; yet, the growth curve indicates a significant increase in colony formers in the spleen during this time of increased production of nucleated erythroid cells. These observations suggest that most of the nucleated erythroid cells produced during this 2-day interval are not the result of the action of erythropoietin directly on colony-forming cells, but the result of the action of erythropoietin on much larger numbers of "erythropoietin-sensitive cells" present in the host bone marrow from the time of transplantation.

Previous experiments (18) have suggested that only a limited number of cells present in bone marrow at the time of transplantation are receptive immediately to erythropoietin stimulation. These experiments also suggested that a recruitment of erythropoietin-sensitive cells occurred following the initial exposure of the marrow to erythropoietin. It was concluded that this recruitment of cells into an erythropoietin sensitive state was due both to the division of stem cells and to the movement of cells not in a proliferative cell cycle into a receptive state. The observation that only a few nucleated erythroid cells were seen in the spleens of the transplanted mice before the 4th day suggests that even though erythropoietin is present during these first 4 days, very few erythropoietin sensitive cells are triggered to differentiate into identifiable erythroid cells. Possibly the recruitment of erythropoietin-sensitive cells is not efficient until the graft becomes adapted to the new environmental conditions of the host. Commencing on the 4th day after transplantation, relatively large numbers of "erythropoietin-sensitive cells" must be recruited for stimulation, in order to account for the marked increase in nucleated erythroid cells seen by the 6th day. This recruitment must be primarily a movement of cells into a receptive stage from a population of cells not in a proliferating cell cycle at the time of transplantation. The finding on the 6th day after transplantation that the total number of colony formers present in the spleens of polycythemic mice receiving erythropoietin is actually greater than the number of colony formers in uninjected polycythemic mice suggests that some of the "erythropoietin sensitive cells" are also derived from dividing stem cells, i.e., colony-forming cells. The removal of colony-forming cells into an erythropoietin-sensitive state is apparently detected by the colony-forming population, which increases to compensate for this removal. It is suggested that since the overall doubling time of colony formers during the first 10 days after transplantation is not altered in the presence of erythropoietin, a decrease in the generation time of colony formers may occur to compensate for the removal of colony-forming cells into the erythropoietin-sensitive state.

The colony-forming cell may either give rise to erythropoietin-sensitive cells or erythropoietin sensitivity could simply correspond to one particular stage in the life cycle of a colony-forming cell. The latter possibility would suggest that increased numbers of colony formers should be detected in hematopoietic tissue in the absence of erythropoietic activity, since colony-forming cells should pass from the erythropoietin-sensitive stage of their life cycles into stages sensitive to agents that direct differentiation into granulocytic and megakaryocytic cells, and eventually the cells should enter a stage where they replicate as colony formers. This latter possibility cannot be completely excluded at the present time, but some information contradicts this interpretation. It has been pointed out that rather large numbers of erythropoietin-sensitive cells must be present in the mouse by the 4th day after transplantation in order to account for the large numbers of erythroid cells observed in the spleen by the

6th day. If these cells were not stimulated to become erythroid cells but instead entered the other cell lines, an easily detectable increase in granulocytic, megakaryocytic or colony-forming cells should be observed. Some evidence for an increase in granulocytic and megakaryocytic colonies was observed (Table 2), but in all experiments no evidence for an increase in colony-forming cells was seen. It should be emphasized that this evidence for an increased granulocytopoiesis is based on counts of microscopic foci of hematopoietic cells which may or may not be equivalent to macroscopic colonies. There is no evidence available at the present time indicating that the microscopic foci are capable upon retransplantation of forming colonies, an essential prerequisite in the assumptions that a colony-forming cell is equivalent to a stem cell. Liron and Feldman (19) have also recently reported an increased incidence of granulocytic colonies in polycythemic animals. Five days after transplantation of  $60 \times 10^4$  bone-marrow cells, large numbers of small foci of erythroid cells are seen in sections of the spleen. If these foci continued proliferating a much larger number of colonies should be visible in the spleen by the 10th day after transplantation than are in fact seen. It is concluded that these erythroid foci were derived from erythropoietin-sensitive cells in the initial inoculum which have a limited proliferative capacity. These cells apparently mature upon stimulation, leave the spleen and do not give rise to colonies detectable by the 10th day after transplantation.

The development of erythroid colonies by the 10th day in polycythemic hosts when erythropoietin was injected on the 8th or 9th day after transplantation suggests that erythropoietin-sensitive cells are continually derived from colony-forming cells even in the absence of erythropoietin. When erythropoietin was injected late after the transplantation of bone marrow, erythroid colonies were seen within well developed colonies containing mature granulocytes, and in areas under the splenic capsule where no other mature hematopoietic cells were evident. Colonies containing mature granulocytic cells were also seen which did not become erythroid. In polycythemic hosts that did not receive erythropoietin, small accumulations of proliferating cells were observed; presumably these accumulations contain erythropoietin-sensitive cells. Were these cells derived from erythropoietin-sensitive cells in the initial inoculum or from colony-forming cells that proliferated and gave rise to erythropoietin-sensitive cells? This question cannot be satisfactorily answered at the present time, but it is probable that the erythropoietin-sensitive cells were derived from proliferating colony formers rather than from proliferating erythropoietin-sensitive cells.

Thus it is concluded, in agreement with Bruce and McCulloch (7) that erythropoietin does not act directly on the colony-forming cell, but upon some cell that is derived from the colony-forming cell. The stimulation of "erythropoietin-sensitive cells" to differentiate into erythroid cells seems to be detected in some manner by the colony-forming cell population and more colony-forming cells are recruited into the "erythropoietin-sensitive cell" population. The presence of an appreciable "erythropoietin-sensitive cell" population in a bone-marrow population probably assists in protecting the colony-forming cell population from being exhausted during the early stages of repopulation of hematopoietic tissue.

IDENTIFICATION OF COLONY-FORMING CELL OR ERYTHROPOIETIN-SENSITIVE CELL The morphological identity of the colony-forming cell and the erythropoietin-sensitive



cell remains unknown. It has been reported previously (20) that the lymphocyte-like cells of the mouse bone marrow had a different pattern of labeling following a single injection of tritiated thymidine than lymphocytes in the blood, lymph or lymphoid tissue. Schooley and Giger (21) suggested on the basis of autoradiographic observations of the marrow of polycythemic mice injected with tritiated thymidine and erythropoietin that these small round or lymphocyte-like cells were probably stem cells. Osmond and Everett (22) presented evidence that the lymphocyte-like cells of the bone marrow are produced as a result of the proliferation of precursor cells present in the bone marrow. Cudkowicz *et al.* (23) utilizing the uptake of the specific DNA analogue, 5-iodo-2'-deoxyuridine-<sup>125</sup>I, measured the proliferative capacity, five days after transplantation of fractions of bone-marrow cells and observed that the proliferative capacity was a function of small and medium "lymphocytes" present in the marrow suspensions. Mel and Schooley (24), in contrast, did not observe a correlation between the transplantation of bone-marrow fractions containing large numbers of small round lymphocyte-like cells and the development of spleen colonies by the 8th or 10th day after transplantation. If the interpretation of the present experiments is correct, it would seem likely that the "erythropoietin-sensitive cell" may correspond to the lymphocyte-like cell of the bone marrow, and the differentiation and proliferation of these cells may be responsible for the proliferative capacity measured by Cudkowicz *et al.* (23) on the 5th day. The lack of a correlation between small round lymphocyte-like cells and the development of spleen colonies suggest that the colony-forming cell is either only a small proportion of these cells or a completely different cell. The colony-forming cell is then envisaged as a cell that gives rise to the small round lymphocyte-like cell which, in turn, is sensitive to differentiative agents directing its division and maturation.

## SUMMARY

The development of erythroid colonies in the spleens of lethally irradiated mice following bone-marrow transplantation was suppressed by the production of polycythemia or the injection of antibody against erythropoietin into the host mice. The injection of exogenous erythropoietin into nonpolycythemic animals did not increase the number of spleen colonies produced by a bone-marrow transplant. The injection of exogenous erythropoietin into polycythemic host mice in some experiments did not significantly alter the number of colonies produced by a bone-marrow transplant, whereas in other experiments a marked increase in the number of spleen colonies occurred. The discrepancy between these experiments is discussed. The overall doubling time of colony-forming cells in the spleens of polycythemic mice was not altered by the injection of exogenous erythropoietin during the first 10 days after bone-marrow transplantation. Some evidence is presented suggesting that the doubling time of colony-forming cells in polycythemic mice receiving erythropoietin was maintained equal to that observed in polycythemic mice not receiving erythropoietin by some change in the proliferation of colony-forming cells. Arguments are presented suggesting that erythropoietin does not act on the colony-forming cell directly, but upon some "erythropoietin-sensitive cell" derived from the colony-forming cell.

## ACKNOWLEDGMENTS

The author wishes to express his appreciation for valuable technical assistance of Virginia W. Havens and Linda N. Cantor.

This work was supported in part by the U. S. Atomic Energy Commission and in part by Cancer Research Funds of the University of California.

## REFERENCES

1. Till, J. E., and McCulloch, E. A.; *Radiation Res.*, 14: 213-222, 1961.
2. McCulloch, E. A., and Till, J. E.; *Radiation Res.* 16: 822-832, 1962.
3. Duplan, J. F.; *Compt. Rend. Soc. Biol.*, 23: 286-289, 1963.
4. Goodman, J. W.; *Transplantation* 1: 334-346, 1963.
5. Goodman, J. W., and Hodgson, G. S.; *Blood* 19: 702-714, 1962.
6. Cole, L. J.; *Am. J. Physiol.*, 204: 265-267, 1963.
7. Becker, A. J.; McCulloch, E. A., and Till, J. E.; *Nature* 197: 452-454, 1963.
8. Welshons, W. J.; *Mammalian Cytogenetics and Related Problems in Radiobiology*. Oxford, Pergamon Press, 1964, pp. 233-243.
9. Bruce, W. R., and McCulloch, E. A.; *Blood* 23: 216-232, 1964.
10. DeGowin, R. L.; Hofstra, D., and Gurney, C. W.; *J. Lab. Clin. Med.* 60: 846-852, 1962.
11. Schooley, J. C., and Garcia, J. F.; *Blood* 25: 204-217, 1964.
12. Siminovitch, L.; McCulloch, E. A., and Till, J. E.; *J. Cell. Comp. Physiol.* 62: 327-336, 1963.
13. McCulloch, E. A., and Till, J. E.; *Radiation Res.* 22: 383-397, 1964.
14. Schooley, J. C.; *Exptl. Haematol.* 7: 79, 1964.
15. Curry, J.; Trentin, J., and Wolf, N.; *Exptl. Haematol.* 7: 80, 1964.
16. Eskuche, I., and Hodgson, G.; *Acta Physiol. Lat. Amer.* 12: 282-290, 1962.
17. Hodgson, G. S.; *Blood* 19: 460-467, 1962.
18. Schooley, J. C.; *Blood* 25: 795-808, 1965.
19. Liron, M., and Feldman, M.; *Transplantation* 3: 509-516, 1965.
20. Schooley, J. C.; Bryant, B. J., and Kelly, L. S.; in *The Kinetics of Cellular Proliferation*, edited by F. Stohlman, Jr., New York, Grune & Stratton, 1959, pp. 208-217.
21. Schooley, J. C., and Giger, C. K.; *Semiannual Report, Donner Laboratory, Lawrence Radiation Laboratory, UCRL-10683*, 176-179, 1962.
22. Osmond, D. G., and Everett, N. B.; *Blood* 23: 1-17, 1964.
23. Cudkowicz, G.; Bennett, M., and Shearer, G. M.; *Science* 144: 866-868, 1964.
24. Mei, H. C., and Schooley, J. C.; in *Actes du Colloque International C.N.R.S. sur "La Greffe des Cellules Hématopoiétiques Allogéniques"*, edited by G. Mathé, J. L. Amiel, and L. Schwarzenberg, Paris, Editions du Centre National de la Recherche Scientifique, 1965, pp. 221-223.

# Influence of Severe Hypoxia on Human Erythropoietin

N67 15946

William E. Siri

The total volume of red blood cells in the healthy person is controlled by the production of red cells whose rate, according to prevailing evidence, is mediated by erythropoietin. Whether or not primary control of erythropoiesis normally is vested in blood oxygen tension is not certain. It is clear, however, that low oxygen tension stimulates erythropoiesis to maintain a compensatory increase in red-cell volume that is related, in an ill-defined way, to degree of hypoxia.

The most comprehensive studies on hematological responses to hypoxia in humans have been those conducted at Morococha, Peru (alt., 14,900 ft;  $P_B$ , 430.6 mm Hg); notably by Hurtado *et al.* (1), Merino (2), Lawrence, Huff, and associates (3, 4), and Reynafarje (5). At this altitude red-cell volume is 50% greater, and plasma-iron turnover is 25% faster than at sea level. Red-cell life span (5, 6) and hemoglobin content appear to be normal.

No investigations comparable to those at Morococha have been conducted, to the author's knowledge, at high altitudes (greater than 15,000 ft), and little has been reported on human erythropoietic activity at intermediate altitudes. In prolonged exposure to severe hypoxia, one may reasonably expect the erythropoietic system to be heavily taxed and its responses more decisive. The influence of hypoxia on the regulation of red-cell volume was therefore investigated in human subjects exposed to oxygen partial pressures ranging from 160 mm Hg (sea level) to 69 mm Hg (21,500 ft). Plasma-iron turnover, blood volume and the ordinary hematological quantities were measured in Andean residents of 12,500 and 17,000 ft, and in climbers at sea level, at 17,800 ft and at 21,500 ft, during an ascent of Mt. Everest.

## METHODS

All subjects were healthy men screened by physical examination, chest X ray, and E. C. G. None had a recent history of blood loss, and all were lean in body composition.

Subjects for the studies at altitudes of 17,800 ft and higher were Caucasian members of the 1963 American Mt. Everest Expedition, 26 to 44 years of age. Base-line values for these subjects were determined at Donner Laboratory (sea level), a month prior to the expedition's departure. The month-long hike to Mt. Everest exposed the climbers gradually to progressively higher altitudes, ensuring partial acclimatization on arrival at the base of operations at 17,800 ft. During the succeeding 63 days on the mountain, climbers spent an average of 30 days at 17,800 ft ( $P_B$ : 383 mm Hg) and 33 days at 21,000 ft ( $P_B$ : 328 mm Hg). The latter period included short trips at higher altitudes (see Fig. 2). Beyond 23,000 ft,

supplemental oxygen provided by an open-circuit breathing apparatus was used while climbing and sleeping. Such excursions were infrequent for any one climber and ranged from one to five days.

Subjects studied at 12,500 ft ( $P_B$ : 474 mm Hg) were young male residents of La Paz, Bolivia. Four Indian miners served as subjects at 17,000 ft, an altitude to which they were acclimatized by 2- to 10-years residence. The studies in Bolivia were conducted at the General Hospital, La Paz, through the courtesy of its Director, Dr. Jorge Ergueta, and at the Laboratory for Cosmic Ray Physics, Chacaltaya (17,000 ft), through the courtesy of the Director, Professor Ismael Escobar.

Plasma volume and plasma iron-turnover were measured with  $^{59}\text{Fe}$ -labeled plasma from the subject. In the Bolivian subjects, red-cell volume was measured directly with  $^{32}\text{P}$ -labeled red cells, but in the Mt. Everest climbers it was derived from the plasma volume and venous hematocrit. Hemoglobin concentrations in the Mt. Everest climbers were determined from finger-tip blood samples with a Coleman No. 25 photohemoglobinometer by the cyanmethemoglobin method. A calibration of  $\pm 0.25$  g/100 ml was maintained in the field with four sealed hemoglobin standards. Capillary tubes were used for micro-hematocrit determinations. For the Bolivian subjects, a Coleman Junior Spectrophotometer and Wintrobe tubes were used for hemoglobin and hematocrit determinations. Blood smears from finger-tip blood were stained with Wrights stain for leucocyte differential counts. Red-cell, white-cell and platelet counts were determined by conventional methods.

Erythropoietin was extracted from 24-hr urine collections by adsorption on collodion membranes (7). Membranes were prepared in advance of the Expedition's departure and stored in distilled water until used. Membranes for the Bolivian studies were freshly prepared as needed. After processing a urine collection, the membrane was dissolved in ether, centrifuged and the solids dried and sealed under nitrogen. Samples were later assayed at Donner Laboratory by the method of DeGown *et al.* (8) (red-cell incorporation of  $^{59}\text{Fe}$  in hypertransfused mice) under the supervision of Dr. D. C. Van Dyke.

Measurements of total-body water were useful for assessing the state of hydration, which, if greatly altered, could influence hemoglobin concentration independently from total hemoglobin. Total-body water was measured in all the subjects with tritiated water, and for the Mt. Everest climbers, these determinations were made prior to the Expedition's departure and repeated near the end of the Expedition when hemoglobin concentrations were at their highest value.

## RESULTS

**PLASMA-IRON TURNOVER** The results of these tests on the climbers and the Bolivian subjects are presented in Table 1. The average values are plotted against altitude in Fig. 1, together with turnover rates reported by Huff *et al.* (4) and Reynafarje *et al.* (5) for acclimatized subjects at sea level and 14,900 ft. Huff's values have been adjusted as explained in the Discussion. The average value of 0.43 mg/kg/day for plasma-iron turnover in the

Table 1. Blood volume and plasma-iron turnover in Mt. Everest climbers and in Andean residents at 12,500 and 17,000 ft

Subject	Alt. 1000 ft	Wt. kg	Hct %	Pl. Vol. ml/kg	R. C. V. ml/kg	Pl. Fe μg/100 ml	Pl Fe rate mg/kg-day
Mt. Everest climbers							
A	0	65.8	48	38.9	35.9	112	0.38
	17.8	63.2	53	40.0	45.0	100	1.15
B	0	91.0	46	37.5	32.0	88	0.43
	21.5	80.6	61	40.0	62.5	93	1.17
C	0	68.9	45	37.9	30.9	114	0.42
	17.8	63.6	53	40.0	45.2	68	0.75
	21.5	61.0	67	29.8	60.6	167	1.31
M	0	93.2	42	34.7	25.2	142	0.47
	17.5	81.6	62	30.5	48.8	82	0.80
Av	0	78.5	45	37.6	31.1	114	0.43
Av	17.5	69.5	56	36.8	44.8	83	0.90
Av	21.5	70.8	64	35.6	61.5	130	1.24
Residents, 12,500 ft							
Sa	12.5	64.5	51	40.4	41.0	62	0.45
Pe	12.5	49.8	53	41.0	43.0	117	0.61
Va	12.5	56.7	51	42.5	43.8	83	0.53
Me	12.5	51.0	49	37.7	36.5	75	0.47
Av	12.5	55.5	51	40.4	41.1	84	0.52
Residents, 17,000 ft							
Th	17	54.0	57	40.8	54.0	---	---
Ca	17	55.5	60	32.7	49.3	76	0.88
Ch	17	60.5	58	40.4	55.6	96	0.94
To	17	62.0	57	40.6	53.3	94	1.15
Av	17	58.0	58	38.6	53.1	89	0.99

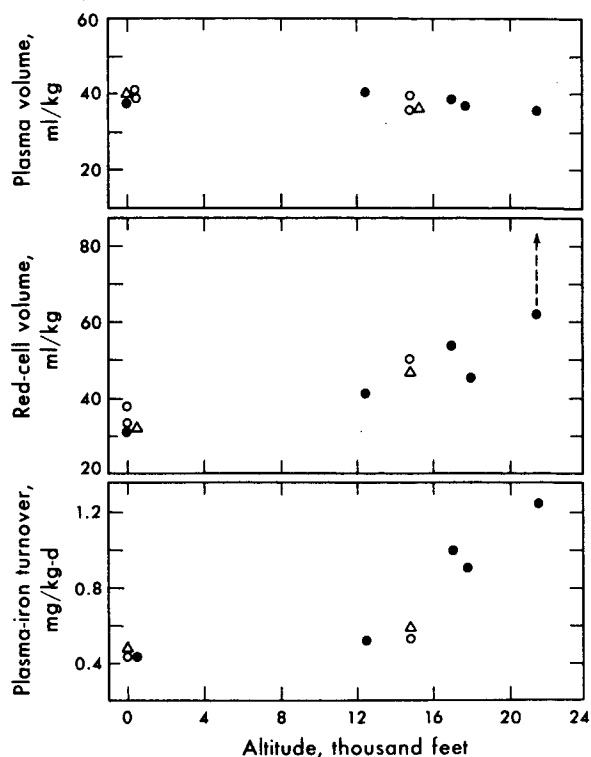


Figure 1. Plasma and red-cell volumes, and plasma-iron turnover in high altitude residents and climbers. Average values from this study are shown by solid points. Open circles represent values from Reynafarje et al. (5) with red-cell volumes adjusted to hematocrits corrected for trapped plasma. Triangles represent data from Huff et al. (3, 4) with plasma-iron turnover adjusted as explained in the text. The vertical dashed line indicates average red-cell volume attained by climbers in six weeks at high altitude. MUB-12205

climbers at sea level is identical to that reported by Reynafarje and consistent with Huff's corrected value. A week after arriving at 17,800 ft (two weeks at altitudes greater than 15,000 ft), the turnover rate of 0.90 mg/kg/day in the climbers was double the rate seen in the same subjects at sea level. Two weeks after arriving at 21,500 ft, the iron-turnover rate was three-fold greater, or 1.24 mg/kg/day.

In Bolivian residents at 12,500 ft, the turnover rate of 0.52 mg/kg/day represents a 20% increase over sea-level values for similar subjects in earlier studies and is consistent with the increase of 25% reported for residents at 14,900 ft (3, 4, 5). The plasma-iron-turnover rate of 0.99 mg/kg/day in Bolivian residents at 17,000 ft is substantially higher than anticipated from the values prevailing at lower altitudes and is comparable to rates seen in persons during the early stage of acclimatization to 14,900 ft.

Plasma-iron concentrations in all the subjects were within the range that is generally considered normal for adult males at sea level. The decrease from 114 to 83  $\mu\text{g}/100\text{ ml}$  plasma in the climbers after two weeks at altitude and the subsequent rise to 130  $\mu\text{g}/100\text{ ml}$  are consistent with changes reported in earlier studies cited.

**HEMOGLOBIN CONCENTRATION** Hemoglobin concentrations in twelve climbers, and grouped average values during the ascent of Mt. Everest are presented in Fig. 2. During the four-week approach march, which involved gradual ascent from sea level to 17,800 ft,

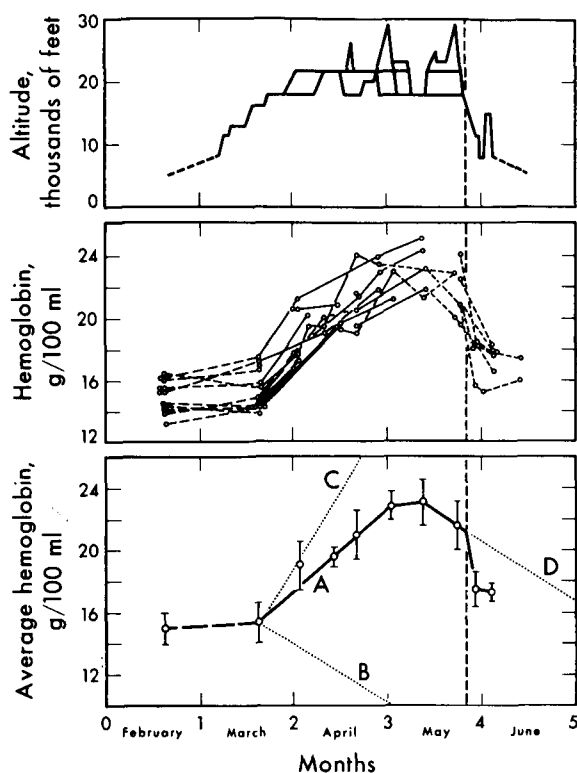
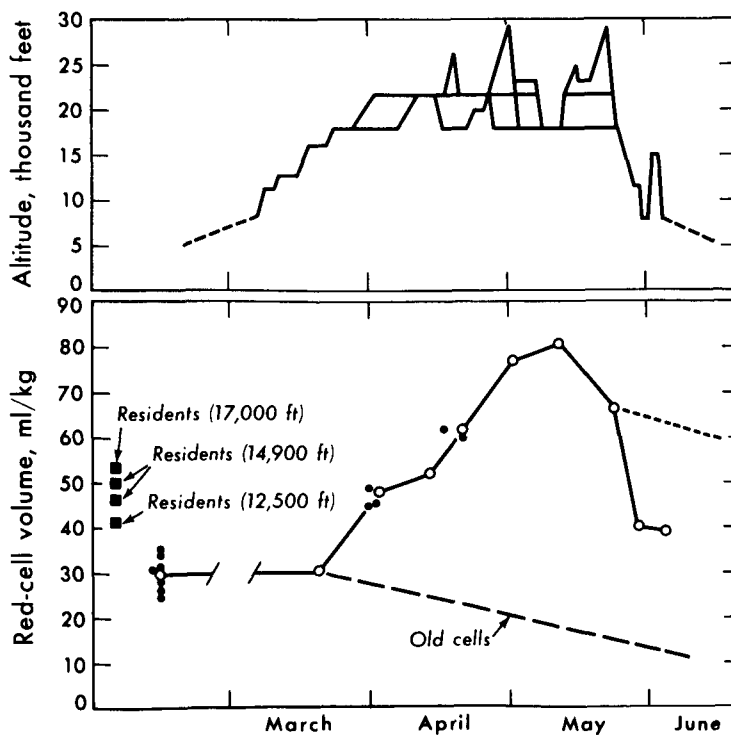


Figure 2. Changes in altitude and in individual and mean hemoglobin concentration during the Mt. Everest Expedition. Average values of hemoglobin concentration for the group are plotted in the bottom panel, line A, with S. D. indicated by bars. Line B represents loss of "old" hemoglobin; line C, the net addition to the circulation of "new" hemoglobin; and line D, the expected reduction in hemoglobin concentration following descent from high altitudes assuming a normal red-cell life span.

MUB-9898

Figure 3. Red-cell volume in Mt. Everest climbers. Solid points are individual measurements; squares are averages for residents at indicated altitudes. Red-cell volume estimated from average hemoglobin concentration in the climbers is represented by open circles. The dashed line represents normal loss of red cells formed prior to stimulated erythropoiesis, and the dotted line indicates expected loss in volume following descent to low altitude.

MUB-12206



hemoglobin concentration changed little from the group average of 15.0 g/100 ml at sea level. After arrival at 17,800 ft, hemoglobin concentration increased at a relatively uniform rate of 0.18 g/100 ml/day for the next 40 days before it showed a tendency to stabilize at a value between 23 and 24 g/100 ml. The maximum hemoglobin concentration observed was in excess of 25 g/100 ml, and in all climbers it exceeded 21 g/100 ml sometime during the expedition.

The apparent drop in concentration while the Expedition was still on Mt. Everest is a consequence of measuring at that point only those climbers encamped at 17,800 ft. However, when the expedition left Mt. Everest and descended rapidly to lower elevations, hemoglobin concentration responded immediately by decreasing from a mean value well over 22 g/100 ml for the whole group (21.6 g/100 ml for the climbers at 17,800 ft) to 17.5 g/100 ml in less than nine days.

The values of hemoglobin concentration and hematocrit in both the climbers and the Bolivian subjects adhered closely to a ratio of 3.0, indicating a relatively constant red-cell hemoglobin content of 36.4 g/100 ml of red cells in all the subjects.

**BLOOD VOLUME** Red-cell and Plasma volumes are presented in Table 1 and summarized in Fig. 1, along with comparable data from Huff *et al.* (4) and Reynafarje *et al.* (5), for comparison of values as a function of altitude. Since the subjects in this and the other studies cited were relatively lean, there is good agreement among the studies on the values of blood volumes at sea level. For the climbers the preexpedition red-cell and plasma volume averaged 31.1 and 37.6 ml/kg, respectively.

The average red-cell volume of 41.1 ml/kg for residents of 12,500 ft is about one third greater than the average volume in comparable Peruvian subjects at sea level (4, 5), and in the climbers. As may be seen from Fig. 1 this is consistent with the 50% increase observed in residents of 14,900 ft. In the four Bolivian residents of 14,900 ft, the volume was 53.1 ml/kg or about 65% greater than the average volume at sea level.

Measurements in the climbers at altitude were made at times when red-cell volumes were still increasing rapidly and therefore do not represent the steady-state values for the respective altitudes at which they were determined. However, the volumes, although transient, were necessary to validate estimates of changes in red-cell volume based on changes in hemoglobin concentration during the expedition. In Fig. 3, the curve of estimated average values shows red-cell volume increasing at the rate of about 1 ml/kg/day to a maximum volume of 80 ml/kg, or two and a half times the sea level average after seven weeks at high altitude.

Plasma volumes from this and other studies shown in Fig. 1 indicate that a slight though definite decrease in volume accompanies the development of polycythemia induced by hypoxia. At most, the reduction appears to be less than 10% in acclimatized subjects. In the climbers the reduction was about 5% at the time of measurement. The relative constancy of the plasma volume in the climbers is consistent with the measurements on total-body water.



Table 2. Leucocyte differential count. The table lists average percentages of leucocytes in Mt. Everest climbers

Cell	Pre-expedition	Expedition	Post-expedition
Segmented	58	60	56
Band cell	< 1	2	2
Eosinophil	3	2	4
Basophil	< 1	< 1	< 1
Lymphocyte	34	32	32
Monocyte	5	4	6

In seven climbers tested after two months at high altitude, when hemoglobin concentration was highest, the average total-body water was only one liter less than the 46.5 liter at sea level.

**LEUCOCYTE COUNTS** During the two months that the climbers were at high altitude on Mt. Everest, leucocyte counts remained within the range 5,000 to 11,500 cells/mm<sup>3</sup>. No significant changes in differential counts were observed as may be seen in Table 2. The apparent small reduction in eosinophil count is not statistically significant. Leucocyte counts, both total and differential, in the Bolivian subjects were in the normal range.

**ERYTHROPOIETIN** Urine collections for erythropoietin assay were obtained from three subjects after 5, 20, and 29 days at 21,500 ft, and from two subjects after 5 days at 23,000 ft. Erythropoietin was also assayed in collections from three Bolivian subjects who had lived at 17,000 ft for two or more years. None of the concentrates prepared from these collections contained detectable quantities of erythropoietin.

## DISCUSSION

Comparing the findings in the Bolivian residents at 12,500 ft with those of earlier studies in similar subjects, (young, lean, male adults) at sea level and 14,900 ft, suggests that to a first approximation red-cell volume, erythropoietic activity and plasma iron-turnover rate increase uniformly but moderately with altitude within this range. The fraction of the measured plasma-iron turnover directly utilized for hemoglobin synthesis also appears to increase directly with altitude. This fraction may be estimated from the data summarized in Fig. 1 for a red-cell hemoglobin content of 36.4 g/100 ml red cells, 3.4 mg Fe/g Hb, and a normal red-cell life span of 120 days. On this basis about 75% of the observed plasma-iron turnover is diverted directly to hemoglobin synthesis at sea level, 85% at 12,500 ft, and 100% at 14,900 ft.

For high altitudes (greater than 15,000 ft), the data presented here, although too limited to support definite conclusions, suggest that red-cell volume and erythropoietic activity follow different relationships both to each other and to altitude. The first indication of this appears in the Bolivian residents at 17,000 ft, in whom red-cell volume was 65% larger

and plasma-iron turnover 100% greater than in sea level residents. These values are larger than would be anticipated from simple projection of values at lower altitudes. Compared to residents at 14,900 ft, in whom the whole of the plasma-iron turnover seems diverted directly to hemoglobin synthesis, the subjects at 17,000 ft appear to utilize only half the iron turnover for this purpose if it is assumed that the red-cell life span is normal.

In the Mt. Everest climbers, direct measurements of blood volume and iron turnover are too few in number to characterize adequately the responses to extreme hypoxia. However, estimates of red-cell volume and rate of red-cell production can be derived from the changes in hemoglobin concentration. It is necessary to assume for this purpose that plasma volume is essentially constant at 36 ml/kg. The validity of this assumption is supported by the  $^{59}\text{Fe}$  measurements of plasma volume and indirectly by the constancy of total-body water. This does not rule out the possibility that plasma volume continued to diminish with increasing polycythemia, but a further reduction of more than 10% seems unlikely. With the red-cell-hemoglobin content expressed as 36.4 g/100 ml cells, and a red-cell density of 1.1 g/ml, red-cell volumes plotted in Fig. 3 were estimated from the formula  $\text{RCV} = 36 \text{ Hb} / (33.3 - \text{Hb})$  ml/kg in which Hb is expressed as g/100 ml.

During the first 52 days on Mt. Everest, hemoglobin concentration increased from 15.3 to 23 g/100 ml, corresponding to an increase in red-cell volume from 31 (measured) to 8.15 ml/kg (estimated), or an average rate of increase of 0.94 ml/kg/day. At the same time, old cells formed prior to stimulated erythropoiesis and which constituted the original volume of 31 ml/kg, were disappearing from the circulation at the rate of 0.26 ml/kg/day, (dashed line in Fig. 3). Thus the rate of production of new cells during this period would be 1.2 ml/kg/day. The corresponding rate of hemoglobin synthesis is 0.43 g/kg/day, or five times the rate at sea level, for which 1.48 mg Fe/kg/day would be required. The estimated rate of iron utilization is substantially greater than the observed rates of plasma-iron turnover, which averaged 1.04 mg/kg/day for the five determinations made during this period of accelerated erythropoiesis. No explanation for the discrepancy is offered. Although it suggests an overestimate of 50% in red-cell-production rate, this large an error seems unlikely in view of the agreement between measured and estimated red-cell volumes.

The precipitous drop in hemoglobin concentration that accompanied descent of the climbers from Mt. Everest is significant because it is not easily explained by hemodilution, and it is far too rapid to be accounted for by complete cessation of erythropoiesis. The reduction from a concentration greater than 22 g/100 ml, by an unknown amount, to 17.5 g/100 ml in nine days or less, which corresponds to an estimated rate of reduction in red-cell volume in excess of 2.2 ml/kg-day, would have called for a 50% increase in plasma volume. Evidence for anything more than 10% is negative. Moreover, it would lead to the untenable conclusion that there was an inconsequential increase in red-cell volume during the preceding two months at high altitude.

At that point in time, 80% or more of the red-cell volume consisted of cells produced in the preceding 65 days. The major part of the volume therefore consisted of a disperse

cohort of relatively young cells, the oldest of which had attained only half the life span of normal cells. This large fraction of the red-cell volume should have remained relatively constant in volume for about 30 days following the climber's descent to low altitudes, assuming a normal life span for these red cells. With complete inhibition of erythropoiesis, which was possible under the circumstances, the total hemoglobin concentration and red-cell volume for a month after the descent from Everest should have decreased slowly and only as a consequence of the continued normal loss of the small remaining fraction of old cells formed prior to the ascent. This would have reduced the hemoglobin concentration about 0.6 g/100 ml and red-cell volume about 2.34 ml/kg in the nine days between observations, (dashed lines in Figs. 2 and 3). In contrast, the observed hemoglobin loss was 4.5 g/100 ml and the estimated red-cell reduction, 29.7 ml/kg.

Although the evidence presented is meager it raises a reasonable doubt about the life span of human red cells formed during high rates of erythropoiesis stimulated by severe hypoxia. Studies on animals show a marked reduction on red-cell life span when the cells are formed during times of intense erythropoietic activity. Neuberger and Niven (9) found a reduction of 30 to 50% for red cells produced in rabbits after bleeding. Berlin and Lotz (10) also found that acute hemorrhage causes a reduction in red-cell life span in the rat. A similar effect was observed by Fryers and Berlin (11) in hypoxic rats in the initial stage of acclimatization. Similar results were reported by Stohlman *et al.* (12) for rats following bleeding, or treatment with phenylhydrazine, or massive doses of erythropoietin.

Although the suggestion has been advanced that iron deficiency may have been responsible for the results in some of the foregoing studies, this criticism does not seem to be valid for the Mt. Everest climbers and Bolivian residents at 17,000 ft, in whom plasma iron concentrations were normal. This is further supported by Hornbein's observation (13) that hemoglobin levels in high-altitude climbers given iron supplement were no different from the levels in their companions who served as controls.

The possibility of shortened red-cell life span in residents at 17,000 ft is suggested by the relationship between the observed red-cell volume and plasma-iron turnover. On the basis of a 120-day life span, only 55% of the measured iron turnover was directly utilized for hemoglobin synthesis. Although this could be considered within normal limits at sea level, it is not characteristic for high altitude. A reduction of about 40% in life span of cells formed at 17,000 ft would be required to account for the expected complete diversion of the plasma-iron turnover to hemoglobin synthesis.

A recent study by Van Dyke *et al.* (14) may have a significant bearing on this question. They found Bolivian residents at 17,000 ft (Chacaltaya) excreted erythropoietin at a rate 20 times greater than humans at sea level. If, as some studies seem to indicate, shortened red-cell life span is sometimes associated with high levels of erythropoietin. Van Dyke's finding reinforces the possibility that a similar effect occurred in our high altitude subjects. A survival curve such as that reported by Stohlman *et al.* (12) for red cells in the rat following administration of large doses of erythropoietin would explain the abrupt drop in hemoglobin

concentration in the climbers when they descended to low altitudes. Our failure to detect erythropoietin in urine collections taken at high altitude is attributed in part to faulty preparation of the concentrates but primarily to their deterioration during several months storage before they could be assayed.

Healthy persons acclimatized to moderate altitudes (less than 15,000 ft) do not normally exhibit leucocytosis nor thrombocytosis (1, 3, 4) although temporary leucocytosis has been observed in the early stage of acclimatization (1). The findings in this study bear out these observations. No meaningful changes in either total or differential leucocyte counts were seen during extended exposure to high altitude. In contrast, climber "A", Table 1, on acute exposure to severe hypoxia for four days in a low pressure chamber preceeding the expedition developed a moderate but significant leucocytosis and thrombocytosis with a depression in eosinophil concentration (15).

## ACKNOWLEDGMENTS

The author gratefully acknowledges the support and encouragement of Dr. John H. Lawrence, Director of Donner Laboratory and Donner Pavilion. For the work in Bolivia, appreciation is expressed for the invaluable assistance of Dr's. Mario Iturraldi, Ovidio Suarez, Nicanor Machicao, Jorge Ergueta, Ismael Escobar, Luis Alexander, Luis Calderon, Luis F. Hartmann, and Mr. Carlos Cardoza.

These studies were supported primarily by the U. S. Atomic Energy Commission. Additional support for the studies on Mt. Everest was received from the National Science Foundation, National Aeronautics and Space Administration and the Air Force Office of Scientific Research.

## REFERENCES

1. Hurtado, A.; Merino, C., and Delgado, E.; Arch. Inter. Med. 75:284-323, 1945.
2. Merino, C. F.; J. Hematol. 5:1-31, 1950.
3. Lawrence, J. H.; Huff, R. B.; Siri, W. E.; Wasserman, L. R., and Hennessy, T. G.; Acta Med. Scand. 142:117-131, 1952.
4. Huff, R. L.; Lawrence, J. H.; Siri, W. E.; Wasserman, L. R., and Hennessy, T. G.; Medicine 30:197-217, 1951.
5. Reynafarje, C.; Lozano, R., and Valdivieso, J.; Blood 14:433-455, 1959.
6. Reynafarje, C.; Berlin, N. I., and Lawrence, J. H.; Soc. Exptl. Biol. Med. 87:101-102, 1954.
7. Van Dyke, D. C.; in Haemopoiesis, edited by G. Wolstenholme and M. O'Connor, London, J. and A. Churchill, Ltd., 1960, pp. 397-417.
8. DeGowin, R. L.; Hofstra, D., and Gurney, C. W.; Proc. Soc. Exptl. Biol. Med. 110:48-51, 1962.
9. Neuberger, A., and Niven, J. S. F.; J. Physiol. 112:292-310, 1951.
10. Berlin, N. I., and Lotz, C.; Proc. Soc. Exptl. Biol. Med. 78:788-790, 1952.
11. Fryers, G. R., and Berlin, N. I.; Am. J. Physiol. 171:465-470, 1952.

12. Stohlman, F., Jr.; Brecher, G., and Moores, R. R.; in Erythropoiesis, edited by L. O. Jacobson and M. Doyle, New York, Grune and Stratton, 1962, 162-172.
13. Hornbein, T. F.; J. Applied Physiol. 17:243-245, 1962.
14. Van Dyke, D. C.; Nohr, M., and Lawrence, J. H.; Erythropoietin in the Urine of Normal and Erythropoietically Abnormal Human Beings. Blood, in press.
15. Siri, W. E.; Van Dyke, D. C.; Winchell, H. S.; Pollycove, M.; Parker, H. G., and Cleveland, A. S.; J. Applied Physiol. 21: 73-80, 1966.

# Studies on the Thymus and the Recirculating Lymphocyte Pool

N67 15947

John C. Schooley and Marvin M. Shrewsbury

Considerable evidence has accumulated to indicate that the thymus has a unique role in the physiology of lymphoid tissue and in the ontogeny of the immune response. Removal of the thymus in young rodents results in a decreased hourly output of lymphocytes from the thoracic duct (1), a diminished lymphocyte population in the blood and lymph nodes (2-4), a severe depression in immunologic responsiveness (5-7) and a progressive wasting (or runting) disease (8). The magnitudes of these various responses are related to the age of the animal at the time of thymus removal. A pronounced decrease in the hourly output of lymphocytes from the thoracic duct occurs following thymectomy in young adult animals (9, 10, 3); but the other alterations found after neonatal thymectomy are either lacking or minimal.

Several lines of evidence suggest that only insignificant numbers of lymphocytes produced in the thymus are released directly into the thoracic duct. Initially Gowans (11) and, more recently, other investigators (1, 12) have presented evidence in favor of the concept of an extensive recirculation of lymphocytes. Schooley and Kelly (1) proposed an explanation of their observed decrease in thoracic duct lymphocyte output following thymectomy in terms of this concept of lymphocyte recirculation. We suggested that normally the thymus contributes significant numbers of lymphocytes to the recirculating lymphocyte pool. Removal of the thymus removes this source of cells and thus decreases the number of recirculating lymphocytes. This decrease is then reflected in a decreased output of thoracic-duct lymphocytes.

In previous experiments the thoracic duct outputs had been determined several months after thymectomy; therefore, we studied in the current experiments the temporal relationships between thymectomy and the first indication of a depression in thoracic duct lymphocyte outputs. In addition, the effects of transplantation of thymic tissue on the thoracic duct lymphocyte outputs were investigated. Also, we have studied the effect of altering the total recirculating lymphocyte pool, utilizing the technique of parabiosis.

## MATERIALS AND METHODS

Specific-pathogen-free male Buffalo rats were thymectomized or sham-operated at about 25 days of age. Thymectomy was performed under ether anesthesia. NIH male Webster mice about four weeks of age (approximately 18 g) were thymectomized or sham-operated. The completeness of thymectomy was determined at autopsy. Any animal that failed to gain weight, showed signs of infection, or contained thymic remnants was discarded. Two weeks after thymectomy animals were paired by weight and parabiosed under sodium pentobarbital anesthesia by a union of skin and body wall without coelio-anastomosis. The normal diet was

supplemented with a liquid diet containing about 1% terramycin until the skin wound healed. Parabionts were divided into groups of intact-intact, intact-thymectomized, and thymectomized-thymectomized partners. Control groups of single thymectomized or sham-thymectomized animals were sham-parabiosed, i. e., the skin incision was made.

Thoracic duct cannulations were performed on individual rats by the technique described by Reinhardt (13). Lymph was collected for at least 90 min from each animal during the morning hours in order to avoid possible diurnal variations. A group of rats was cannulated one week after thymectomy or sham-operation. The parabionts and their controls were cannulated one month after the union.

Lymph was collected from the abdominal thoracic duct of sham-operated and thymectomized mice from one to 14 days after operation by a procedure previously described (14). Blood was collected from the inferior vena cava of another group of similarly operated mice. The mice were anesthetized with sodium pentobarbital for these collections. Two successive collections of lymph of about 10 to 15 min were made for each animal. The precise time of collection was measured. Lymph was collected in a calibrated polyethylene tube as it flowed from the thoracic duct and the lymph volume measured.

The volume of lymph was measured in all experiments. The number of leukocytes in the lymph and blood was counted using a hemocytometer. All mononuclear cells observed in lymph were assumed to be lymphocytes. Differential counts of blood smears were made and the total lymphocyte content per  $\text{mm}^3$  of blood was calculated. The hourly output of lymphocytes from the thoracic duct was calculated.

The thymus (of intact animals), spleen, and various groups of regional lymph nodes were dissected out of the parabionts, cleaned of fat and adjacent tissues, and immediately weighed. The mesenteric, axillary, brachial, mediastinal, inguinal, and superficial and deep cervical lymph nodes were weighed. The total weight of all these representative groups of lymph nodes was calculated. Portions of these tissues were fixed in neutral formalin, embedded and stained with hematoxylin and eosin for histological examination.

Thymuses obtained from newborn male rats were transplanted subcutaneously into the inguinal or axillary region of newborn male Buffalo rats. One group of rats was transplanted with ten donor thymuses at birth, thymectomized 25 days later, and the thoracic duct cannulated seven days later. Another group received multiple thymuses at birth and the thoracic duct was cannulated about two months later. In both groups the hourly output of lymphocytes from the thoracic duct and the blood lymphocyte level were measured, and the transplants were weighed at autopsy and fixed for histological examination.

## RESULTS

The hourly output of lymphocytes from the thoracic duct of rats was decreased by more than 50% by the 7th day after thymectomy (Table 1). This marked decrease in the output of lymphocytes from the thoracic duct did not occur if the thymectomized rat contained a

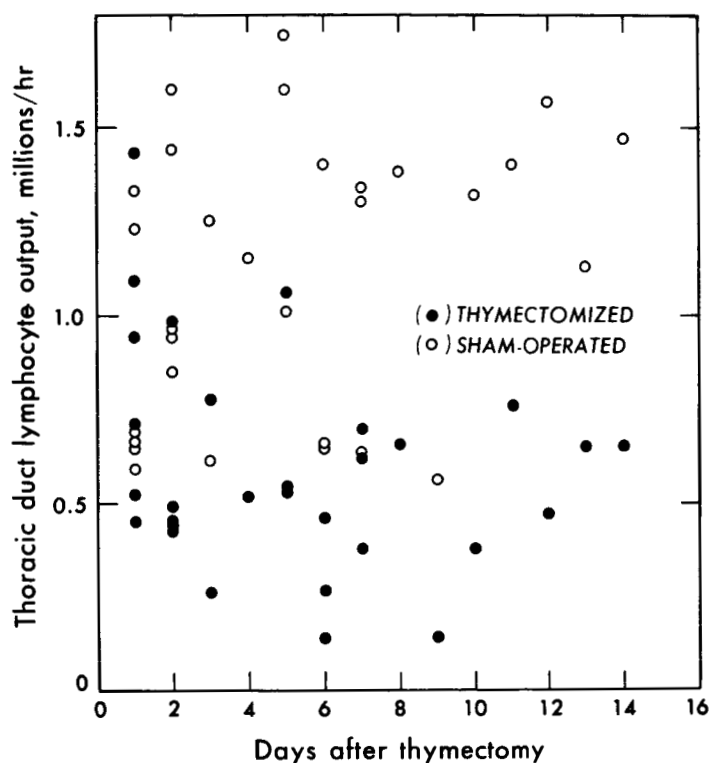


Figure 1. MUB-4478

subcutaneous transplant of the thymus in the axillary or inguinal region at the time that the normal thymus was removed. A tendency towards a decrease in the output of lymphocytes from the thoracic duct was observed in another group of rats as early as the third day after thymectomy.

The changes in the hourly output of lymphocytes from the thoracic duct in mice following thymectomy are shown in Fig. 1. Each point represents the value for one mouse. In spite of individual variability it is obvious that a marked decline in the output of lymphocytes occurs by the second or third day after thymectomy. During the first three days after operation the average output of lymphocytes from the thoracic ducts of all the sham-operated mice was  $0.98 \pm 0.10$  million cells/hr whereas the average output from all the thymectomized mice was  $0.69 \pm 0.09$  million cells/hr. Although this includes the values obtained at one day after operation the differences are significant ( $0.05 > P > 0.025$ ). During the next three days the output of lymphocytes from the sham-operated mice was  $1.2 \pm 0.17$  million cells/hr, but the output of the thymectomized mice declined to  $0.50 \pm 0.11$  million cells/hr. This decrease of more than 50% in the output of lymphocytes after thymectomy was highly significant ( $P < 0.001$ ). During the first four days after thymectomy the blood lymphocyte levels of both groups of mice were unchanged, but from the fifth to tenth day the blood lymphocyte levels of the thymectomized group decreased to about 20% of the sham-operated control group. The changes in the blood lymphocyte levels in the mouse following thymectomy agree with the observations of Metcalf (15).



Table 1. Output of thoracic-duct lymphocytes 7 days after thymectomy of the rat

	Number of animals	Body weight (grams)	Lymphocyte output (millions/hr)
Sham-operated	7	110±6	10.7±0.7
Thymectomized	7	122±4	4.0±0.7
Thymus transplants + Thymectomy	11	125±6	12.6±2.3

Table 2. Effect of multiple thymic transplants on the output of thoracic-duct lymphocytes

Treatment	Animal weight (grams)	Thymic weight (mg)	Thymic transplant weight (mg)	Lymphocyte output (cells/million/hr)
Unoperated controls	207+10	493+17	—	27.2+2.42
Neo-natally transplanted with 6-10 thymuses	204+7.8	546+7.7	1550+192	32.3+3.26

The results shown in Table 1 indicate that the depression in output of lymphocytes from the thoracic duct seven days after thymectomy does not occur in young rats if they contain subcutaneous thymic transplants. The neonatally transplanted thymuses weighed as much as the normal host thymus at this time. One month later, however, the neonatally transplanted thymuses were only about one third the size of the normal thymus, and seven days after thymectomy the output of lymphocytes from the thoracic duct was  $16.1 \pm 2.1$  million cells/hr whereas the output of lymphocytes from normal animals of the same age was  $26.6 \pm 1.8$  million cells/hr. Thus, in these older animals the presence of a small thymic graft did not prevent the decrease in the output of lymphocytes from the thoracic duct following thymectomy. Histologically the thymic grafts in the young and older hosts had the structural pattern characteristic of the normal thymus.

The effect of multiple thymic transplants on the output of lymphocytes from the thoracic duct is shown in Table 2. The thymuses were transplanted into newborn rats and the

Table 3. Lymph-node weights of parabionts (milligrams)

	Mesenteric	Axillary	Brachial	Mediastinal	Inguinal	Superior cervical	Deep cervical	All nodes	Spleen	Thymus
Sham-operated single										
Intact										
(10 animals - $279 \pm 6.7$ )*	$171 \pm 9.8$	$34.3 \pm 2.9$	$25.1 \pm 2.3$	$41.1 \pm 4.9$	$29.7 \pm 2.7$	$132 \pm 7.1$	$46.5 \pm 4.0$	$479.7 \pm 16.8$	$515 \pm 17$	$434 \pm 17$
Sham-operated single										
Thymectomized										
(10 animals - $285 \pm 6.3$ )	$139 \pm 9.1$	$29.5 \pm 3.8$	$24.7 \pm 2.9$	$36.3 \pm 3.6$	$20.2 \pm 1.6$	$78.7 \pm 6.3$	$30.1 \pm 4.1$	$358.7 \pm 16.7$	$483 \pm 12$	
Parabionts										
Intact	$146 \pm 5.0$	$41.4 \pm 2.8$	$29.7 \pm 3.5$	$43.3 \pm 3.2$	$47.6 \pm 4.1$	$124 \pm 8.0$	$47.0 \pm 5.0$	$484.1 \pm 17.5$	$579 \pm 30$	$456 \pm 8.9$
Intact	$154 \pm 8.3$	$41.6 \pm 3.2$	$35.5 \pm 2.5$	$46.0 \pm 4.7$	$44.9 \pm 6.2$	$113 \pm 5.3$	$34.8 \pm 4.5$	$469.6 \pm 11.6$	$552 \pm 20$	$450 \pm 15$
(10 pairs - $539 \pm 9.6$ )										
Intact	$133 \pm 7.5$	$37.8 \pm 1.6$	$28.1 \pm 4.4$	$39.3 \pm 4.2$	$36.2 \pm 3.9$	$109 \pm 5.3$	$40.1 \pm 5.9$	$423.2 \pm 12.0$	$497 \pm 20$	$417 \pm 18$
Thymectomized	$148 \pm 7.5$	$37.3 \pm 2.8$	$26.9 \pm 2.5$	$48.7 \pm 7.1$	$37.4 \pm 3.0$	$95.3 \pm 4.5$	$29.2 \pm 2.1$	$423.0 \pm 21.0$	$517 \pm 21$	
(10 pairs - $550 \pm 12$ )										
Thymectomized	$131 \pm 10$	$32.3 \pm 2.0$	$28.5 \pm 3.2$	$37.1 \pm 5.9$	$27.0 \pm 4.3$	$87.7 \pm 6.2$	$37.4 \pm 7.9$	$381.4 \pm 27.3$	$493 \pm 19$	
Thymectomized	$128 \pm 9.8$	$38.0 \pm 6.2$	$26.5 \pm 2.7$	$35.0 \pm 3.7$	$30.3 \pm 4.1$	$88.0 \pm 6.0$	$32.1 \pm 6.1$	$377.4 \pm 27.2$	$463 \pm 27$	
(10 pairs - $528 \pm 13$ )										

\*(No. of animals - Average weight)

Table 4. Thoracic-duct lymphocyte output

Treatment	Lymph volume (mm <sup>3</sup> /hr)	Lymphocyte output (millions/hr)
Intact		
Sham-operated (11)	$500 \pm 50$	$19.2 \pm 2.3$
Thymectomized		
Sham-operated (10)	$440 \pm 30$	$7.7 \pm 0.8$
Parabionts (10)		
Intact	$600 \pm 60$	$29.4 \pm 3.0$
Intact	$540 \pm 50$	$29.9 \pm 3.0$
Intact	$510 \pm 40$	$19.6 \pm 2.1$
Thymectomized	$590 \pm 40$	$21.7 \pm 2.6$
Thymectomized	$540 \pm 40$	$8.8 \pm 1.1$
Thymectomized	$510 \pm 30$	$6.7 \pm 0.8$

thoracic ducts of the host animals were cannulated at two months of age. No significant increase in the output of lymphocytes from the thoracic duct was observed in rats bearing multiple thymic transplants. The blood lymphocyte levels of the rats bearing multiple thymic transplants were indistinguishable from the control animals.

As shown in Table 3, lymph-node weights of single thymectomized rats or of thymectomized-thymectomized parabionts were significantly decreased compared to the values of appropriate sham-operated controls. However, the weights of these same representative

groups of lymph nodes were significantly increased towards normal values in a thymectomized rat joined by parabiosis to a normal rat. The hourly output of lymphocytes from the thoracic duct of single thymectomized rats or thymectomized-thymectomized parabionts indicated in Table 4 was also markedly decreased relative to the sham-operated control animals. The output of intact-intact parabionts was significantly greater than the value for single intact sham-operated animals. The reason for this is unknown, although it may be related to minor immunologic differences between the two parabiosed rats. However, no evidence of parbiotic intoxication was observed in the various parabionts, and skin grafts transplanted between different rats were viable indefinitely. The output of lymphocytes from the thoracic duct of a thymectomized rat joined to an intact animal was identical to the value of single intact animals and to the output of the intact member of the parabiont. Thus, the effect of thymectomy on the hourly output of lymphocytes from the thoracic duct and on the weights of peripheral lymphoid tissue was virtually abolished if the thymectomized rat was joined by parabiosis to a normal rat.

## DISCUSSION

The evidence for an extensive recirculating pool of lymphocytes, initially proposed by Gowans (11), appears well established. The route of recirculation of lymphocytes from blood to lymph in the rat appears to be via the post-capillary venules of the lymph nodes (16); the route of recirculation in the rabbit may, however, differ (17). The immediate depression of thoracic-duct lymphocyte output following extracorporeal irradiation of the blood suggested to Cronkite *et al.*, (18) that blood lymphocytes are supplying the lymph with lymphocytes rather than the reverse. It seems reasonable, therefore, to assume that the measurement of the output of lymphocytes from the thoracic duct is a reasonable index of the size of the recirculating lymphocyte pool.

A significant decrease of about 50% in the output of lymphocytes from the thoracic duct was found within a week after thymectomy in the rat and within three days after thymectomy in the mouse. This decrease in lymphocyte output was not observed after removal of the normal rat thymus, if the animal contained a subcutaneous thymic graft of about the same size as the normal thymus. These data extend and corroborate previous observations from this laboratory (1) and give further support for the view that the thymus is of considerable importance in regulating the size of the recirculating lymphocyte pool in the adult animal.

Relatively pronounced decreases in the output of lymphocytes from the thoracic duct and in the level of blood lymphocytes occur soon after administration of adrenal corticoids, ACTH, or adrenaline (19, 10). Comparisons of the effects of thymectomy were always made with sham-operated animals in order to minimize any effects of these hormones, presumably released as a result of operative trauma, although a systematic study of possible differential effects of these hormones on normal and thymectomized animals was not made. The finding that the level of blood lymphocytes in the thymectomized rat did not drop, relative to the sham-operated rat, until about five days after operation suggests that the observed results are not due to operative trauma. There are several possible ways that the thymus could regulate the size of the recirculating lymphocyte pool. The thymus could contribute large numbers of

lymphocytes to the pool, or supply some humoral agent that either regulated lymphocytopoiesis in the peripheral lymphoid tissue or is necessary for the differentiation of some primitive precursor stem cell into lymphoid cells. Certainly none of these possibilities are mutually exclusive.

Mitotic indices and measurements of DNA turnovers indicate that large numbers of cells are produced in the thymus. The route by which these cells, produced in the thymus, eventually enter the recirculating lymphocyte pool, if indeed they do enter the pool, is unknown. Evidence has been presented (4) for the view that if large numbers of cells do emigrate from the thymus, they do not leave via lymphatic channels that empty directly into the thoracic duct. Sainte-Marie and Leblond (20), on the basis of morphological observations and counts of lymphocytes within the arterial and venous vessels supplying the thymus, concluded that lymphocytes arising in the thymic cortex migrated to the medulla and then entered the blood stream. Ernström *et al.* (21) collected blood from the carotid artery near the origin of the thymic arteries and from the thymic veins and observed an increased percentage of lymphocytes in the venous blood. More recently, Ernström and Larsson (22) have demonstrated that lymphocytes having a low mitochondrial content are more numerous in thymic vein blood, which suggested that the cells leaving the thymus are small lymphocytes. Nossal (23), utilizing autoradiographic techniques, followed the migration of cells from the thymus of guinea pigs after local labeling with  $H^3$ -thymidine and demonstrated that small lymphocytes emigrate from the thymus and settle in the peripheral lymphoid tissue. These experiments all suggest that some cells normally leave the thymus to enter the peripheral lymphocyte pool, but regrettably there are no data available indicating quantitatively the magnitude of the emigration.

Metcalf (2) has shown that the presence of almost twelve times the normal amount of thymic tissue in mice does not increase the blood lymphocyte levels or the weights of the host lymphoid tissue. The present experiments corroborate these findings and indicate, in addition, that the presence of about three times the normal thymic tissue in rats does not elevate the hourly output of lymphocytes from the thoracic duct. The failure of multiple thymic grafts to elevate either the blood lymphocyte levels or the thoracic duct lymphocyte output is difficult to reconcile with the concept that the thymus contributes large numbers of cells to the recirculating lymphocyte pool, especially since the recent autoradiographic evidence of Matsuyama *et al.* (24) indicates that lymphopoiesis in thymic grafts is identical with normal thymic tissue.

Another observation difficult to reconcile with the concept that the thymus is a major source of thoracic duct lymphocytes is the brief remark of Gowans (25) that transfusions of suspensions of thymic lymphocytes failed to elevate the output of lymphocytes from the thoracic duct although the transfusion of thoracic duct cells elevates the output within 4 to 12 hr after transfusion (11). Everett (26) has also stated briefly that following massive transfusions of labeled thymic lymphocytes, labeled cells were rarely observed in the thoracic-duct lymph. These findings require further investigation and could be of considerable importance. If thymic lymphocytes do enter the blood but do not enter the rapidly recirculating lymphocyte pool until after some delay, it is possible that it is during this delay period that the relatively

immunologically inactive thymic lymphocyte becomes an active immunologically competent cell.

Metcalf (27), Osoba and Miller (28) and Levey et al. (29) have implicated a humoral factor, produced by the thymus, in the regulation of lymphopoiesis. It is possible that the removal of the source of this factor by thymectomy is responsible for the decreased size of the recirculating lymphocyte pool, but other data suggest to us that such a humoral factor is not necessary for the proliferation of differentiated lymphoid tissue. For example, although a significant decrease in the mass of peripheral lymphoid tissue occurs by 60 days after the thymectomy of 6- to 8-day-old rats, the fractional cell renewal of the remaining lymphoid tissue is indistinguishable from that found in sham-operated animals on a weight basis (1). This indicates that active lymphopoiesis occurs in thymectomized rats even in the absence of the thymus.

Miller et al. (30) and Cross et al. (31) noted that the thymus was necessary for restoration of immunologic activity and lymphoid tissue in adult irradiated mice, following syngenic bone-marrow transplantation, but not after syngenic spleen transplantation. They concluded that immunologically competent cells present in the splenic transplant could function in the absence of the thymus.

The chromosome marker studies of Micklem et al. (32) indicate that "stem cells" capable of repopulating the thymus, lymph nodes, and spleen are present in the bone marrow, but not in the thymus, lymph nodes, or thoracic-duct lymph. They consider that, although the experiments were performed with regenerating tissues, it is possible that in the normal animal the cells of the thymus and a considerable fraction of the lymph node lymphocytes are constantly being derived from bone-marrow stem cells. It is thus possible that the decreased output of lymphocytes from the thoracic duct after thymectomy is the result of a failure of bone-marrow stem cells to differentiate into lymphoid cells. Such an explanation would necessarily assume that considerable numbers of stem cells are involved in this process, since the decreased thoracic-duct lymphocyte output occurs so rapidly after thymectomy.

The previous studies all suggest that there are two populations of lymphocytes: one population requiring the presence of the thymus for proliferation and the other population capable of proliferating in the absence of the thymus. Several investigators (33, 34, 16, 35) have presented evidence for the existence of two populations of lymphocytes, of which one population appears to have a relatively long life and the other a short life. The lymphocyte transfusion experiments of Gowans and Knight (16) also indicate the existence of two lymphocyte populations: one that recirculates rapidly and the other that recirculates slowly. The findings of McGregor and Gowans (36) that after chronic drainage of lymphocytes from a thoracic duct fistula in rats, the primary immune response is severely depressed or abolished whereas the secondary response is relatively unaffected, indicate that the rapidly recirculating lymphocytes are mostly noncommitted immunologically competent cells. The rapidity with which the output of lymphocytes from the thoracic duct decreases after thymectomy is consistent with the concept that an appreciable population of short-lived small lymphocytes requires the

presence of the thymus for their development. The magnitude of the decrease in small lymphocytes is consistent with the data of Robinson *et al.* (35), showing that the maximum size of the short-lived population of small lymphocytes is about 40% of the small lymphocytes of the blood. Thus, we conclude that removal of the thymus affects a population of short-lived small lymphocytes that recirculates rapidly and are probably derived from the differentiation of some precursor "stem cell" present in the bone marrow.

The thymus is necessary for the restoration of lymphoid tissue and the output of lymphocytes from the thoracic duct of the thymectomized member of a parabiont. This restoration could also be either the result of the movement of cells or a humoral agent produced by the thymus of the intact member into the thymectomized member. Autoradiographic observations (1) and experiments with chromosome markers (37) indicate that an extensive exchange of lymphocytes can occur within the lymphatic systems of normal animals after parabiosis. Ford and coworkers (38) have observed that this exchange is barely affected if both partners are thymectomized; but if only one partner is thymectomized an asymmetric exchange of lymphoid cells generally occurs with a migration of cells from the member containing a thymus into the thymectomized partner. A quantitative measure of the rate of this exchange is unavailable, and the relative role of a humoral factor derived from the thymus of the intact member on lymphopoiesis in the parabiont can not be excluded in any explanation of the recovery of the recirculating lymphocyte pool in these experiments.

## SUMMARY

A marked decrease in the recirculating pool of lymphocytes, as measured by the hourly output of lymphocytes from the thoracic duct, occurs within a week after thymectomy. This decrease was prevented if the thymectomized animal contained a subcutaneous thymic transplant or was joined by parabiosis to an animal containing a normal thymus, indicating that the thymus is intimately concerned in the regulation of a considerable portion of the recirculating lymphocyte pool. The simplest explanation of these findings is that the thymus is a major source of lymphoid cells, which migrate from the thymus, probably directly into the blood stream, and eventually enter the rapidly recirculating small lymphocyte pool. This conclusion must, however, remain tentative, since data are not available indicating the magnitude of the emigration of lymphocytes from the thymus, although there is good evidence that some emigration occurs. The role a humoral factor produced by the thymus may have in explaining the present experiments cannot be properly evaluated until the extent of lymphocyte emigration from the thymus is known. The failure of multiple thymic transplants to elevate either the blood lymphocyte level or the output of lymphocytes from the thoracic duct suggests that some homeostatic mechanism regulates the level of thymus derived or thymus controlled lymphocytes in the recirculating lymphocyte pool. The rapidity with which the output of lymphocytes from the thoracic duct declines after thymectomy indicates that the thymus regulation is concerned primarily with a short-lived population of lymphocytes, regardless of whether these cells are derived directly from the thymus or through the proliferation of lymphoid cells elsewhere regulated by a humoral thymic factor.

## ACKNOWLEDGMENTS

Supported in part by the U. S. Atomic Energy Commission and in part by Cancer Research Funds of the University of California

## REFERENCES AND NOTES

1. Schooley, J. C., and Kelly, L. S.; in *The Thymus in Immunobiology*, edited by R. A. Good and A. E. Gabrielsen, New York, Harper & Row, 1964, p. 236-253.
2. Metcalf, D.; *Australian J. Exptl. Biol. Med. Sci.* 41:437-448, 1963.
3. Schooley, J. C., and Kelly, L. S.; Lawrence Radiation Laboratory Report UCRL-8513, 57-59, 1958.
4. Waksman, B. H.; Arnason, B. G., and Janković, B. D.; *J. Exptl. Med.* 116:187-206, 1962.
5. Arnason, B. G.; Janković, B. D.; Waksman, B. H., and Wennersten, C.; *J. Exptl. Med.* 116:177-186, 1962.
6. Martinez, C.; Kersey, J.; Papermaster, B. W., and Good, R. A.; *Proc. Soc. Exptl. Biol. Med.* 109:193-196, 1962.
7. Miller, J. F. A. P.; *Proc. Royal Soc. Ser. B.* 156:415-428, 1962.
8. Parrott, D. M. V., and East, J.; *Nature* 195:347-348, 1962.
9. Bierring, F.; in *Ciba Foundation Symposium on Haemopoiesis*, edited by G. E. W. Wolstenholme and M. O'Connor, London, Churchill, 1960, p. 185-198.
10. Reinhardt, W. O., and Yoffey, J. M.; *Amer. J. Physiol.* 187:493-500, 1956.
11. Gowans, J. L.; *J. Physiol.* 146:54-69, 1959.
12. Shorter, R. G., and Bollman, J. L.; *Amer. J. Physiol.* 198:1014-1018, 1960.
13. Reinhardt, W. O.; *Proc. Soc. Exptl. Biol. Med.* 58:123-124, 1945.
14. Shrewsbury, M. M.; *Proc. Soc. Exptl. Biol. Med.* 99:53-54, 1958.
15. Metcalf, D.; *Brit. J. Haematol.* 6:324-333, 1960.
16. Gowans, J. L., and Knight, E. J.; *Proc. Royal Soc. B.* 159:257-282, 1964.
17. Fichtelius, K. E., and Bryant, B. J.; in *The Thymus in Immunobiology*, edited by R. A. Good and A. E. Gabrielsen, New York, Harper & Row, 1964, p. 274-287.
18. Cronkite, E. P.; Jansen, C. R.; Cottier, H.; Rai, K., and Sipe, C. R.; *Ann. N. Y. Acad. Sci.* 113:566-577, 1964.
19. Hungerford, G. F.; Reinhardt, W. O., and Li, C. H.; *Blood* 7:193-206, 1952.
20. Sainte-Marie, G., and Leblond, C. P.; *Blood* 23:275-299, 1964.
21. Ernström, V.; Gyllenstein, L., and Larsson, B.; *Nature* 207:540-541, 1965.
22. Ernström, V., and Larsson, B.; *Acta Pathol. Microbiol. Scand.* 65:203-214, 1965.
23. Nossal, G. J. V.; *Ann. N. Y. Acad. Sci.* 120:171-181, 1964.
24. Matsuyama, M.; Wiadrowski, M. N., and Metcalf, D.; *J. Exptl. Med.* 123:559-576, 1966.
25. Gowans, J. L.; in *The Thymus in Immunobiology*, edited by R. A. Good and A. E. Gabrielsen, New York, Harper & Row, 1964, p. 287.
26. Everett, N. B.; in *The Thymus in Immunobiology*, edited by R. A. Good and A. E. Gabrielsen, New York, Harper & Row, 1964, p. 287.
27. Metcalf, D.; *Brit. J. Cancer* 10:442-457, 1956.
28. Osoba, D., and Miller, J. F. A. P.; *J. Exptl. Med.* 119:177-194, 1964.

# Serum-Lipoprotein Distribution and Protein Analysis by Refractometry

N67 15948

Frank T. Lindgren, Norman K. Freeman, Robert D. Wills,  
Alicia M. Ewing and Lin C. Jensen

It is the purpose of this paper to consider potential relationships between the serum-lipoprotein distribution and the other principal serum macromolecules, i. e., the serum proteins. These relationships would certainly be of interest in the full discussion of the metabolic role of lipids. A logical question arises as to how one can accurately measure serum protein or those protein macromolecules exclusive of the lipoproteins. In the past, total serum protein usually has been measured by a variety of techniques, including both chemical and physical methods. The former include measurement of total protein nitrogen by modifications (1) of the original Kjeldahl procedure, by such colorimetric reactions as the Folin phenol reagent developed by Lowry *et al.* (2), or the biuret reagent described by Gornall *et al.* (3). These chemical methods have certain limitations; for example, each class of protein may have slightly different nitrogen or tyrosine and tryptophane content. Further, the analytical methods themselves are difficult to carry out with accuracy and reproducibility. On the other hand, physical methods for quantitative serum protein analysis, including electrophoretic (4) and ultracentrifugal (5) techniques, usually lack either precision and/or simplicity.

## MATERIALS AND METHODS

For more than 60 years, the serum proteins have been determined by refractometry (6). This measurement, however, includes both the serum small molecule background as well as the total content of serum-lipoprotein macromolecules. Because the small molecule background is nearly constant, and a valid correction can be applied, this method actually measures quite accurately the total serum macromolecules. The measurement of serum proteins by refractometry has recently been reviewed extensively by Naumann (7); yet the influence of serum lipoproteins on the accuracy of this method for total serum-protein measurement has not been fully discussed. For instance, serum-lipoprotein content contributes substantially and in varying amounts to the serum-macromolecular measurement. Also, lipoprotein specific refractive increments (8-10) are different for each lipoprotein class and are substantially lower than those of the uncomplexed proteins (11).

Since lipoproteins are measured in salt solutions of various densities and refractive indices, there is a slight complication in evaluating the refractive index contribution of the total lipoprotein spectra to the measurement obtained in total serum refractometry. Knowledge is required of the change in the specific refractive increments of each lipoprotein class with change in the refractive index of the reference medium. For macromolecules of small particle size, the relationship is approximately given by the familiar formula (12, 13):



29. Levey, R. H.; Trainin, N., and Law, L. W.; J. Nat. Cancer Inst. 31:199-217, 1963.
30. Miller, J. F. A. P.; Doak, S. M. A., and Cross, A. M.; Proc. Soc. Exptl. Biol. Med. 112:785-792, 1963.
31. Cross, A. M.; Leuchars, E., and Miller, J. F. A. P.; J. Exptl. Med. 119:837-850, 1964.
32. Micklem, H.; Ford, C.; Evans, E., and Gray, J.; Information exchange Group No. 5, Scientific Memo No. 54, Radiobiological Research Unit, Harwell, 1965, p. 1-48.
33. Caffrey, R. W.; Rieke, W. O., and Everett, N. B.; Acta Haematol. 28:145-154, 1962.
34. Craddock, C. G.; Nakai, G. S.; Fukuta, H., and Vanslager, L. M.; J. Exptl. Med. 120:389-412, 1964.
35. Robinson, S. H.; Brecher, G.; Lourie, I. S., and Haley, J. E.; Blood 26:281-295, 1965.
36. McGregor, D. D., and Gowans, J. L.; J. Exptl. Med. 117:303-320, 1963.
37. Harris, J. E.; Ford, C. E.; Barnes, D. W. H., and Evans, E. P.; Nature 201:886-887, 1964.
38. Ford, C. E.; Xth Congress of the International Society of Hematology, Stockholm, 1964.

Marvin M. Shrewsbury's present address is Department of Biology, San Jose State College, San Jose, Calif.

$dn/dc = 3n_1(m^2 - 1)/2D(m^2 + 2)$ , where  $D$  is the density of the anhydrous macromolecule,  $n_1$  is the refractive index of the solvent, and  $m$  is the ratio of the refractive index of the solute to the solvent. Figure 1 shows the almost linear form of this relationship, in which the various curves are slightly displaced (or rotated) to fit through available experimental specific refractive increment values and the calculated or estimated refractive index of the anhydrous macromolecule. Thus, from these relationships, it is possible to convert the measured refractive increment of each lipoprotein class to the appropriate value it would have in a serum background environment.

We have made the above calculations on sera from a small population of nonfasting normal males and females. The subjects were clinically normal adults, ages 35 to 49, employed at the Lawrence Radiation Laboratory, Livermore, California. Very low-density- and low-density-lipoprotein values were measured by precision refractometry (10) at 5,893 Å, and high-density data were evaluated from ultracentrifugal analysis (14), in which the wavelength used is 5,460 Å. Thus, for very low-density lipoproteins ( $S_f$  20-10<sup>5</sup>), a specific refractive increment of 0.00158 Δn/g/100 ml (10), as measured in 0.199 Molal NaCl, is used. For low-density lipoproteins ( $S_f$  0-20), a specific refractive increment of 0.00154 (9), as measured in 1.745 Molal NaCl, is used with correction to anticipated value of 0.00166 Δn/g/100 ml in 0.199 Molal NaCl. High-density lipoproteins were measured in 0.199 Molal NaCl plus 2.771 Molal NaBr using a specific refractive increment of 0.00149 Δn/g/100 ml (15). Similarly, corrections were made using a value of 0.00173 Δn/g/100 ml for high-density lipoproteins in 0.199 Molal NaCl. Because of the uncertainty of the high-density specific refractive increment, no correction was made for dispersion.

Extrapolation to 5,893 Å of the Perlmann and Longsworth (14) specific refractive increment data for the serum proteins (at 5,770 Å, 5,460 Å and 4,358 Å) was made using a best fit Cauchy plot. From this it was estimated that the refractive increment of the serum proteins (such as serum albumin and globulin) would be approximately 1% lower at 5,893 Å than at 5,460 Å. Accordingly, their value at the latter wavelength has been corrected to 0.00185 Δn/g/100 ml for calculations of total serum protein content from measurements at the sodium D line.

The refractive index contribution of the serum small-molecule background was evaluated from the 2nd ml infranatant of an unaltered serum preparative run with corrections for sedimentation of the small molecule solutes (10). Subtracting the corrected lipoprotein and serum background refractive increments from the total serum refractive increment (5,893 Å) measured by precision refractometry (16) yields the total serum-protein macromolecules whose densities are greater than 1.20 g/ml, excluding essentially all the known lipoproteins. Such a measurement, of course, includes complex proteins such as mucoproteins and any lipoproteins that might exist in the density region of 1.20-1.33 g/ml. The amounts of both are normally very small.

## RESULTS AND DISCUSSION

The mean values and standard deviations of serum-protein concentrations determined

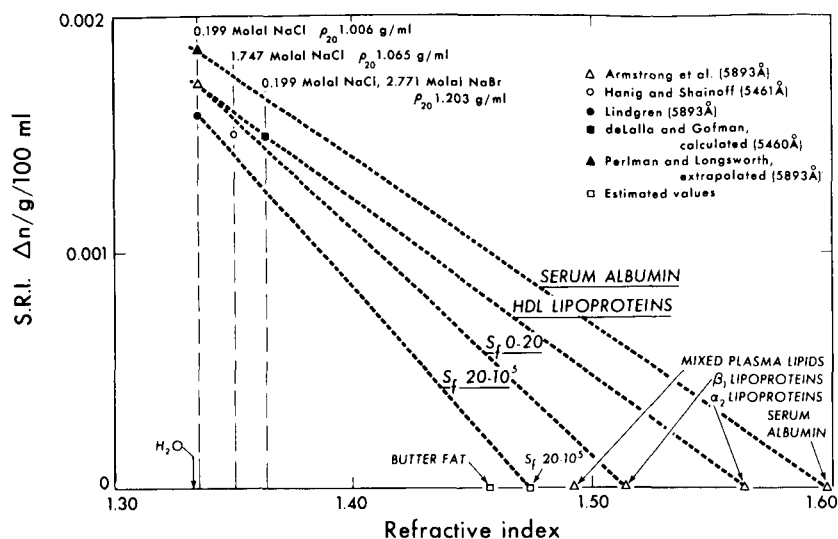


Figure 1. Relationship between specific refractive increment of serum proteins and lipoprotein classes and the refractive index of the reference media. MUB-8384

from our refractometric data, together with the calculations by other formulae are given in Table 1. For the purposes of clarity and comparison with other serum protein data, we have defined three quantities. These are total serum macromolecules, total serum protein (excluding all the known lipoproteins) and total real protein (which includes the protein moieties of the serum lipoproteins). Thus, these values illustrate the ca 900 mg% contribution of the lipoproteins to the total serum macromolecules, approximately 300 mg% of which is lipoprotein. Within our small populations, no significant differences were observed between males and females in either total serum protein or total real protein. We have broken our data into these components because of the procedure for calibration of the refractometric method (7). The usual calibration has been to compare refractive increment above the water reference against, either total real-serum protein evaluated by conventional chemical methods, or a standard protein solution, such as serum albumin. The former procedure ignores the contribution of non-protein moieties of the serum macromolecules, particularly the lipoproteins of density less than 1.20 g/ml. On the other hand, the latter, neglecting differences in specific refractive increment, would approximate the serum content of total macromolecules. Table 1 also presents the usual calculations, showing the wide discrepancies observed between the various regression formulae from the literature. These have been proposed by Sunderman (17), Drinkman and McKeon (18), and Bausch and Lomb (19).

Figure 2 shows all the components measured by serum refractometry, together with the mean refractive increment values and their standard deviations for our small populations. It is apparent that neither the total serum proteins (excluding the known lipoproteins) nor total real protein can be measured accurately by serum refractometry unless the total content of serum lipoproteins is considered. Although the usual differences in serum lipoprotein content between the males and females were observed (20, 14), it is interesting to note the significantly elevated ( $p > .01$ ) serum small-molecule background in the male group. This is of additional interest because the standard deviations of these values are only slightly higher than the relative accuracy of the precision refractometry itself.

The individual calculations for total serum protein (excluding the lipoproteins) are plotted in Fig. 3, along with the regression formulae of Sunderman (17), Drinkman and McKeon (18), and Bausch and Lomb (19). Gross discrepancies for total serum protein amounting to the order of 1,000 mg%, as calculated by these three regression formulae, are readily apparent. It is therefore understandable why in the past this refractive index method for serum-protein determination has been in a state of controversy, and has not received widespread acceptance as a reliable analytic procedure. However, considering the accuracy of precision refractometry of serum as well as the accuracy of the calculated contributions of lipoproteins to the total serum refractive increment, this improved version of serum refractometry should have great potential accuracy. It further would have the stability inherent in a physical rather than a chemical measurement. Here our anticipated accuracy, based on the limiting factor of reproducibility of lipoprotein analysis (a standard error of measurement of approximately  $\pm 5\%$ ), should be the order of 50 to 100 mg% for total serum proteins (exclusive of the lipoproteins). Such factors as small differences in specific refractive increment among various classes of serum proteins (8, 11), which would be the order of 1%, also must be considered. However, such a revised measurement of total serum protein with a potential error in the neighborhood of 1 to 2% represents substantial improvement over the refractometric method whose several regressive formulae differed by as much as 15% within the normal range of serum values!

If it were necessary to isolate and measure lipoproteins either by refractometry or the ultracentrifuge to make all these corrections (which has been done with a small computer program), such a method of defining total serum macromolecules, total real protein and non-lipoprotein protein would perhaps have limited application. However, lipoproteins and lipoprotein  $\Delta n$  may be estimated adequately for this correction from serum-lipid measurements. For instance, the three major classes of serum lipoproteins may be estimated from values of total serum-cholesteryl esters, glycerides and phospholipids. Table 2 presents these regression equations together with their approximate correlations to the ultracentrifugal lipoprotein data. Because of differences in lipoprotein distribution in the male and female populations, two sets of regression formulae have been given. In general, either total serum lipid, or a combination of serum-triglyceride and cholesteryl-ester values may be used to calculate total lipoprotein  $\Delta n$ . However, for the females, inclusion of serum phospholipid tends to improve the calculation slightly. Table 3 presents regression formulae for total lipoprotein  $\Delta n$  as calculated from total serum lipid and from combinations of serum triglyceride, serum-cholesteryl ester and serum phospholipid. The correlation coefficients refer to the relationship between the total lipoprotein  $\Delta n$  obtained from actual lipoprotein measurement and the derived  $\Delta n$  value calculated from lipid data. It is to be understood that these values are slightly higher than the correlation coefficients to be expected when the regression formula is used to predict  $\Delta n$  in another population. This is because the coefficients were calculated by a least squares method to optimize the relationship of the derived  $\Delta n$  variable to the calculated  $\Delta n$  value (within one population). Random variation of values would therefore tend to lower the correlation when the same regression coefficients are used for prediction in another population. It is evident, however, that lipoprotein  $\Delta n$  can be estimated with considerable accuracy from these serum lipid parameters. Perhaps the most promising application of this method

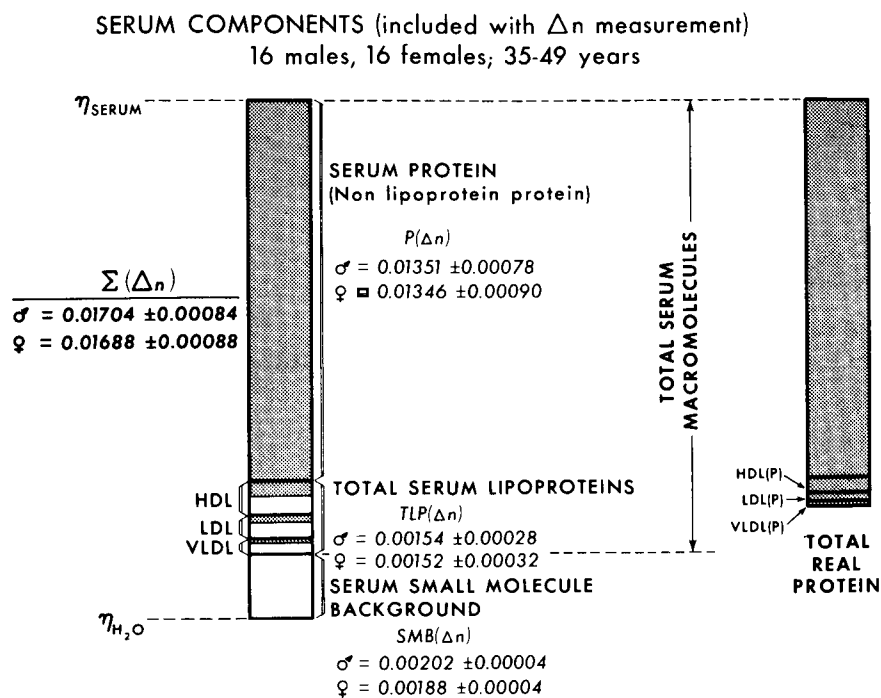


Figure 2. Serum components included with  $\Delta n$  measurement, giving mean values  $\pm$  standard deviations for 16 males, 16 females, 35 to 49 years.

MUB-8383

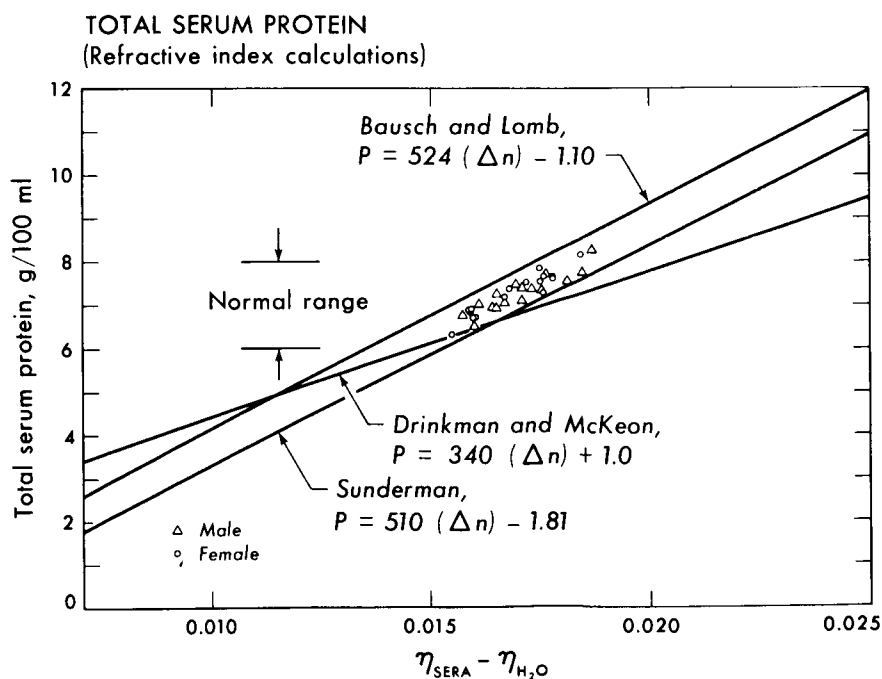


Figure 3. Individual total serum-protein values for our male and female populations showing the three commonly used regression formulae.

MUB-8385

Table 1. Serum protein concentrations  
16 Males, 16 Females, 35-49 Years

Method	Males	Females
Total serum macromolecules	8,158 ± 462	8,133 ± 465
Total real protein	7,525 ± 415	7,553 ± 482
Total serum protein	7,263 ± 420	7,237 ± 485
Sunderman* (1944)	6,882 ± 430	6,797 ± 447
Drinkman-McKeon* (1962)	6,795 ± 287	6,738 ± 298
Bausch and Lomb* (1963)	7,831 ± 442	7,744 ± 459

\*Usual  $\Delta n$  calculation.

Table 2. Lipoprotein-lipid regression formulae

Normal males	
$S_f$ 20-400 =	$0.92 \text{ (STG)} + 0.04 \text{ (SCE)} + 0.29 \text{ (SPL)} - 122 \quad r = 0.99$
$S_f$ 0-20 =	$0.06 \text{ (STG)} + 2.46 \text{ (SCE)} - 1.61 \text{ (SPL)} + 66 \quad r = 0.91$
HDL =	$-0.83 \text{ (STG)} - 1.52 \text{ (SCE)} + 4.28 \text{ (SPL)} - 249 \quad r = 0.85$
Normal females	
$S_f$ 20-400 =	$1.11 \text{ (STG)} + 0.08 \text{ (SCE)} - 0.30 \text{ (SPL)} - 1 \quad r = 0.96$
$S_f$ 0-20 =	$0.30 \text{ (STG)} + 1.87 \text{ (SCE)} - 0.89 \text{ (SPL)} + 56 \quad r = 0.82$
HDL =	$1.13 \text{ (STG)} - 0.60 \text{ (SCE)} + 3.13 \text{ (SPL)} - 132 \quad r = 0.84$

Lipid Values in mg/100 ml.

Table 3. Regression formulae for total lipoprotein  $\Delta n$ \*

Normal males	
$\Delta n \text{ (TLP)} = 1.704K \text{ (TGL)} + 0.00015$	$r = 0.96$
$\Delta n \text{ (TLP)} = 1.248K \text{ (STG)} + 3.605K \text{ (SCE)} + 0.00011$	$r = 0.98$
$\Delta n \text{ (TLP)} = 0.860K \text{ (STG)} + 1.803K \text{ (SCE)} + 3.454K \text{ (SPL)} - 0.00018$	$r = 0.99$
Normal females	
$\Delta n \text{ (TLP)} = 1.867K \text{ (TGL)} + 0.00017$	$r = 0.95$
$\Delta n \text{ (TLP)} = 2.558K \text{ (STG)} + 3.776K \text{ (SCE)} + 0.00015$	$r = 0.90$
$\Delta n \text{ (TLP)} = 0.335K \text{ (STG)} + 2.269K \text{ (SCE)} + 3.690K \text{ (SPL)} - 0.00020$	$r = 0.95$

\*Lipid abbreviations are TLP (total lipoprotein), TGL (total gravimetric lipid), STG (serum triglyceride), SCE (serum cholesteryl ester) and SPL (serum phospholipid). Lipid values are in mg/100 ml.  $K = 10^{-6} \text{ (mg/100 ml.)}^{-1}$ .

may be its value as a screening test for possible lipid or protein abnormalities. This would be especially true for small animal studies because of the very limited amounts of serum required for analysis. Thus, serum refractometry can be done on one drop of serum, and the serum-cholesteryl ester and triglyceride can be done simultaneously by the high-resolution infrared spectrometry technique of Freeman (21) on as little as 0.050 ml of serum. Further, the infrared lipid analysis has been partly automated (22) and is sufficiently simple and reproducible that complete automation appears to be possible.

In order to utilize serum refractometry to measure accurately the total serum-protein macromolecules exclusive of the lipoproteins, it is necessary to measure or estimate the serum-lipoprotein spectra. This revised technique may become important because of possible interrelationships between serum protein and lipid metabolism. In the present preliminary study of normal males and females, however, only low-order non-significant correlations were observed. Yet, in many of the known hyper- and hypoproteinemias (7), where both lipid and protein abnormalities may exist, there indeed may be fruitful application of precision serum refractometry in combination with measurement or estimation of the serum lipoproteins.

## ACKNOWLEDGMENTS

We wish to thank Ruth Szekeley, Medical Department, Lawrence Radiation Laboratory, Livermore, for her invaluable aid in arranging and obtaining the blood samples used in this study.

This work was supported by Research Grants 5-R01-HE-01882-11 and 5-R01-HE-02029-11 from the National Heart Institute, Public Health Service, Bethesda, Maryland, and by the United States Atomic Energy Commission.

## REFERENCES

1. Zipf, R. E.; Katchman, B. J., and Sunderman, F. W.; in *Serum Proteins and Dysproteinemias*, edited by F. W. Sunderman and F. W. Sunderman, Jr., Philadelphia, J. B. Lippincott Co., 1964, p. 40.
2. Lowry, O. H.; Rosebrough, N. J.; Farr, A. L., and Randall, R. J.; *J. Biol. Chem.* 193:265, 1951.
3. Gornall, A. G.; Bardawill, C. J., and David, M. M.; *J. Biol. Chem.* 177:751, 1949.
4. Williams, F. G., and Nixon, M. C.; in *Serum Proteins and the Dysproteinemias*, edited by F. W. Sunderman and F. W. Sunderman, Jr., Philadelphia, J. B. Lippincott Co., 1964, p. 110.
5. deLalla, O. F.; Lawrence Radiation Laboratory Report UCRL-8550, November, 1958.
6. Reiss, E.; *Inaug. Diss.*, Strassburg, 1902.
7. Naumann, H. N.; in *Serum Proteins and the Dysproteinemias*, edited by F. W. Sunderman and F. W. Sunderman, Jr., Philadelphia, J. B. Lippincott Co., 1964, p. 86.
8. Armstrong, S. H.; Budka, M. J. E.; Morrison, K. C., and Hasson, M.; *J. Am. Chem. Soc.* 69:1747, 1947.
9. Hanig, M., and Shainoff, J. R.; *J. Biol. Chem.* 219:479, 1956.

10. Lindgren, F. R.; Nichols, A. V.; Freeman, N. K.; Wills, R. D.; Wing, L., and Gullberg, J. E.; *J. Lipid Research* 5:68, 1964.
11. Perlmann, G. E., and Longsworth, L. G.; *J. Am. Chem. Soc.* 70:2719, 1948.
12. Zimm, H., and Dandliker, W. B.; *J. Phys. Chem.* 58:644, 1954.
13. Heller, W., and Pugh, T. L.; *J. Colloid Sci.* 12:294, 1957.
14. Ewing, A. M.; Freeman, N. K., and Lindgren, F. T.; in *Advances of Lipid Research*, Vol. 3, edited by R. Paoletti and D. Kritchevsky, New York, Academic Press Inc., 1965, p. 25.
15. deLalla, O., and Gofman, J. W.; in *Methods of Biochemical Analysis*, Vol. 1, edited by D. Glick, New York, Interscience, 1954, p. 459.
16. Bauer, N.; Fajans, K., and Lewin, S. Z.; in *Physical Methods of Organic Chemistry*, 3rd ed., Vol. 1, edited by A. Weissberger, New York, Interscience Publisher, 1960, p. 1239.
17. Sunderman, F. W.; *J. Biol. Chem.* 153:139, 1944.
18. Drinkman, A., and McKeon, F. A.; *Am. J. Clin. Pathol.* 38:392, 1962.
19. Bausch and Lomb, Abbe-3L Refractometer Reference Manual; Serum Protein Meter Reference Manual, Rochester 2, New York, 1963.
20. deLalla, O. F., and Gofman, J. W.; in *Blood and Other Body Fluids*, edited by D. S. Dittmer, Washington, D. C., Federation of American Societies for Experimental Biology, 1961, p. 64.
21. Freeman, N. K.; *J. Lipid Res.* 5:236, 1964.
22. Freeman, N. K.; Semiannual Report, Donner Laboratory, Lawrence Radiation Laboratory, UCRL-16613, 1965.



# Studies on Deficient Mammalian Cells Isolated from X-Irradiation Cultures

N67 15949

Paul W. Todd

The finding by Puck (1) and by Elkind and Sutton (2) that single cells exposed to X radiation develop into colonies of a variety of sizes stimulated a series of studies by Sinclair (3). He was able to classify colonies of Chinese-hamster cells that developed after graded doses of X radiation into "small" and "m". "Small" colonies appeared to contain a lower percentage of viable progeny cells; the progeny cells had a longer doubling time; they were less resistant to subsequent exposure to X radiation; and all of these characteristics appeared to be independent of the chromosome number.

A series of experiments were conducted to answer the following questions raised by Sinclair's results:

1. Are similar small-colony-forming (herein called "deficient") cells produced in X-irradiated cultures of human cells?
2. Are deficient cells produced with greater efficiency by high-LET (linear energy transfer) radiations than by X rays?
3. Do deficient mammalian cells bear any resemblance to the respiratory (or cytochrome) deficient yeasts, or "petites" discovered by Ephrussi (4) and found in irradiated cultures by Raut and Simpson (5)?
4. Do deficient cells have heritable chromosome aberrations such as those found in irradiated pig-kidney-cell cultures by Ruddle (6)?

## MATERIALS AND METHODS

**CELLS** Cultured mammalian cells used in these experiments were human kidney line T1 (7, 8) and Chinese-hamster bone-marrow M3-1 cells obtained from an adult male Chinese hamster originally from Yerganian's inbred stock (9). Lines of deficient cells were obtained by selecting cells from small aberrant colonies that appeared in cultures having received 500 rads of X radiation.

**MEDIA** Human kidney cells were cultured in Eagle's minimum essential medium (MEM) (10) containing 10% fetal bovine serum. Chinese-hamster cells were cultured in medium similar to Elkind's HU-15 (2). For respirometry, cells were suspended in MEM for suspension cultures (11). All media contained 50 units per milliliter each of penicillin and streptomycin. All solutions were obtained from Microbiological Associates, Bethesda, Md.

**X IRRADIATION** For X-ray dose-response experiments 35 mm covered plastic dishes, on which a specified number of cells had been plated 4 hr previously and on which  $5 \times 10^4$  cells killed by 4,000 rads of X radiation had been growing for at least 20 hr (12), were irradiated in air with medium present. Viable colonies were allowed to develop from surviving cells, with medium changes as required (usually every 5 days).

**HEAVY-ION IRRADIATION** The medium was removed for all heavy-ion irradiations, and uncovered dishes were held in small compartments of a wheel that enabled them to be irradiated serially by the beam. The compartments were sealed with a mylar-film cover and the atmosphere inside replaced by flowing air saturated with water vapor and 4% in  $\text{CO}_2$  during irradiation. The medium was then replaced.

**DOSIMETRY** X irradiations were performed with a Machlett OEG-60 X-ray tube powered by a Picker 60-kV full-wave rectifier. The tube was operated at 50 kV and filtered by  $0.473 \text{ g/cm}^2$  of aluminum. The half-value layer of this radiation was  $0.045 \text{ g/cm}^2$  in copper,  $0.265 \text{ g/cm}^2$  in aluminum, and  $1.30 \text{ g/cm}^2$  in water. The doses reported here are based on an output of 387 rads/min at 25 mA, as estimated by ferrous sulfate dosimetry and extrapolating to zero thickness of the solution at the surface of a plastic petri dish (13).

Heavy-ion irradiations were performed at the Berkeley heavy-ion linear accelerator (HILAC). Doses were measured with an integrating ionization chamber that interrupted the beam automatically after a preset dose. The chamber was constructed of two aluminized mylar foils and is described in greater detail elsewhere (14). The chamber was calibrated by microscopic measurements of its dimensions and by evaluation of its response to X rays. The agreement with X-ray dosimetry was within the error limits of the measurements (about 4%).

**KARYOLOGY** Chromosome preparations were made by the air-dry method of Rothfels and Siminovitch (15), except that 0.17% NaCl is used instead of water in making the medium hypotonic (16).

**RESPIROMETRY** Oxygen consumption was measured by classical manometric techniques (17). Equal numbers of cells were equilibrated in 2 ml of MEM for suspension at  $37.0^\circ\text{C}$  for 5 to 10 min before continuous measurement of pressure began. Pyruvate was initially absent, and glucose was initially present at a concentration of 1 g/liter.

## RESULTS

**HUMAN CELLS** The colony-size distributions of control and irradiated cultures of human kidney cells are shown in Fig. 1. Figure 2 presents the dose-response curve for the progeny of cells selected from a small aberrant colony that developed after exposure to 500 rads of X radiation. This line was designated T91M as shown on the figure. The cells of this line were more radiosensitive and grew more slowly than the normal T1 cells, as can be seen by comparison of the survival and growth curves for the two lines.

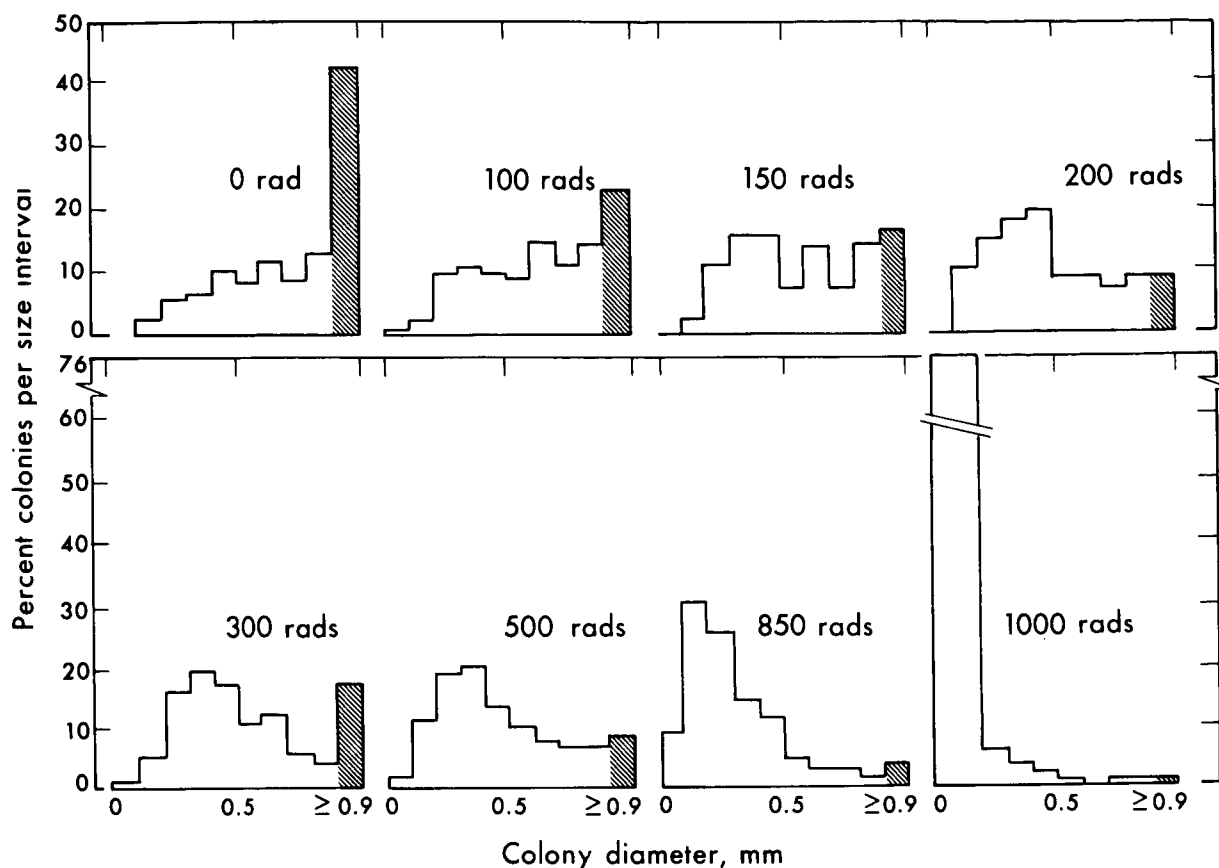


Figure 1. Colony-size distributions of T1 cells exposed to various doses of 50 kVp X rays and allowed to grow 12 days. The ordinate is percent of cells per 0.1 mm diameter interval. Uppermost size class is artificially high because of the inclusion of all colonies greater than 1.0 mm in diameter. Corresponding surviving fractions were:

100 rads:  $0.771 \pm 0.060$   
 150 rads:  $0.587 \pm 0.044$   
 200 rads:  $0.621 \pm 0.077$   
 300 rads:  $0.366 \pm 0.045$   
 500 rads:  $0.100 \pm 0.008$   
 850 rads:  $0.0102 \pm 0.0008$

MUB-4488

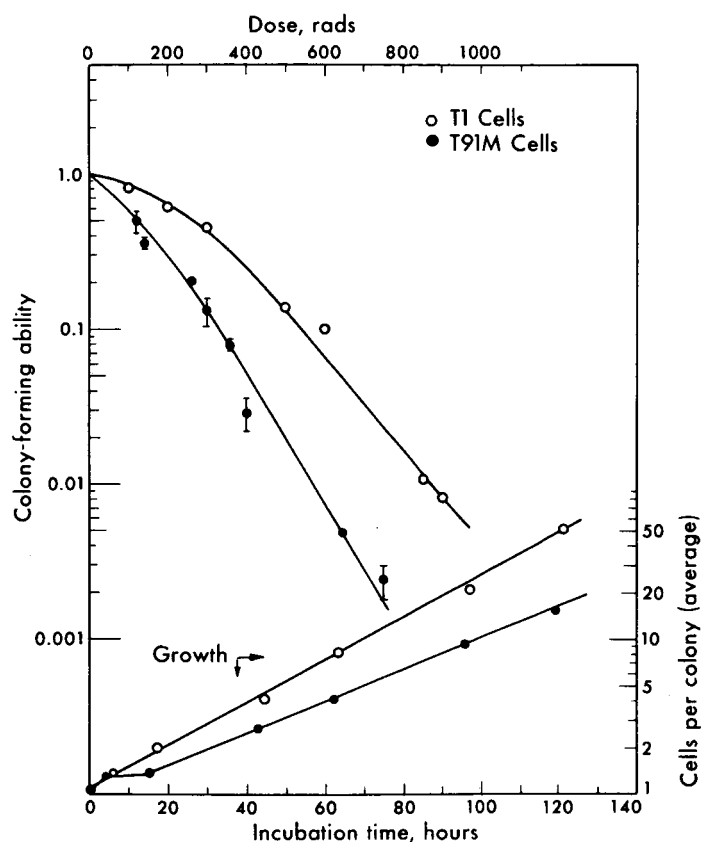


Figure 2. Growth and X-ray survival curves of T91M deficient human kidney cells (solid circles) compared to those of normal T1 cells (open circles). Plating efficiency was  $137.5 \pm 11.0\%$  for T1 cells and  $38.8 \pm 11.9\%$  for T91M cells. MU-34663

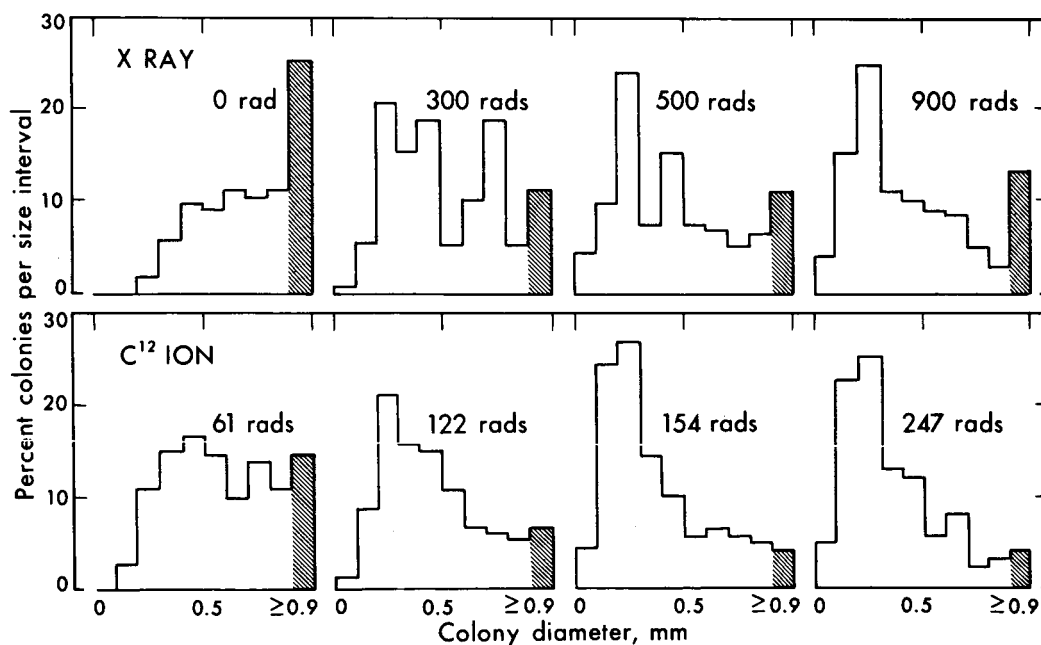


Figure 3. Colony-size distribution of T1 cells exposed to various doses of 50 kVp X rays and <sup>12</sup>C ions. Histograms are formed on the same basis as described in Fig. 1 after 12 days of growth.

MUB-4489

**HIGH-LET RADIATION** Colony-size distributions for cultures irradiated with graded doses of X rays ( $\text{LET} \approx 5 \text{ keV}/\mu$ ) and fast carbon ions ( $\text{LET} \approx 200 \text{ keV}/\mu$ ) are compared in Fig. 3. Lower doses of carbon ions were delivered.

**RESPIRATORY DEFICIENCY** The time course of oxygen consumption by the deficient T91M human kidney line is compared with that of the parent T1 line in Fig. 4a. Figure 4b presents a similar paired comparison of normal and deficient Chinese-hamster cell lines.

**KARYOLOGY** Four sublines derived from irradiated Chinese-hamster M3-1 cells were selected and tested for increased radiosensitivity and decreased growth rates. According to Fig. 5, which compares growth and X-ray survival of the deficient lines to those of the normal parent line, at least three of these lines differed from normal.

At the same time, the karyotypes of these four lines were compared to that of normal M3-1 cells. That no observable change from the near-diploid chromosome number occurred is indicated in Fig. 6, and selected strict diploid idiograms obtained from all lines did not appear to differ qualitatively, as indicated in Fig. 7. No abnormal (broken, dicentric, ring, etc.) chromosomes were seen in any of the cultures except those that are said to arise spontaneously in hamster cell cultures (18, 19).

## CONCLUSIONS

The questions asked at the outset can be answered in the following manner:

1. Colonies of deficient cells appear in X-irradiated cultures of human as well as hamster cells.
2. High-LET radiation is more effective than X radiation in the production of deficient cells, by the criterion of small-colony development.
3. Deficient cells are respiratory deficient only to the extent that they consume less oxygen than do normal cells. Further biochemical characterization is required to determine the relationship between these cells and cytochrome-deficient microorganisms.
4. Hamster cells do not express their inherited deficiencies visibly in their karyotypes. This does not conclude, however, that heritable chromosome aberrations cannot result in cellular deficiencies of the type described here.

## ACKNOWLEDGMENTS

The author is grateful to Drs. Warren K. Sinclair, Robert H. Haynes, and Cornelius A. Tobias for interesting discussions of the problem, and to Dr. Tobias for his continued support. The responsible assistance of Willie M. Jackson and A. -M. Mamoon is gratefully acknowledged.

This research was jointly supported by the U. S. Atomic Energy Commission and the National Aeronautics and Space Administration.

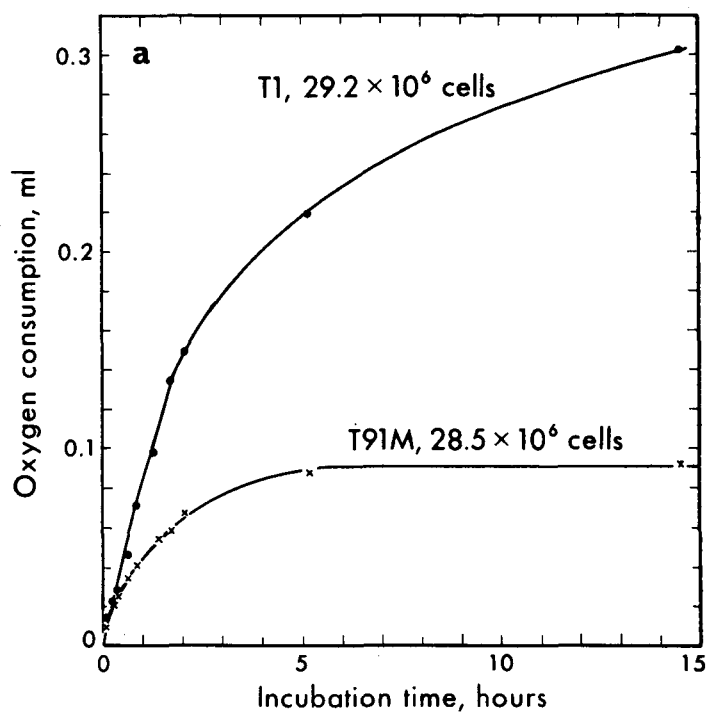


Figure 4a. Oxygen consumption curves for parallel cultures of T1 cells and T91M cells in MEM spinner medium initially containing 1 g/liter glucose and no pyruvate. Initial slopes are nearly equal, but total substrate utilization appears to be less. MU-34664

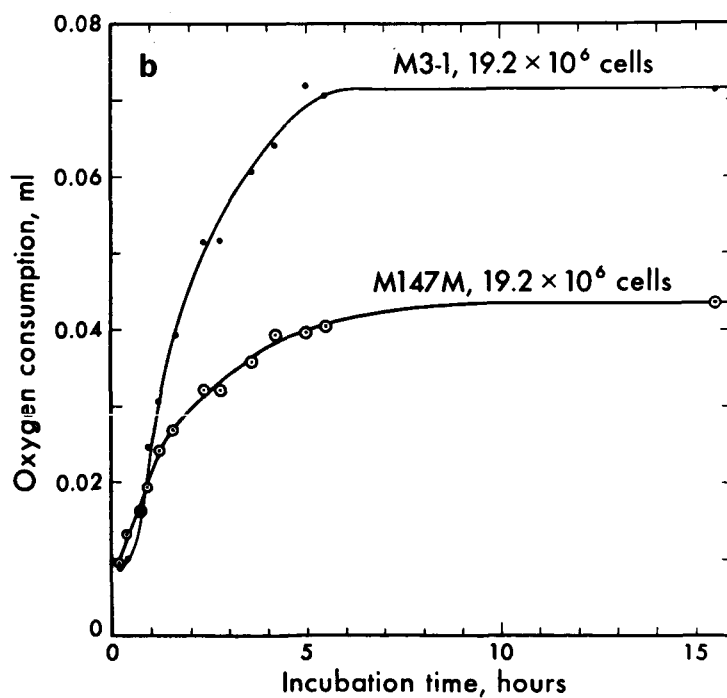


Figure 4b. Oxygen-consumption curves for parallel cultures of M3-1 and M147M cells in MEM spinner medium containing 1 g/liter glucose and no pyruvate. Initial slopes are similar, but total substrate utilization appears to be less.

MU-34671

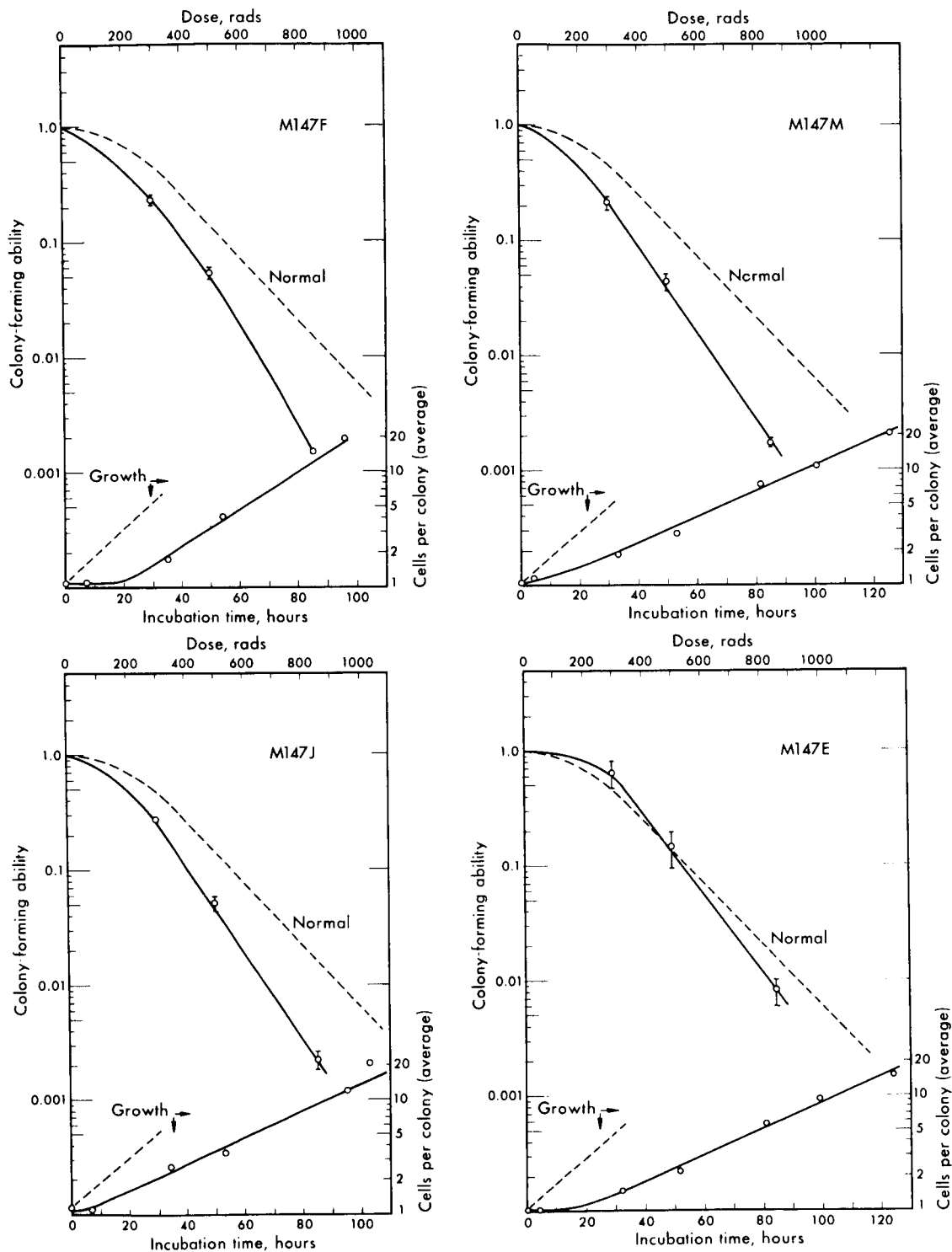


Figure 5. Growth and radiation-survival curves for four sublines of Chinese-hamster cells derived from single irradiated M3-1 cells. Dashed curve corresponds to results expected with M3-1 cells. The radiation-survival curve of line M147E did not appear to differ from the normal.

MU-34669

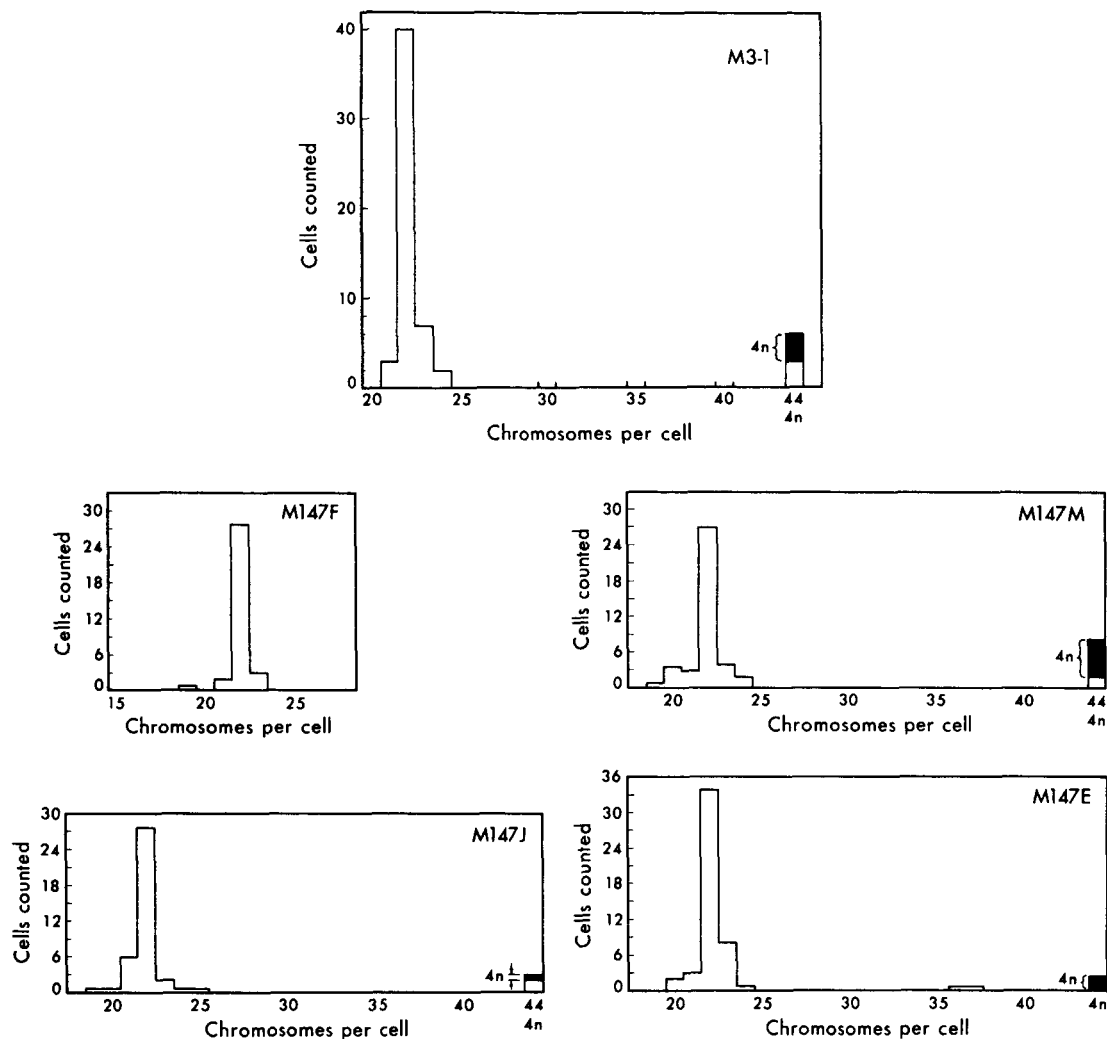


Figure 6. Chromosome number distributions of cultures of four sublines of Chinese-hamster cells derived from single irradiated M3-1 cells -- the same lines as were used to obtain the data of Fig. 5. Chromosome-number distribution of Chinese-hamster bone-marrow M3-1 cells is presented in top graph for comparison. Shaded areas denoted "4n" represent approximately tetraploid cells in which the number of chromosomes could not be clearly determined.

MUB-4465



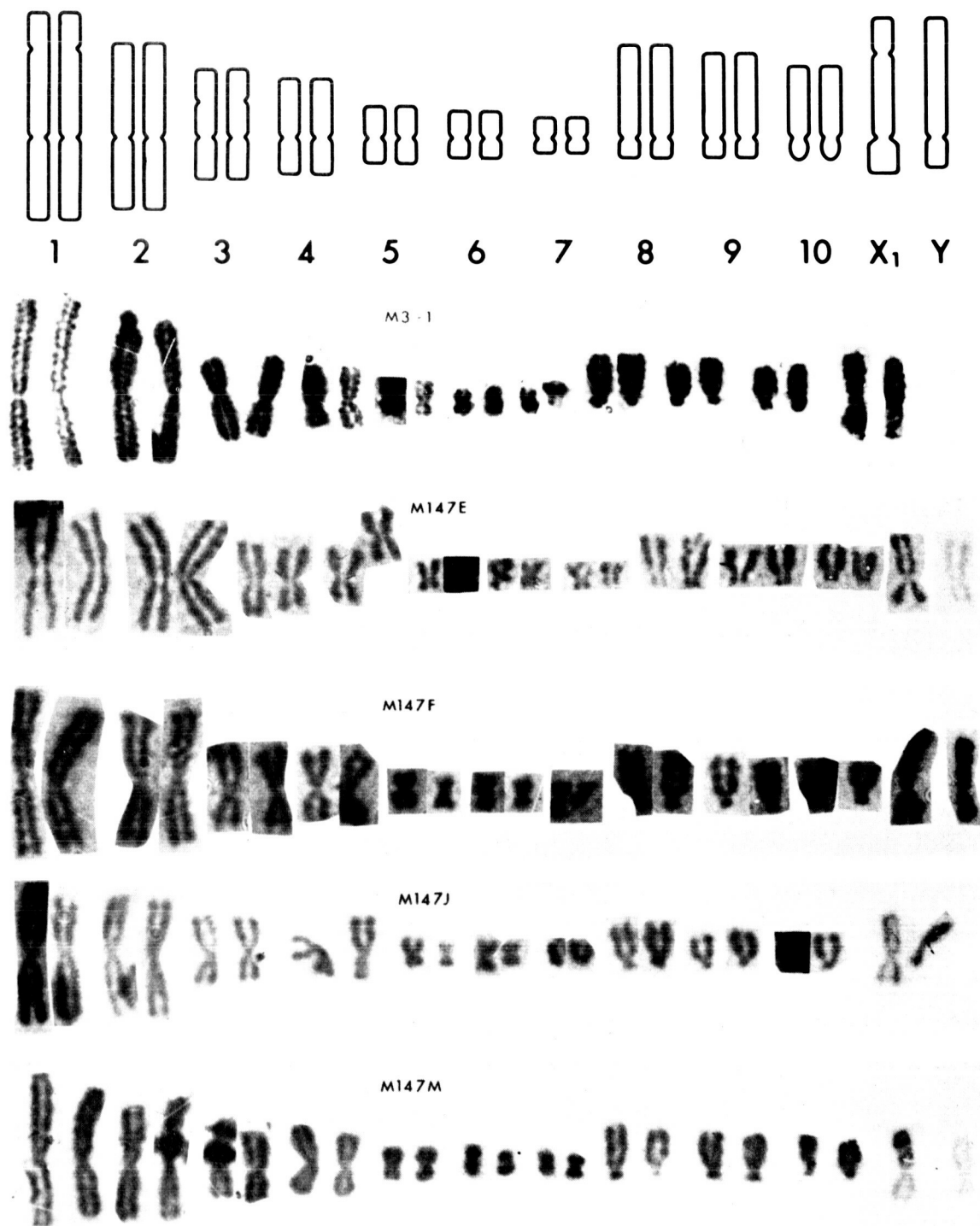


Figure 7. Idiograms of diploid cells from four sublines of Chinese-hamster cells derived from single irradiated M3-1 cells (the same lines as were used to obtain the data of Fig. 5), compared to that of the unirradiated parent M3-1 line and the schematic diploid karyotype (20).  
ZN-4431

## REFERENCES

1. Puck, T. T.; Progr. in Biophys. 10:237, 1960.
2. Elkind, M. M., and Sutton, H.; Radiation Res. 13:556, 1960.
3. Sinclair, W. K.; Radiation Res. 21:581, 1964.
4. Ephrussi, B.: Nucleo-Cytoplasmic Relations in Microorganisms, Oxford, Clarendon Press, 1953.
5. Raut, C., and Simpson, W. L.; Arch. Biochem. Biophys. 57:218, 1955.
6. Ruddle, F. H.; Cancer Res. 21:885, 1961.
7. Barendsen, G. W.; Beusker, T. L. J.; Vergroesen, A. J., and Budke, L.; Radiation Res. 13:841, 1960.
8. Van der Veen, J.; Bots, L., and Mes, A.; Arch. ges. Virusforsch. 8:230, 1958.
9. Yerganian, G.; J. National Cancer Inst. 20:705, 1958.
10. Eagle, H.; Science 130:432, 1959.
11. Microbiological Associates, Catalog and Price List p. 11 (Bethesda, Md., 1964).
12. Puck, T. T., and Marcus, P. I.; Proc. National Acad. Sci. U. S. 41:433, 1955.
13. Weiss, J.; Allen, W. O., and Schwarz, H. A.; Brookhaven National Laboratory Report BNL-2319.
14. Todd, P. W.; Lawrence Radiation Laboratory Report UCRL-11614, 1964 (unpublished).
15. Rothfels, K. H., and Siminovitch, L.; Stain Technol. 33:73, 1958.
16. Tjio, J. H., and Puck, T. T.; J. Exptl. Med. 108:259, 1958.
17. Umbreit, W. W.; Burris, R. H., and Stauffer, J. F.: Manometric Techniques, Minneapolis, Burgess Publ. Co., 1961.
18. Ford, D. K.; Canadian Cancer Conf. 3:171, 1959.
19. Ford, D. K.; Wakonig, R., and Yerganian, G.; J. National Cancer Inst. 22:765, 1959.
20. Yerganian, G.; in Methodology in Mammalian Genetics, edited by W. J. Burdette, San Francisco, Holden-Day Co., 1963, p. 469.

# Fluctuations of Energy Loss by Heavy Charged Particles in Thin Absorbers

N67 15950

Howard D. Maccabee, Mudundi R. Raju and Cornelius A. Tobias

When a charged particle passes through matter, it loses energy by a series of collisions with the electrons of the material. In first approximation, the probability of an energy loss  $\epsilon$  in a single electronic collision is proportional to  $\epsilon^{-2}$  (1). Thus collisions resulting in large energy transfers to an electron are relatively infrequent compared to small-energy-loss collisions. Although they are relatively infrequent, the large-energy-loss collisions account for a significant proportion of the total energy transfer. In a thin absorber (one in which the total energy lost is small compared to the kinetic energy of the particle), the probable number of large-energy-loss collisions may be so small that the random statistical fluctuations in this number result in significant fluctuations in the energy lost in this mode, and thus fluctuations in the total energy transfer will occur. This phenomenon has been theoretically investigated by Landau (1), Symon (2), Vavilov (3) and others. Experimental investigations have been carried out by Gooding and Eisberg (4), Rosenzweig and Rossi (5), and Grew (6), all of whom compared their data with the theory of Symon.

In Vavilov's exact treatment, the dimensionless parameter  $\kappa$  is introduced, and it is shown that for  $\kappa \ll 1$  the fluctuations are large, while for  $\kappa \gg 1$ , the fluctuations are negligible, and the normal Gaussian shape of the total energy loss distribution is valid.

$$\kappa = 0.150 \left( \frac{SZz^2}{A} \right) \left( \frac{1-\beta^2}{\beta^4} \right) \quad \text{where}$$

$S$  = thickness of absorber in  $\text{g/cm}^2$

$Z$  = atomic number of absorber

$A$  = atomic weight of absorber

$z$  = charge on incident particle

$\beta$  = speed of incident particle  $\div$  speed of light

$\kappa$  may be thought of as a measure of the ratio of the total energy loss to the maximum possible energy loss in a single collision, i. e., an estimate of the number of large-energy-loss collisions suffered by the particle in passage. The purpose of our investigation is to verify experimentally the Vavilov theory over the whole range of  $\kappa$ , and to determine its implications for biological targets.

## METHOD

In a previous paper (7) we have described the advantages of Lithium-drifted Silicon semiconductor detectors for this work, the general method used and the results of several

preliminary experiments. In the preliminary experiments we found significant deviations between the theoretical energy-loss distributions and those we measured. We surmised that these discrepancies on the low-energy-loss side of the curves were due to edge effects in our detectors, i.e., the sensitive thickness is slightly less at the edges than at the center, and some beam particles pass through at the edges without "seeing" the full detector thickness. In order to correct this geometrical problem in the present series of experiments, we used another smaller detector as a coincidence gate to eliminate all pulses from particles passing through the edges of the "analyzing" detector. A block diagram of the experimental setup is shown in Fig. 1.

## RESULTS

We have performed a series of ten experiments at the 184-in. synchro-cyclotron using 730-MeV protons and 910-MeV alpha particles, covering the range of  $\kappa$  from 0.0033 to 1.02. The results of three typical experiments are shown in Figs. 2, 3, and 4. Figure 2 is a plot of the data from a run with 730-MeV protons passing through a Silicon detector of thickness  $0.66 \text{ g/cm}^2$ , yielding  $\kappa = 0.0338$ . The solid curve is a plot of the Vavilov theoretical distribution as computed from the program of Seltzer and Berger (8). Figure 3 is a plot of the data from 910-MeV alpha particles passing through a detector of thickness  $0.413 \text{ g/cm}^2$ , yielding  $\kappa = 0.638$ . Figure 4 is a plot of the data from 730-MeV protons passing through a detector of thickness  $0.0645 \text{ g/cm}^2$ , yielding  $\kappa = 0.0033$ .

## DISCUSSION

Agreement between the measured energy-loss distributions and the theory is good in Figs. 2 and 3. Figure 2 is typical of what may be called the Landau spectrum, occurring at small  $\kappa$  values. The distribution is very asymmetrical, with a long high-energy-loss "tail," and a broad peak around the most probable energy loss (which is significantly less than the mean energy loss). Figure 3 is typical of intermediate values of  $\kappa$  i.e.  $\kappa \sim 1$ . The distribution is very similar to the "expected" Gaussian, but with slight asymmetry, and the most probable energy loss is slightly less than the mean.

In figure 4 there is considerable disagreement between experiment and theory, with the measured distribution much broader than the theoretical. Upon closer examination, however, we find that the full width of the theoretical distribution at half maximum (FWHM) is 29 KeV, while the FWHM resolution of the measuring system at room temperature is approximately 40 KeV. Adding these two quantities in quadrature yields an expected value of 49.5 KeV; this is in good agreement with the measured value. Thus physical resolution limitations on our present measuring system prevent direct verification of the theory in this region of very small  $\kappa$ . In order to surmount this obstacle, we are attempting to improve the resolution of our system to the neighborhood of 5 KeV by cooling our detectors with liquid nitrogen and using special low-noise electronics as developed by Goulding (9).

Work is continuing on several other aspects of this problem, especially on the tabulation of our findings into a form that will be convenient and useful to future experimenters.

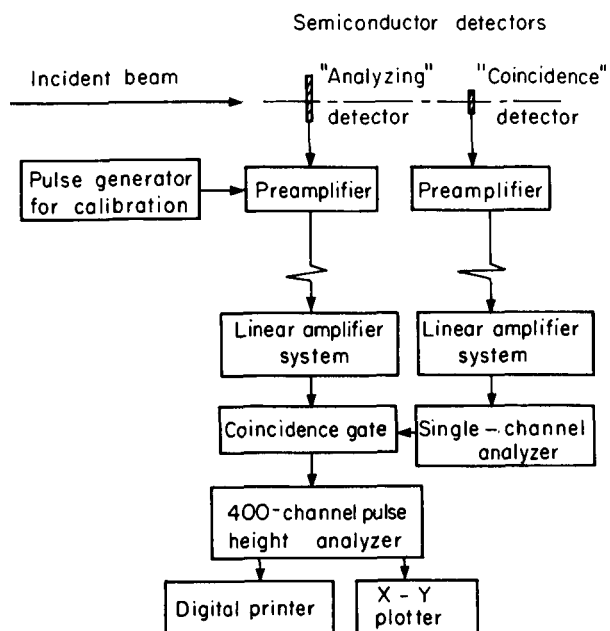
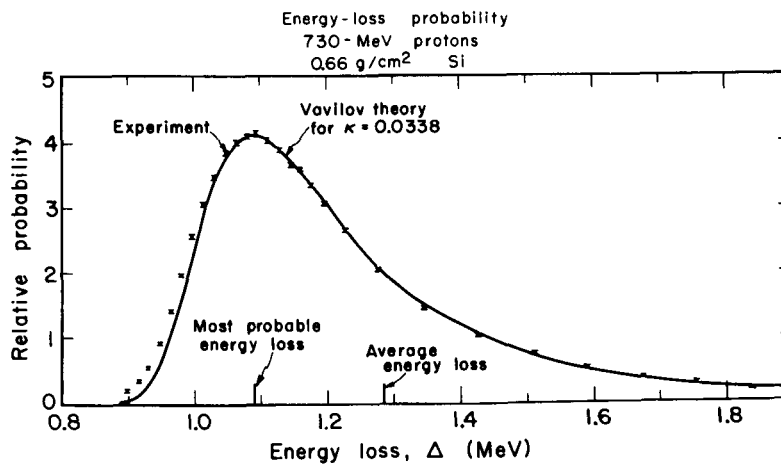


Figure 1. Block diagram of experimental setup.  
MUB-9083

Figure 2. Energy loss probability, 730-MeV protons in  $0.66 \text{ g/cm}^2$  silicon  $\kappa = 0.0338$ .  
MUB-9086



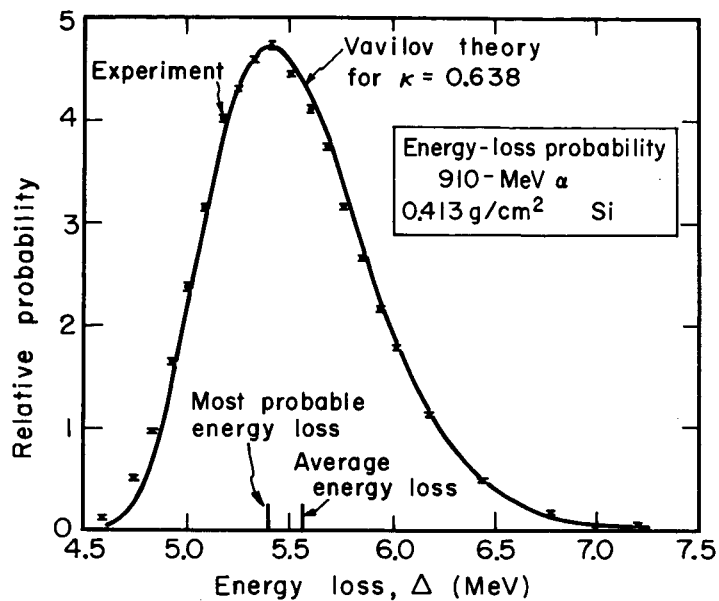


Figure 3. Energy loss probability. 910-MeV alpha particles in 0.413 g/cm<sup>2</sup> silicon  $\kappa = 0.638$ . MUB-9084

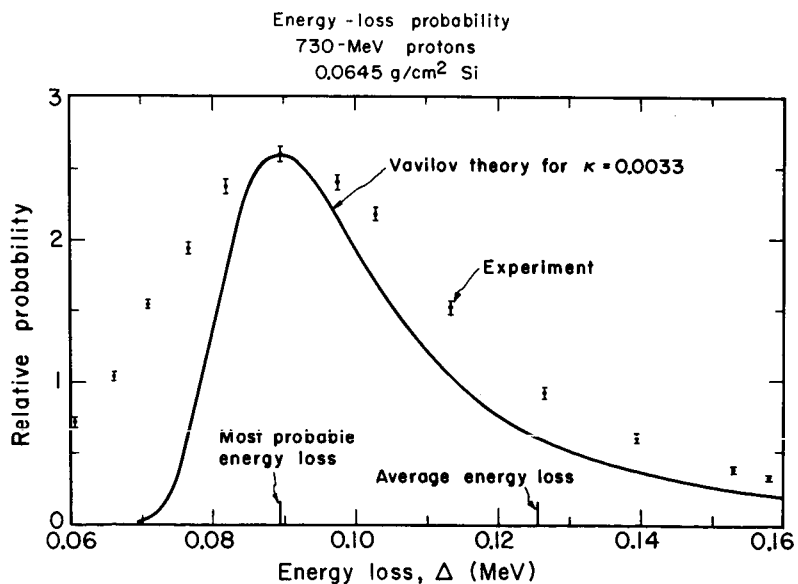


Figure 4. Energy loss probability. 730-MeV protons in 0.0645 g/cm<sup>2</sup> silicon  $\kappa = 0.0033$ . MUB-9085

It is clear that the living cell, and indeed the cell nucleus, acts as a thin absorber with respect to most forms of charged particulate radiation, and thus significant fluctuations in the energy transferred to such biological "targets" are expected. The implications of these fluctuations for radiobiology are also being examined.

### ACKNOWLEDGMENTS

We are obliged to F. Goulding and D. Landis for help with electronics, R. Lothrop for detectors, J. Howard and D. Love for cyclotron operation and V. Brady for computer programming. This work was supported by the National Aeronautics and Space Administration. Mr. Maccabee wishes to thank the Atomic Energy Commission for continued fellowship support.

### REFERENCES

1. Landau, L.; J. Phys. U.S.S.R. 8:201, 1944.
2. Symon, K. R.; Ph.D. Thesis, Harvard Univ., 1948; summarized in High Energy Particles (B. Rossi), New York, Prentice-Hall, 1952, p. 32.
3. Vavilov, P. V.; Zh. Experm. i. Teor. Fiz. 32:920, 1957; English transl: Soviet Phys. JETP 5:749, 1957.
4. Gooding, T. V., and Eisberg, R. M.; Phys. Rev. 105:357, 1957.
5. Rosenzweig, W., and Rossi, H. H.; Columbia Radiological Research Laboratory Report NYO-10716, Nov., 1963 (unpublished).
6. Grew, G.; IEEE Trans. NS-12 No. 1:308, 1965.
7. Maccabee, H., and Raju, M.; Semiannual Report, Donner Laboratory, Lawrence Radiation Laboratory, UCRL-16246: 103, 1965; Nucl. Instr. Methods 37:176, 1965.
8. Seltzer, S., and Berger, M.; NAS-NRC Pub. #1133:187, 1964.
9. Goulding, F. S.; Lawrence Radiation Laboratory Report UCRL-16231:87.

# Secondary-Electron Distribution for Heavy Ions

Nobuo Oda and John T. Lyman

N67 15951

Although it is well known that the contribution of delta rays to the radiation effect of heavy ions is quite significant, our knowledge of  $\delta$  rays is very poor experimentally as well as theoretically. Thus far almost all the  $\delta$ -ray corrections have been made with several simplified assumptions, on the processes of  $\delta$ -ray production as well as on their slowing down, which have not yet been verified by the experiment. Although it is most desirable to obtain complete experimental knowledge of the physical properties of the  $\delta$  rays, some specific information on  $\delta$  rays may suffice (depending on the methods of interpretation of the radiation effects, which used to be the target-theoretical analysis) for the study of the biological effect. Therefore, first let us consider two alternative possible approaches to the  $\delta$ -ray correction.

## TARGET THEORY AND DELTA-RAY CORRECTION

The two alternative approaches are "space-averaged picture" and "extended-track picture."

**SPACE-AVERAGED PICTURE** The exact formulation of this approach was first given by Lea (1). Lea derived the  $\delta$ -ray correction in terms of the "associated volume," in which the so-called overlapping factor  $F$  was calculated on the assumption of a "one-ionization model." A similar approach has been applied by Dolphin and Hutchinson (2) to heavy-ion irradiation of enzymes. The reason why we call this method "space-averaged picture" is that this method does not take into account the spatial correlation between  $\delta$ -ray tracks and the primary track, but regards  $\delta$  rays as distributed uniformly in space, with the intercorrelation among ions along the same  $\delta$ -ray track considered as taken into account through the overlapping factor,  $F$ . A reformulated form of this approach may be given (3) as (i) derivation of the slowing-down spectrum of  $\delta$  rays,  $\phi_{\delta}(E)$ , from the primary particle flux  $\phi_p(E)$ ; (ii) derivation of the inactivation cross section (or volume) with the use of the total differential flux,  $\phi_t = \phi_p(E) + \phi_{\delta}(E)$ , following the calculation method given in reference 3.

This space-averaged picture is a good approximation for the target, which is relatively small compared with the average  $\delta$ -ray range. The most important quantity in this picture is naturally the slowing-down spectrum of  $\delta$  rays,  $\phi_{\delta}(E)$ , which can be theoretically derived through:

- a. The production of secondary electrons by the primary particles, which can be described in terms of the emission cross section of secondary electrons with energies between  $E$  and  $E + dE$  per atom per unit primary flux,  $d\sigma(E)$ . This quantity is usually assumed to be described by the Rutherford formula



for the knock-on collision, but, for the low-energy secondary electrons, some deviation must be expected. This cross section has to be measured for the low-energy secondary electrons.

- b. The slowing-down process of secondary electrons, which requires information on the collision cross section of electrons over the energy range from the maximum  $\delta$ -ray energy down to nearly zero energy for the biologically important substances. Theoretical calculations have been performed, so far, with the use of the theoretical formulae for the stopping power (Bethe-Bloch formula) and for the collision cross section (Møller formula) by Spencer and Fano (4). However, this slowing-down theory has been experimentally examined only at energies above about 50 keV, and its validity below this energy is still not established.

Unfortunately, the maximum energy of  $\delta$  rays for heavy ions with energy 10 MeV/amu (extensively used for radiobiological experiments with the Hilac) is only about 20 keV. This implies that there is now no slowing-down theory available for the slowing-down spectrum associated with heavy-ion beams produced by the Hilac. For electron energies below about 10 keV, the cross section for inelastic collisions depends critically on the electron energy because of the changing participation of inner-shell electrons in the collision process.

A number of measurements at energies below 10 keV has been made for studies of electrons backscattered from solids (5, 6) as well as of the transmission of electrons through thin foils (7). From these measurements, some important information can be derived for electron energies from 10 keV down to 1 keV. For example, the range-energy relation shows no significant dependence on the atomic number of material when the range is measured in mass per unit area, the scattering process is predominantly inelastic, and an estimate of the mean free path for inelastic collisions is in good agreement with the prediction of the Bohr-Bethe theory when the inner-shell effect is taken into account. We can make use of such information to derive the slowing-down spectrum for the energy range down to 1 keV.

It may be expected that the theory will have to be extensively modified before it is valid for electron slowing-down at energies of the order of K-shell binding energy or less. (The electron slowing-down spectrum has not yet been directly measured.) At the same time, it is readily understood that experimental study of such quantities as the emission cross section of secondary electrons with heavy ions, and the collision cross section as well as the stopping power of low-energy electrons, is required before any working theory of the electron slowing-down in the low-energy region can be established.

**EXTENDED-TRACK PICTURE** In this picture, the fundamental quantities may be the differential flux of secondary electrons, expressed as  $\phi_{\delta}(E, r)$ , where  $r$  is the distance from the track of the primary particle, or the energy flux per unit surface out of the cylinder having radius  $r$  and the primary particle track as axis,  $D(r)$ . Unfortunately, there is little relevant experimental data on either of the above quantities.

The quantity  $D(r)$  can be derived in principle from knowledge of  $\phi_\delta(E, r)$ , but can also be derived approximately from the combination of the emission cross section of secondary electrons by heavy ions and the energy-dissipation distribution expressed as a function of distance from the secondary electron source. The latter was calculated by Spencer (8) for the primary electron energies above 25 keV for media of low atomic number, but for energies below that the Spencer theory cannot be expected to be valid and other treatment might be useful, such as the utilization of the range-energy curve for electrons.

This picture properly takes into account the high concentration of activation events in the vicinity of the primary track and also strongly relates to the "track" model of water radiolysis (9). This model, based on the diffusion kinetics of radicals, taking account of the effects of the distribution of spur sizes and  $\delta$ -ray tracks, has been fairly successful in explaining molecular yield effects (10). This model is a kind of indirect-action model in terms of radiation biology, and along these lines we shall be able to construct an indirect-action theory of biological action, as an extension of the pioneer work by Zirkle and Tobias (11).

Along the latter line, Hutchinson (12) has made some calculations on  $D(r)$ , based on several assumptions on the production of secondary electrons, the range-energy relation, and the overall rate of energy deposition of an electron at a distance  $r$  from the primary ion track. Here, we do not go into the details of the  $\delta$ -ray correction for the extended-track picture.

#### LOW-ENERGY SECONDARY-ELECTRON FLUX PRODUCED BY HIGH-ENERGY HEAVY IONS

Even if the slowing-down spectrum of secondary electrons were obtained, by theoretical calculations, from the information discussed previously (b), such a spectrum cannot cover the energy range below about 1 keV. Therefore, direct measurement of the lower-energy part of the slowing-down spectrum would be most desirable--if it were possible.

As a first step in measuring the low-energy secondary-electron flux from heavy ions, an experiment has been done with the Hilac to measure the absolute yield and the slowing-down spectrum of secondary electrons with energies below 50 eV (13). This experiment corresponds to the direct measurement of  $\phi_\delta(E)$ , described under Space-Averaged Picture, which is the differential flux of secondary electrons at a point in a medium bombarded with heavy ions.

Some of the results are discussed here. The apparatus is shown in Fig. 1, where the target consists of three foils, each of which has thickness approximately equal to the range of the maximum-energy  $\delta$  rays. The primary energy of heavy ions was varied with the use of aluminum absorber wheels, and the primary beam intensity was measured by a Faraday cup. A negative voltage (-1200 V) was applied on the suppressor ring between the target and the Faraday cup to prevent disturbance of the reading of the primary beam on the Faraday cup by exchange of secondary electrons produced both from the rear surface of the target and from the Faraday cup. We carried out this measurement at a vacuum of the order of  $10^{-8}$  torr.

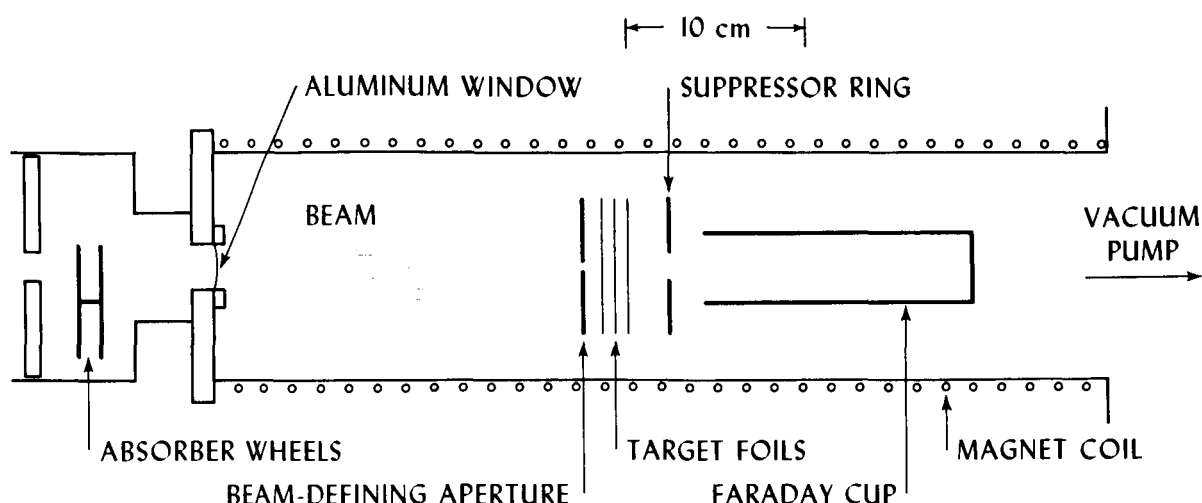


Figure 1. Schematic diagram of the experimental apparatus. MUB-8229

Applying retardation potentials on two outside target foils, we can get the voltage-current curve from the reading of electron current on the central foil. From the voltage-current curve, we can derive the absolute yield as well as the energy spectrum of secondary electrons. To derive the latter, two kinds of angular distribution of secondary electrons were assumed, that is, the isotropic distribution and the cosine distribution. The energy spectra for Al with He ions are shown in Figs. 2 and 3.

It is interesting to see that the energy spectrum is almost insensitive to the assumed angular distribution as well as to the primary energy. The energies, the stopping powers, and the effective charges of the primary heavy ions at several points, such as in the target and at the rear of the target, were derived with the use of data by Northcliffe (14) and Roll and Steigert (15).

In Fig. 4 the yields are plotted as a function of  $Z_{\text{eff}}^2$  for various ions and a Ni target. The yield means the total number of secondary electrons with energies below 45 eV. It is to be noted that the yields for various ions with the same velocity lie on the straight line passing through the origin, and the yields for ions of different velocity deviate from that line. This fact seems to imply that the yield is proportional to the total LET of the primary ions, because the total LET is proportional to  $Z_{\text{eff}}^2$ . However, that this is not the case is shown in Fig. 5, where the yields are plotted as a function of the total LET. From Fig. 5 it is easily seen that the yields with different velocities for each kind of ion are not proportional to the corresponding total LET's. For each kind of ion, the higher-velocity primary particle has the higher specific yield (yield per unit energy absorption).

The following results are obtained from the data: (i) When the velocities of primary ions are the same, the yields for each kind of ion are proportional to the total LET's.

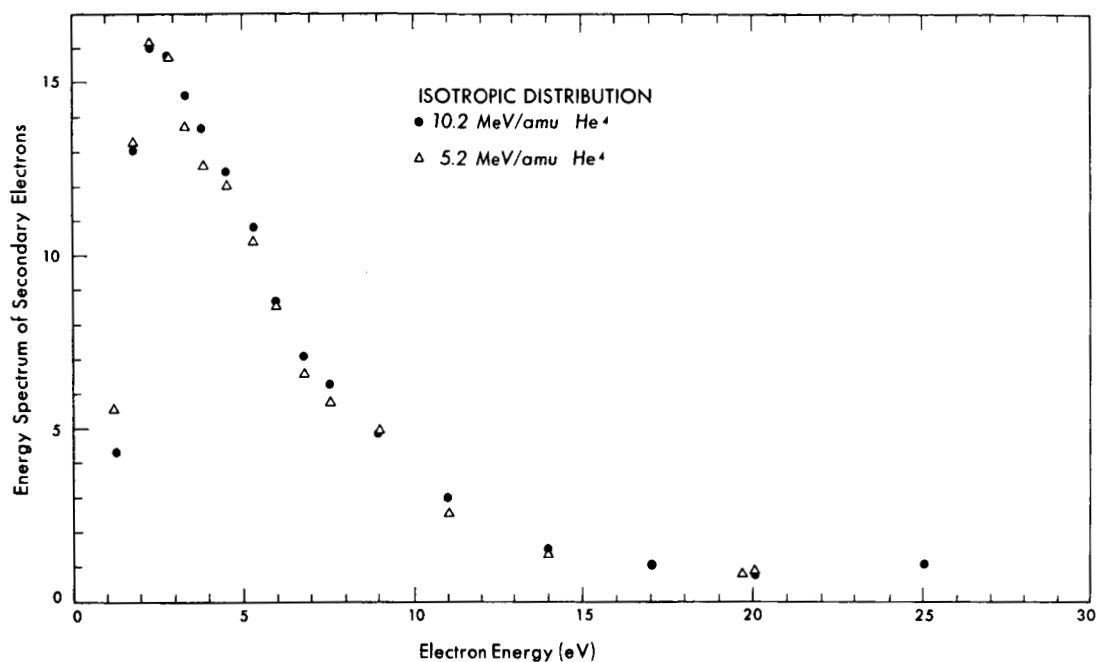


Figure 2. Differential energy spectrum assuming an isotropic angular distribution, for secondary electrons from an Al foil bombarded with  $^4\text{He}$  ions.  
MUB-8230

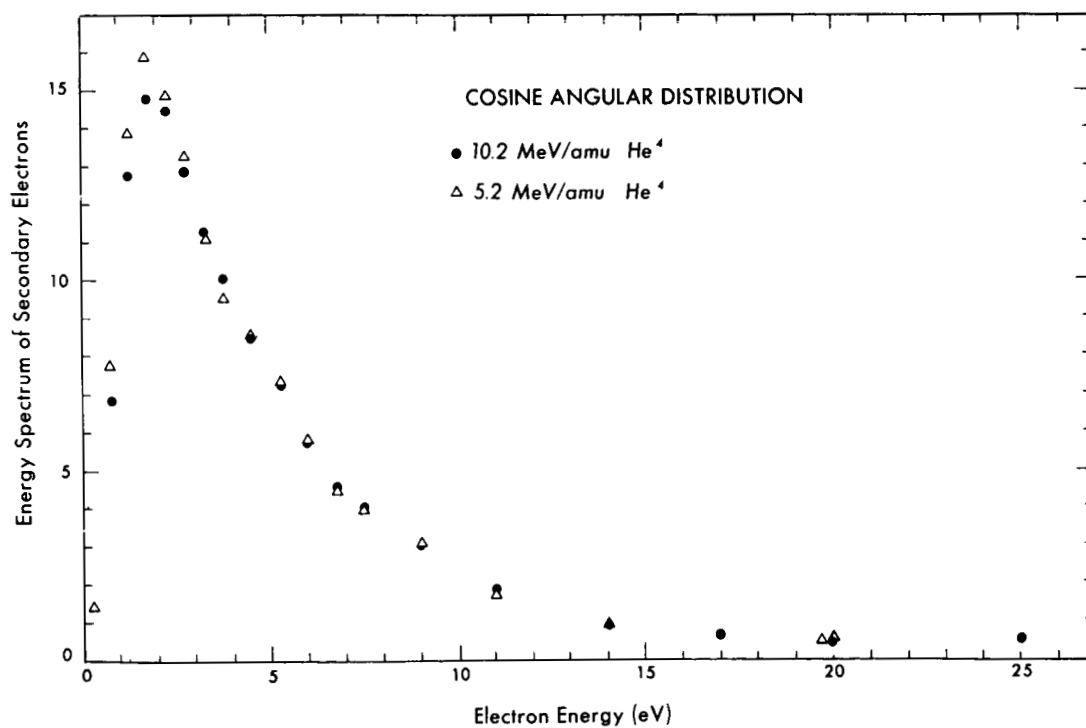


Figure 3. Differential energy spectrum, assuming a cosine angular distribution, for secondary electrons from an Al foil bombarded with  $^4\text{He}$  ions.  
MUB-8231

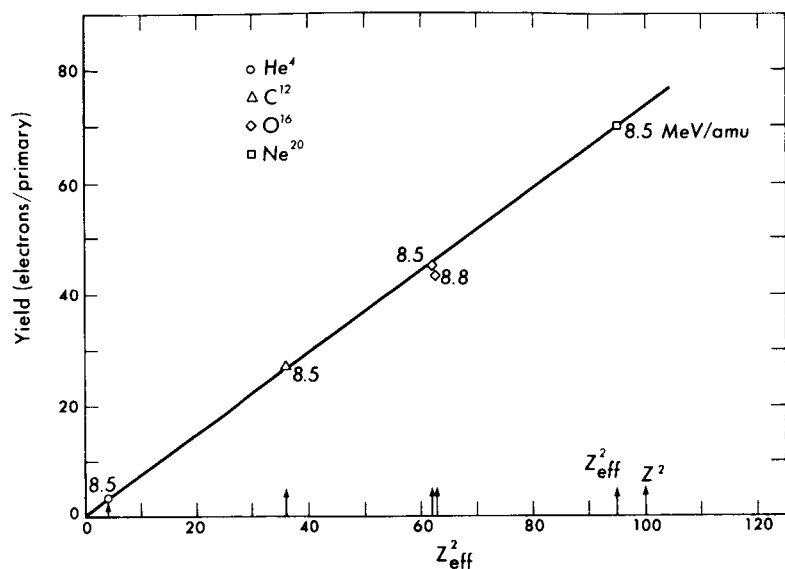


Figure 4. Total yield of electrons from a Ni foil as a function of  $Z^2$  for 8.5-MeV/amu heavy ions. MUB-8232

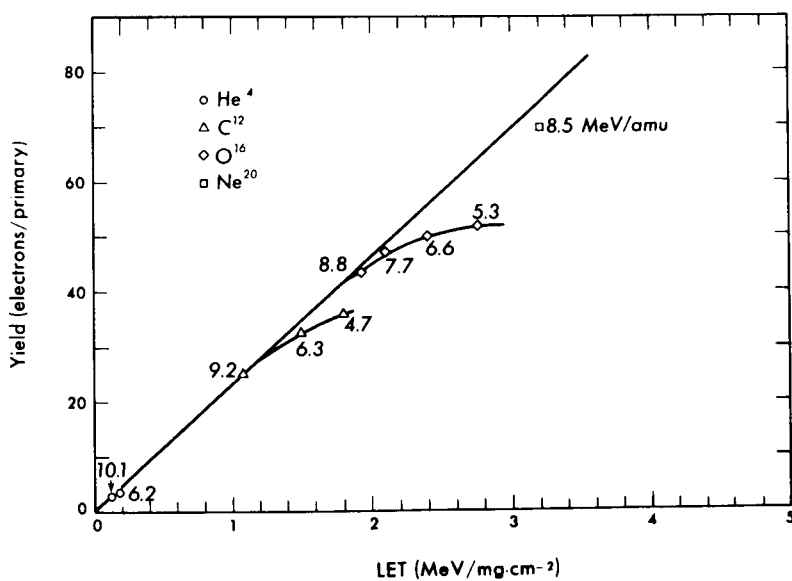


Figure 5. Total yield of electrons from a Ni foil as a function of the total LET for heavy ions with different velocities. MUB-8233

(ii) When the velocities are different, the specific yield for higher velocity is higher than that for lower velocity. These results seem to be strongly related to the production of high-energy secondary electrons ( $\delta$  rays) by the primary particles, because the maximum energy of  $\delta$  rays is proportional to the energy of the primary particles. It is surprising that the low-energy part of the electron slowing-down spectra shows a strong dependence on the maximum energy of  $\delta$  rays.

The yield corresponds to the plane flux when it is normalized per unit energy interval. The spherical flux can readily be derived from the above plane flux, if the appropriate angular distribution of secondary electrons is assumed.

## EFFECTS OF LOW-ENERGY SECONDARY ELECTRONS

Although the role played by low-energy secondary electrons in biological effects has not been much investigated so far, several related problems have received considerable attention in recent years. Several examples are presented in the following, which suggest the importance of studying the behavior of the low-energy part of secondary electron flux.

**THE TRIPLET (METASTABLE) STATE EXCITATION** The excitation of forbidden spin states by electron impact is a resonant process, so that only the electrons with energies close to excitation energy are effective in this process (16). For example, in gases triplet excitations can play an important role, and the relatively long lifetime of the lowest triplet state compared with that of allowed states permits it to participate in chemical reactions while still in the excited state. From this point of view, the significance of the slow electrons should not be ignored.

**SUBEXCITATION ELECTRONS** The important role played by the subexcitation electrons for the total ionic yield in the gas and the yield of F centers in ionic crystals, in both of which some admixed contaminants play a significant role, has been pointed out by Platzman (17, 18). Thus, for the cases in which minor components experience major effects, the usually accepted statement that the primary absorption of energy from ionizing radiation by different components of a system is in approximate proportion to their molecular concentrations may be grossly erroneous. For biological molecules, it is highly possible that the role of the lower-energy electrons might not be a minor one, because the crucial molecular bonds for the radiation effects may in a sense be regarded as some minor components. Further, it is to be noted that for gases 15 to 20% of the absorbed energy comes from the subexcitation electrons, in the case of high-energy radiations.

**CAVITY IONIZATION CHAMBER (GREENING EFFECT)** It is well known that the cavity ionization chamber shows the polarity effect when used at very low gas pressure. This phenomenon has been explained by Greening (19) to be due to the low-energy electron distribution emerging from the walls of an irradiated chamber, and is called the Greening effect. This effect restricts the exact applicability of the cavity principle which is supposed to be exactly valid at the limit of low gas pressure. This should have some bearing on the dosimetry of heavy ions when the cavity chamber is used, but no experimental work on this has been done yet.

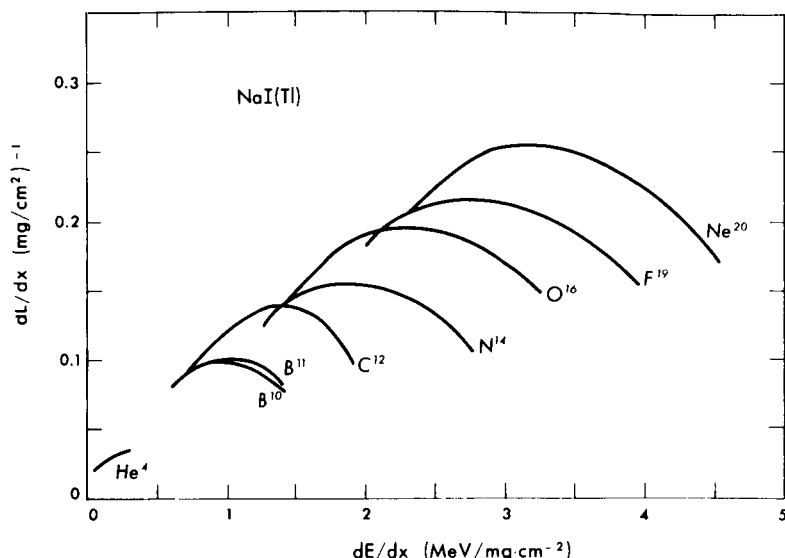


Figure 6. Specific fluorescence of a NaI(Tl) crystal as a function of the total LET. Redrawn from Reference 20. MUB-8234

**FLUORESCENT RESPONSE OF SCINTILLATION CRYSTAL TO HEAVY IONS** The fluorescence of a scintillation crystal caused by ionizing radiation is a kind of radiation effect, and has been studied by many people. Results obtained by Newman *et al.* (20, 21) with heavy ions are very interesting from the viewpoint taken in this paper. The specific fluorescence ( $dL/dx$ ) is shown as a function of the total LET in Fig. 6.

It should be very interesting to note that the specific fluorescence is not a function of the total LET alone, but is instead a function of the velocity of the primary heavy ions, just as is the yield curve of the low-energy secondary electrons shown in Fig. 5. It is probable that this similarity might show some fundamental interrelation between the fluorescence effect and the low-energy electron flux. Meyer and Murray (22) gave a theoretical interpretation of this phenomenon based on the extended-track picture. However, since the fluorescence effect is one of the phenomena in which a minor component (i. e., fluorescent center) plays a major role, it is possible that the low-energy electron flux might significantly contribute to that effect. As in a sense the specific fluorescence corresponds to the inactivation cross section in radiation biology, much more experimental work should be done in radiation biology, too, with heavy ions with different energies, to elucidate the mechanism of the  $\delta$ -ray effects.

## SUMMARY

Two kinds of approaches to the  $\delta$ -ray correction for heavy ions are discussed: "space averaged picture" and "extended track picture." The fundamental quantity for the "space averaged picture" is the differential flux (slowing-down spectrum)  $\phi_\delta(E)$  of  $\delta$  rays. Experimental results on the low-energy part of  $\phi_\delta(E)$  are presented, that is, on the energy spectrum and the absolute yield values. The most interesting results are as follows: (i) When the velocities of primary ions are the same, the yields for each kind of ion are proportional to the total LET's. (ii) When the velocities are different, the yield for higher velocity is higher than that for lower velocity. The discussion of several related problems

suggests the importance of studies on the behavior of energy spectra of secondary electron flux.

### ACKNOWLEDGMENTS

The authors are much indebted to Dr. C. A. Tobias, whose interest made this work possible, and to Jerry Howard and David Love, for their excellent technical assistance.

We also wish to thank Drs. E. Newman and F. E. Steigert for permission to use their graph of the specific fluorescence of a NaI(Tl) crystal (Fig. 6).

This work was supported jointly by the U. S. Atomic Energy Commission and National Aeronautics and Space Administration.

### REFERENCES AND NOTES

1. Lea, D. E.: *Actions of Radiations on Living Cells*, Cambridge, The Cambridge University Press, England, 1954.
2. Dolphin, G., and Hutchinson, F.; *Radiation Res.* 13:403-414, 1960.
3. Oda, N.; Relationships between primary energy transfer and target theory, presented at panel on "Biophysical Aspect of Radiation Quality," Vienna, April 1965 (in press), IAEA.
4. Spencer, L. V., and Fano, V.; *Phys. Rev.* 93:1172-1181, 1954.
5. Sternglass, E. J.; *Phys. Rev.* 95:345-358, 1954.
6. Holliday, J. E., and Sternglass, E. J.; *J. Appl. Phys.* 28:1189-1193, 1957.
7. Kanter, H.; *Phys. Rev.* 121:461-471, 1961.
8. Spencer, L. V.; *Energy Dissipation by Fast Electrons*, NBS Monograph 1, U. S. Department of Commerce, Washington, D. C., 1959.
9. For a review on the "track" model see Magee, J. L.; *Ann. Rev. Phys. Chem.* 12:389-410, 1961; Hart, E. J., and Platzman, R. L.; in *Mechanisms in Radiobiology Vol. 1*, edited by M. Errera and A. Forssberg, New York, Academic Press, 1961, Chap. 2.
10. Kuppermann, A.; in *The Chemical and Biological Action of Radiations Vol. 5*, edited by M. Haissinsky, New York, Academic Press, 1961, pp. 85-166.
11. Zirkle, R. E., and Tobias, C. A.; *Arch. Biochem. Biophys.* 47:282-306, 1953.
12. Hutchinson, F.; in *Medical and Biological Aspects of the Energies of Space* edited by P. A. Campbell, New York and London, Columbia University Press, 1961.
13. Oda, N., and Lyman, J. T.; Measurements of the energy spectrum and the yield of low-energy secondary electrons for high-energy heavy ions (in preparation).
14. Northcliffe, L. C.; *Phys. Rev.* 120:1744-1757, 1960.
15. Roll, P. G., and Steigert, F. E.; *Nuclear Phys.* 17:54-66, 1960.
16. Massey, H. S.; and Burhop, E. H. S.; *Electronic and Ionic Impact Phenomena*, London, Oxford University Press, 1952, p. 145.
17. Platzman, R. L.; *Radiation Res.* 2:1-7, 1955.
18. Platzman, R. L.; *Intern. J. Appl. Rad. Isotopes* 10:116-127, 1961.
19. Greening, J. R.; *Brit. J. Radiol.* 27:163-170, 1954.
20. Newman, E., and Steigert, F. E.; *Phys. Rev.* 118:1575-1578, 1960.
21. Newman, E.; Smith, A. M., and Steigert, F. E.; *Phys. Rev.* 122:1520-1524, 1961.



22. Meyer, A., and Murray, R. B.; Phys. Rev. 128:98-105, 1962.

Nobuo Oda's present address is Tokyo Institute of Technology, Meguro-Ku, Tokyo.

# The Interpretation of Microbial Inactivation and Recovery Phenomena

Robert H. Haynes

N67 15952

A central problem in radiobiology is learning what determines whether a cell will reproduce after irradiation and form a clone under suitable growth conditions. Two related problems are: why is division delayed and how do mutations arise in those cells that do survive. These are important questions in biology, and in trying to answer them we have learned much about cellular responses to specific structural alterations in DNA. Furthermore, recent studies on the recovery of microorganisms after irradiation or chemical treatment indicate that complex enzymic mechanisms exist that serve, in a rather general way, to protect the informational structure of DNA against change. Facts relevant to an understanding of inactivation and recovery come from five types of experiment:

- 1) Microbiological assay of radiation dose-response curves under various conditions that modify radiosensitivity;
- 2) Cytological observation of changes in cell morphology or growth pattern after irradiation;
- 3) Genetic analysis of genes controlling radiosensitivity;  
Biochemical studies of macromolecular synthesis after irradiation;
- 4) Chemical identification of the primary and secondary structural changes produced by radiation in the nucleic acids.

This work has increased our understanding of cell survival and death after irradiation, and it promises also to shed new light on mutagenesis and genetic recombination. Studies on the inactivation of various strains of *Escherichia coli* by ultraviolet light (UV) have played a key role in the development of recent ideas in this field, but there is good reason for thinking that similar concepts apply also to the effects of ionizing radiation and a variety of chemical agents known to attack DNA (1). It is the purpose of this paper to outline the phenomenological background of these developments in molecular radiation biology, and to show that the assumptions of classical target theory can be modified to provide a new mathematical interpretation of radiation survival curves (2). Recent reviews in this field are those of Rupert & Harm, Kimball, Adler, Davies & Evans (3), Weiss (4) and Setlow (5).

## THE CONCEPT OF INTRACELLULAR TARGETS

Biology provides scant support for a view of the cell as such an intimately coupled and uniformly sensitive network of structure and function that disturbance or damage to any part is likely to destroy the rest. Rather, in the light of the modern view of the gene and the central dogma of molecular biology, the early radiobiologists appear quite perceptive in their

assumption that cells contain non-redundant "targets" whose structural integrity is essential for survival. Damage to these targets was assumed to be lethal, whereas damage in other cell components was regarded as irrelevant to inactivation (6).

A given macromolecule or organelle can be an important target for two independent reasons: first, because of its biochemical relevance to the particular end-point being measured, and second, on account of its chemical sensitivity to attack. Obviously, a target must be relevant to the end-point, although it need not be especially sensitive chemically. In the case of inactivation by 2537 Å ultraviolet light, DNA is biochemically "relevant", and it is chemically "sensitive" because of its high specific absorption coefficient at this wavelength.

Allowing that the target hypothesis provides a suitable starting point for thinking about cellular inactivation, the problem can be conveniently subdivided into four broad questions:

- 1) What are the most important target macromolecules for damage relevant to this end-point?
- 2) What kinds of structural defects are produced under various irradiation conditions within these macromolecules?
- 3) How do these defects arise initially from the fast physico-chemical reactions that occur upon absorption of the radiation?
- 4) How does the presence of these defects lead to biosynthetic and replicative failure?

Relatively simple chemical answers may be sufficient for the first two questions, although the second two demand a detailed description of the physical and biochemical processes involved. Present evidence strongly supports the view that DNA is the most important target for microbial inactivation by UV, ionizing radiations and certain chemical mutagens, such as nitrogen mustard (HN2) (1). In this paper I will deal primarily with questions on the assumption that "DNA" is the answer to question one, although obviously no final answers can be given to any of the questions at the present time. Question three is not considered in detail, and it would appear that identification and enumeration of the various kinds of stable defects formed in DNA are sufficient for an understanding of the biological problems with which we are presently concerned.

## EVIDENCE THAT DNA IS AN IMPORTANT TARGET FOR INACTIVATION

There is no indication that DNA is the only target relevant to inactivation by X rays, UV or HN2. However, there is reason to believe that it is an important one, and no other macromolecular target has so far been explicitly identified, although a substantial portion of X-ray induced lethality may be attributed to "non-DNA" targets (7).

The best evidence for DNA as an X-ray and UV target comes from studies on the sensitizing effect of incorporated halogenated base analogs, such as 5-bromouracil (5-BU), in a variety of biological systems including bacteria and mammalian cells, phages and transforming DNA (8-12). For example, Szybalski and Lorkiewicz have shown that the increase

in X-ray sensitivity of *B. subtilis* produced by 5-BU is closely paralleled by a corresponding increase in sensitivity of the transforming DNA extracted from the same cultures (13). RNA can be ruled out as a target since no sensitization is observed in *E. coli* grown in the presence of 5-fluorouracil which, unlike 5-BU, is incorporated into RNA but not into DNA (10). However, it is not clear why 5-BU incorporation has no effect on the sensitivity of *E. coli* to nitrogen mustard, although it does sensitize to attack by mitomycin C (14).

Other lines of evidence that are often cited are as follows:

- 1) DNA synthesis is the most UV-sensitive macromolecular process (15);
- 2) The X-ray sensitivity of organisms ranging from viruses to mammalian cells is correlated with their total DNA content (16);
- 3) Bacterial sensitivity to UV, X rays and HN2 is correlated with the DNA base composition (2, 17);
- 4) X rays, UV and HN2 are all mutagenic and capable of producing chromosome aberrations (18-20);
- 5) The action spectrum for UV inactivation and mutation of various organisms is congruent with a nucleic acid absorption spectrum (21);
- 6) The ploidy of yeast influences its sensitivity to X rays, UV and HN2 (22, 23).

These results provide mostly qualitative, indirect evidence for DNA as a target; however it is difficult to conceive of an experiment that would settle the matter beyond any shadow of doubt. Nevertheless, it may be assumed with fair certainty that DNA is the principal target for inactivation and the success of many experimental predictions based on this view has greatly enhanced its credibility.

## THE DNA INACTIVATION MECHANISM

The first clear demonstration of the role of specific DNA structural defects in killing and recovery phenomena came from studies on UV inactivation and photoreactivation. Here it was shown that UV-induced pyrimidine dimers block DNA synthesis and that enzymic photoreactivation is based on the cleavage of these dimers in situ (24-28). This illustrates what seems to have become the central doctrine of molecular radiation biology: radiation-induced structural defects in DNA, unless repaired, inhibit cell multiplication by blocking the normal biosynthetic activities of the macromolecule. On this basis, survival after irradiation should be determined jointly by the probability of formation and subsequent repair of such DNA defects (1, 2). It is likely that the principal lethal event caused by the presence of unrepaired defects in DNA is irreversible blockage of normal replication; however, alterations in messenger RNA transcription, or lysogenic induction may also be important concomitant mechanisms (29, 30).

It should be emphasized that pyrimidine dimers are the only DNA structural defects that so far have been directly implicated in microbial inactivation. The correlation of the formation of any molecular species with a particular biological effect is hazardous and open to the objection that some other chemically undetected product is involved in the effect. Criticisms of this kind cannot be dismissed lightly since the resolution of most physico-chemical

measurements is greatly outstripped by the potentialities of biological amplification. Clearly, chemical prominence is no guarantee of biological relevance, even under very restrictive experimental conditions.

An oversimplified, but nonetheless useful, DNA inactivation mechanism is outlined schematically in Fig. 1. It attempts to summarize in the most general way the conclusions of many recent studies with *E. coli*. The physico-chemical reactions that give rise to the initial DNA defects are complete within milliseconds and so it is unlikely that they can be influenced by any concomitant metabolic activity. However, the biochemical events crucial to survival occur slowly during the first few hours of postirradiation incubation, and it is these processes that can be significantly affected by the physiological state of the cells. This emphasizes that radiosensitivity can be modified at two distinct levels: by altering either the fast physico-chemical reactions involved in the formation of the initial defects, or the slow biochemical processes involved in their repair. Alterations in the target itself, for example 5-BU incorporation, might affect sensitivity by giving rise to changes at either level (34, 32), although inhibition of repair replication now seems to be regarded as the most important mechanism of 5-BU sensitization (33). In any case, sensitization by attenuation or failure of repair can be invoked to account for a variety of phenomena, including the existence of shoulders on survival curves, synergistic interactions among various inactivating agents, the sensitizing effects of compounds that either bind or are incorporated into DNA (e.g., acridine dyes and 5-BU respectively) (1), and the effects of such "physiological" variables as stage in the mitotic cycle, time of harvesting from batch cultures and the type of growth medium (7).

The diagram (Fig. 1) is intended to illustrate two main postulates:

- 1) Certain DNA structural defects irreversibly block normal DNA synthesis upon reaching the growing point of the bacterial chromosome. This seems to be well-established for UV-induced pyrimidine dimers (28).
- 2) Repair and normal replication are competitive processes in that the onset of repair tends to slow down or inhibit normal replication. (There is no direct evidence for this idea, but it seems essential for the formulation of a simple and logically consistent picture of inactivation.)

These postulates can be applied to the macromolecular events in UV-resistant and sensitive strains of *E. coli* as follows:

In sensitive strains, such as  $B_{s-1}$ , there is no repair, so that after a dose of UV sufficient to form at least one dimer per chromosome, normal replication continues for a brief period until the defect reaches the growing point (25). This irreversibly blocks further synthesis, and cell multiplication is impossible.

In resistant strains, such as  $B/r$ , we assume the existence of a number (perhaps a few hundred) of repair enzyme complexes that attack the defects momentarily after they are formed. According to the second postulate this rapid onset of repair accounts for the immediate cessation of DNA synthesis in  $B/r$  as compared with its more delayed, but irreversible, inhibition in  $B_{s-1}$  (25). At low doses few defects are formed, so that relatively little repair occurs and normal replication is slowed

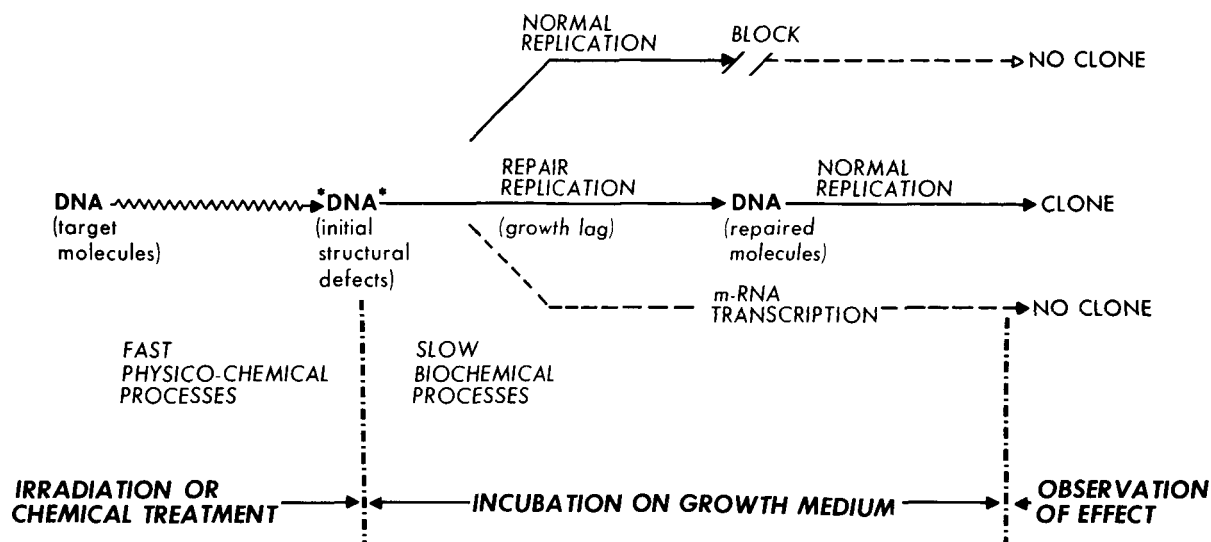


Figure 1. A schematic outline of the most general features of the DNA inactivation mechanism for bacteria. As for many radiobiological effects, it is convenient to distinguish three main stages: 1) Irradiation and the immediate physico-chemical absorption processes; 2) Biochemical responses during incubation on the growth medium; 3) Observation of the net biological effect in terms of clone-forming ability. Here it is assumed that DNA is one of the principal targets for damage relevant to cellular inactivation; that chemically stable structural defects (represented by asterisks) are formed in DNA by either the direct or indirect action of the radiation; that the presence of these defects triggers repair replication; and that if all the potentially lethal defects are repaired, normal replication resumes and a clone may be formed. Repair and normal replication are regarded as competitive processes and if, for any reason, normal replication proceeds before repair is complete, its subsequent irreversible blockage by an unrepaired defect makes clone formation impossible. A possible alternate route to lethality would be via blocked or erroneous m-RNA transcription. MUB-10757

only briefly before it resumes at the normal rate if no damage remains. At moderate doses such that the number of defects equals or exceeds the number of functional repair complexes, there would be a greater chance that a potentially repairable defect would escape repair and reach the growing point upon resumption of normal replication. This suggests that there would be an ever increasing probability of death because of a decreasing efficiency of repair with increasing dose.

Thus, pyrimidine dimers may act as either permanent or temporary blocks to normal replication, depending on whether they are to be found at the growing point or in association

with a repair complex. And competition between repair and normal replication provides a convenient explanation for the origin of the UV-induced lag in growth and DNA synthesis in *E. coli* B/r. However, it is difficult even to guess the reason for the suggested competition. It seems unlikely that the precursor pool or energy supply would be sufficiently limited for this to be a factor. It may be simply that the physical attachment of the repair complexes is sufficient to retard the rate of advance of the parental strands past the growing point.

Another manifestation of the competition between repair and normal replication is that subsidiary treatments or events that tend independently to inhibit DNA synthesis or prolong the postirradiation growth lag appear to enhance viability by increasing the time available for repair (34-36). As indicated in Fig. 1, completion of repair and resumption of normal DNA synthesis leads to the formation of a visible colony or clone. However, if there exist inactivation mechanisms other than that based on damage to DNA, resumption of normal replication is more properly regarded as a necessary, but not sufficient, condition for clone formation.

### DNA REPAIR IN DARK REACTIVATION OF UV DAMAGE IN *E. COLI*

The existence of postirradiation processes capable of suppressing the expression of the initial molecular damage has been recognized for some time, and a variety of terms has been used to describe them, for example, reactivation, recovery, restoration, rescue, etc. The word repair is reserved to denote the actual enzymic steps that are involved in such processes. If these phenomena are based on the restoration of structural defects in DNA, then at least three modes of repair are possible a priori: 1) direct repair of the defects in situ (as in photoreactivation); 2) replacement of the defects by local DNA synthesis (as in dark reactivation in *E. coli* B/r); and 3) "bypass" of the defects by recombination between homologous DNA molecules (dark recovery in diploid yeast may be an example of this mechanism (37).

The UV resistance of *E. coli* B/r (Fig. 2) and other similar strains relative to that of sensitive strains such as  $B_{s-1}$  has been attributed to the presence in B/r of a reactivation mechanism capable of repairing UV-induced pyrimidine dimers in DNA (32, 38). This mechanism is either absent or nonfunctional in  $B_{s-1}$ . There is good evidence that repair is effected through a multi-step "cut and patch" process involving nuclease excision of single strand oligo-nucleotide fragments containing pyrimidine dimers, DNA degradation and non-conservative repolymerization, or repair replication, which fills in the resulting gaps (39-43). A suitable "repair replication" reaction in which the 3' -hydroxyl terminus of the gap would serve as a primer for the insertion of nucleotides in the sequence determined by base-pairing with the opposite strand has been described in vitro (44). The sequence and coordination of the overall process is still uncertain. Originally it was suggested that repair is initiated by dimer excision followed by extensive exonuclease degradation of the defective strand in the 5' → 3' direction; this enlarged gap would then be closed by 3' → 5' repolymerization and a rejoining of the last phosphodiester bond. However, the biochemical observations appear to be equally consistent with a model in which repair is initiated by an incision, or single-strand break, adjacent to the defect. This would allow repair replication to begin immediately at the exposed 3' -hydroxyl terminus accompanied by a "peeling back" of the defective strand, with or without its concomitant degradation. A final cut to release the defective strand together with

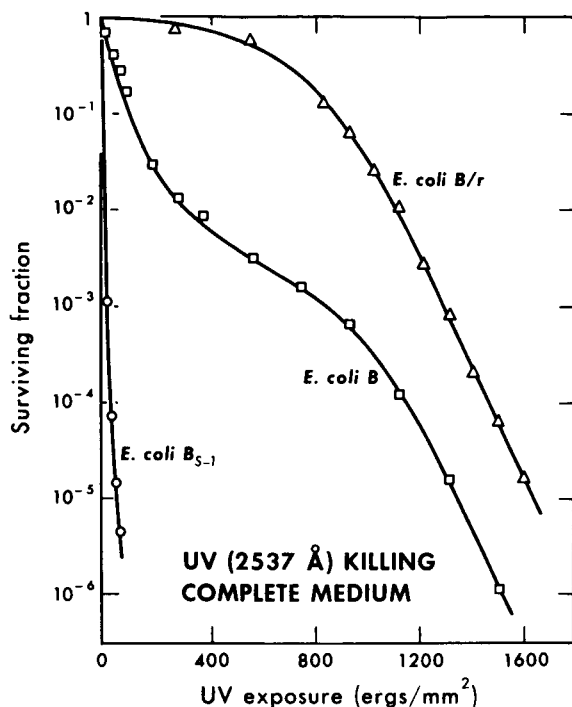
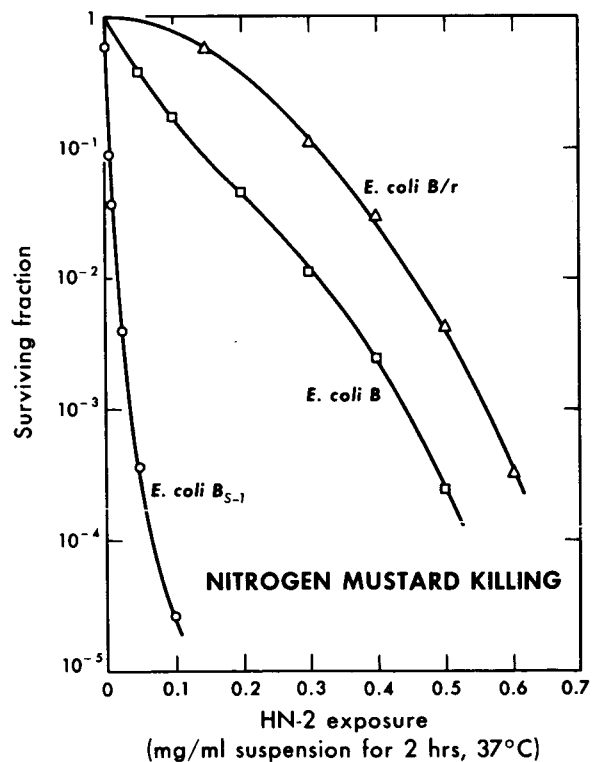


Figure 2. Comparative survival curves of stationary phase *E. coli* B/r, B and B<sub>S-1</sub> for inactivation by 2,537 Å ultraviolet light. The cells were grown overnight in peptone broth, washed and resuspended for irradiation in phosphate buffer, and plated on nutrient (salt) agar. MUB-12202

Figure 3. Comparative survival curves for stationary phase *E. coli* B/r, B and B<sub>S-1</sub> for inactivation by nitrogen mustard (methyl bis (β chloro-ethyl) amine hydrochloride). Buffered suspensions of the cells were incubated with various initial concentrations of the drug for two hours at 37°C and then plated on nutrient (salt) agar to determine survival. MUB-12203





the rejoining step would complete the process. Such a scheme might be called "patch and cut" rather than "cut and patch". At present it appears difficult to devise an experiment that would distinguish unequivocally between these two models, although the latter is attractive because it does not involve the introduction of long, vulnerable single strand gaps in the course of repair.

## GENERALITY OF REPAIR REPLICATION

There are two important questions regarding the generality of repair replication: first, can excision-repair restore defects other than pyrimidine dimers, and second, does such a repair system exist in other organisms? Both of these questions can now be answered in the affirmative. Excision-repair has been demonstrated in *E. coli* B/r after attack by nitrogen mustard, mitomycin C and X rays as well as UV, and similar effects have been observed in *B. subtilis* and *M. radiodurans*. However, it remains possible that different macromolecular events may be involved in the recovery phenomena that occur in yeast and other higher cells.

Survival curves indicating the relative sensitivities of *E. coli* B/r, B and B<sub>s-1</sub> to attack by nitrogen mustard are shown in Fig. 3. The response pattern of these three strains is obviously similar to that observed for ultraviolet light (Fig. 2). The principal DNA defects formed by HN2 are interstrand guanine-guanine cross-links that bear no chemical resemblance to the pyrimidine dimers formed by UV (45,46). This, together with the involvement of nucleases in DNA repair, led to the suggestion that it is not the altered bases themselves that are "recognized" by the repair enzymes, but rather some associated secondary structural alterations, or "kinks", in the phosphodiester backbone (1,47). (It is obvious from the helicity of DNA that a backbone distortion must accompany pyrimidine dimerization.) This idea is supported by three independent biochemical observations: 1) repair replication in *E. coli* TAU-bar after HN2 attack is similar to that observed after UV (48); 2) elimination of alkylated di-guanyl residues from the DNA of *E. coli* T<sup>-</sup>A<sup>-</sup>U<sup>-</sup> after attack by sulfur mustard (49); 3) conversion of HN2 cross-linked DNA to a normally denaturable form in *E. coli* B/r but not in *E. coli* B<sub>s-1</sub> (50). We conclude that DNA defects produced by the bifunctional alkylating agents, nitrogen and sulfur mustard, can be repaired by the excision-repair mechanism (51, 52), although it remains difficult to visualize exactly how the interstrand cross-links produced by these agents are eliminated.

A similar situation holds for attack by the DNA cross-linking antibiotic mitomycin C, which mimics some of the effects of UV and gives rise to more extensive DNA degradation in reactivating than in non-reactivating mutants of *E. coli* K12 (53). This has also been interpreted as evidence for excision-repair of the DNA structural defects produced by this drug.

On the basis of the relative sensitivities of *E. coli* B/r, B and B<sub>s-1</sub> to X rays, and the dose-response pattern of the synergistic interaction between UV and X rays, it was argued that certain X-ray-induced defects in DNA are susceptible of repair in B/r (1,2,23). Recent studies on DNA degradation and resynthesis after X irradiation in *E. coli* B/r and B<sub>s-1</sub> reinforce the view that X-ray-induced defects (as yet unidentified chemically) may be eliminated

by the excision-repair mechanism (54). But because of the ability of X rays to produce single-strand breaks, repair in this instance need not be initiated by endonuclease attack in the region of the defects (55, 56). That is, mutants that are UV sensitive because they are unable to introduce the initial incisions required for repair need not be sensitive to agents that are themselves capable of producing single-strand breaks. In such instances repair could occur if the cells were capable at least of carrying out the repolymerization and rejoining steps of the process. For example, several UV-sensitive mutants of *E. coli* K12 are X-ray resistant (39), as is an *hcr*<sup>-</sup> and UV-sensitive mutant of *E. coli* WP2 (56).

In an elegant series of experiments, Strauss and his colleagues have put forth strong evidence for the existence of a similar multi-step excision-repair system in *B. subtilis* (57-60). They have been able to make use of transformation as well as phage- and cell-survival assays to show that UV-resistant strains can also repair DNA defects produced by HN2 and the monofunctional alkylating agent, methyl methane sulphonate (MMS). However, the initial incision enzymes are not required for the repair of MMS damage since it, like X rays (but unlike UV or HN2), produces single-strand breaks (58). Accordingly, they have found UV sensitive strains that are resistant to MMS, and an MMS-sensitive strain that is sensitive to UV (59, 60). The latter observation is crucial for the current theory since any organism deficient in the final steps of repair should not be able to repair UV damage. In further support of these ideas, Bridges and Munson have shown that *E. coli* WP2 *hcr*<sup>-</sup>, which is UV sensitive and  $\gamma$ -ray resistant, is sensitive to HN2 but resistant to MMS (56).

The above results indicate that a variety of chemically distinct DNA structural defects are susceptible of excision-repair in reactivating strains of *E. coli* and *B. subtilis*. The recognition step in repair may be considered formally equivalent to threading the DNA through a close fitting protein "sleeve" that gauges the closeness-of-fit of the polynucleotide strands to the Watson-Crick structure (48). Such a mechanism might even be able to detect mispairing of normal bases in certain circumstances (61). Strains defective in repair would then exhibit an abnormally high spontaneous mutation rate since repair would tend to maintain genetic stability.

In view of the impressive versatility of excision-repair, it is natural to ask if there are any lesions that cannot be repaired. Studies with mammalian cells indicate that high-LET (linear energy transfer) radiations produce a greater proportion of irreversible damage than do X rays (62, 63), and it is not implausible to imagine that unrepairable DNA damage might be produced within the columns of dense ionization formed along the tracks of such particles (64-66). In a series of experiments with beams of stripped atomic nuclei (9 MeV/amu) from the heavy-ion linear accelerator at Berkeley (67), we found that the differential sensitivity of B/r and B<sub>s-1</sub> declines as the LET of the particles increases, and that the two strains are equally sensitive to partially stripped argon nuclei (Fig. 4). The simplest interpretation of these results is that the fraction of repairable defects (owing to small ionization clusters) declines with increasing LET. This could be attributed to an increasing probability of producing unrepairable DNA double-strand breaks by densely ionizing particles (64-66). However attractive this interpretation, it remains open to the criticism that DNA may be a relatively less

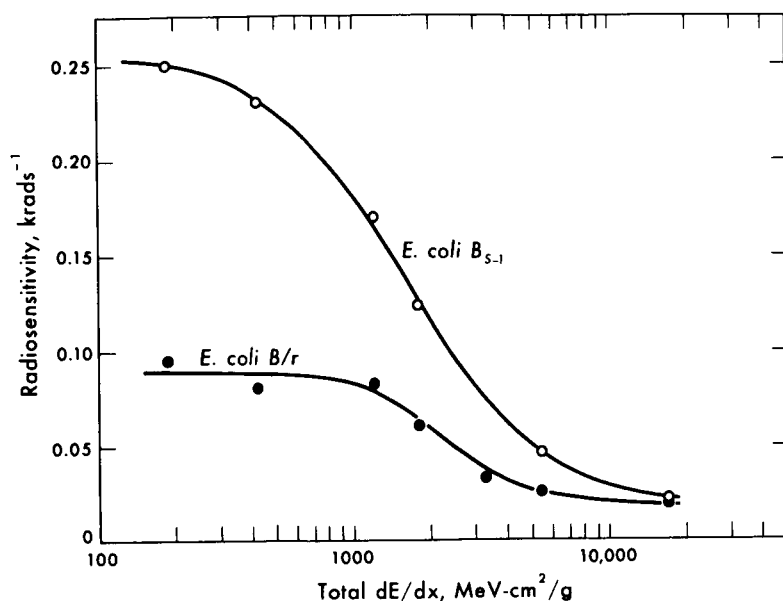
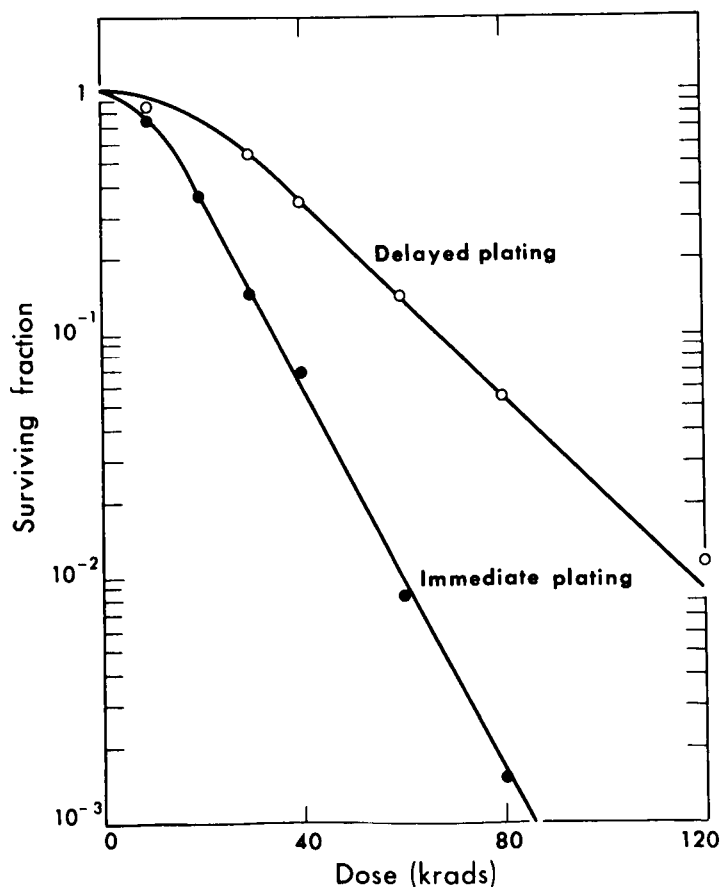


Figure 4. Radiosensitivity ( $LD_{90}^{-1}$ ) of *E. coli* B/r and B<sub>s-1</sub>, irradiated under fully oxygenated conditions, as a function of the total mass stopping power of the various heavy-ion beams (9 MeV/amu) produced by the Berkeley HILAC. All collisional losses (including  $\delta$ -electrons) were included in the calculation of dE/dx, which is used as an approximate mean LET.  
MUB-9397

Figure 5. Recovery of diploid yeast (*Saccharomyces cerevisiae*, strain X841) elicited by 48-hr storage (delayed plating) after irradiation with stripped neon nuclei (9 MeV/amu) under fully oxygenated conditions. The magnitude of recovery is the same as that observed for X-ray or 40-MeV alpha-particle irradiation despite the 30 fold increase in LET.  
MU-35521



important target for these high-LET particles, and that lethality might be due to membrane damage or other processes.

There is evidence for the existence of excision-repair mechanisms in bacteria other than E. coli and B. subtilis. Analysis of the interaction between UV and X rays in Micrococcus radiodurans suggests that the great radioresistance of this organism is due to an extremely efficient DNA repair mechanism (68); and the dramatic way in which it excises pyrimidine dimers has been appropriately described by Jane Setlow (69) as "a sort of molecular striptease"! In addition, I have observed synergistic UV-X-ray interactions in the following species (in each case the maximum UV-induced X-ray sensitization is given in parentheses): M. lysodeikticus (1.4), Ps. aeruginosa (1.7), Ps. fluorescens (1.7), E. carotovora (1.3), E. coli B/r (3.0), H. influenzae (1.9), and M. pyogenes aureus (1.4). It should be noted that E. coli B/r is unusual because the interaction is significantly greater than in any of the other bacteria studied, including E. carotovora, whose DNA base composition is similar to that of coli. If these interactions are correctly interpreted as being caused by the inhibition of repair (1, 2), then it would appear that repair is fairly common among bacteria, although the mechanism in B/r may be unusually efficient.

Recovery after irradiation has been observed in organisms of wide phylogenetic distribution, and in many instances DNA repair might be involved, but it is by no means certain that the enzymic steps are the same in each case. Liquid-holding recovery in diploid yeast and dark reactivation in E. coli are similar in that both appear to be enzymic, energy-requiring processes capable of reversing damage caused by X rays, UV or HN2, but incapable of dealing with damage caused by heat or acridine-sensitized photodynamic action (70, 71). However, they differ markedly in their response to densely ionizing radiation. We have just seen that it is unlikely that high-LET damage can be repaired in E. coli; however, both the survival-curve shoulder and the magnitude of recovery in diploid yeast are independent of LET (Fig. 5) (37). The macromolecular basis of recovery in yeast is unknown but these results strongly suggest that it differs in some fundamental way from excision-repair in E. coli.

## REPAIR AND INTERPRETATION OF SURVIVAL CURVES

In classical target theory, lethality is regarded as the inexorable outcome of the accumulation of an appropriate number of physical "hits" in the target volume(s) (6, 72, 73). Hits are assumed to be independent, randomly distributed events whose number is proportional to dose. For ionizing radiations they have been equated with the number of primary ion pairs (or 110 eV ion clusters) that are discharged in the target volume.\* All relevant hits are assumed to be equally effective and to have unit probability of producing the observed effect. The adjustable parameters in the survival-curve equations characterize the number of hits or targets and their intrinsic sensitivity, (or target volume). Target or hit multiplicity means

---

\*The ideas of target theory and the direct action of ionizing radiation were originally closely linked in the minds of many people. However, this strict "bang, bang, you're dead!" view was subsequently modified to include indirect action by allowing for attack on the target by radiation-induced free radicals diffusing in from the immediate environment (73, 74).

that the basic response is discontinuous, and that at the level of the individual cell there is a threshold dose for inactivation. The observation of smoothly bending shoulders on survival curves is therefore attributed to statistical fluctuations in the number of hits to be found among the cells of an irradiated population at any level of dose. No allowance is made for repair, and the fate of a cell is assumed to be determined the moment irradiation is over. However, if some of the initial hits can be removed by repair before they have had an opportunity to be expressed biologically (Fig. 1), it is meaningless to ask if a cell is "alive" or "dead" immediately after irradiation. Classical theory erred in associating lethality so closely with the initial absorption events, and the target-theoretical equations used to describe survival curves should be modified to allow for the possibility of repair (2).

Lethality is intrinsically an all-or-nothing response, since all that is determined in the plating assay is whether or not a lethal event has occurred in any cell, and every cell either is or is not inactivated. We will call a lethal event a "hit", even though more than one physical absorption event may be necessary to produce it. The occurrence of more than one lethal event in any given cell is in principle unobservable, and we do not admit the definition of "sublethal" hits. If we assume that these "hits" are independent of one another, distributed randomly throughout the population, and since one lethal hit is by definition sufficient to inactivate, then clearly, the surviving fraction (S) of cells decreases exponentially as the expected number of hits per cell increases, i.e.,

$$-\ln S = \left\{ \begin{array}{l} \text{Expected number of} \\ \text{lethal hits per cell} \end{array} \right\} . \quad (1)$$

But what is a "lethal hit"? On the basis of the inactivation mechanism outlined in Fig. 1, it is an "unrepaired DNA structural defect", that, at the end of the time available for repair, constitutes an irreversible block to DNA synthesis. Thus, the initially formed DNA structural defects, may be regarded, before the onset of repair, as potentially lethal hits; any remaining after repair are obligatory lethal hits. That is,

$$\begin{aligned} -\ln S &= \{ \text{Expected number of unrepaired defects per cell} \} \\ &= \left\{ \begin{array}{l} \text{Number of defects} \\ \text{formed initially by} \\ \text{the radiation} \end{array} \right\} - \left\{ \begin{array}{l} \text{Number of defects} \\ \text{removed by repair} \end{array} \right\} \end{aligned} \quad (2)$$

$$\text{or} \quad -\ln S = F(x) - R(x) \quad (3)$$

where F and R indicate that the two curly-bracketed quantities in equation 2 depend on the radiation dose x.

In order to use equation 3 we must make some reasonable inference as to the explicit form of F(x) and R(x). F(x) describes the way in which the potentially lethal DNA defects increase with dose. In principle, this can be determined chemically. However, the simplest assumption, as in classical target theory, is that the number of initial defects is proportional to dose, i.e.,  $F(x) = kx$ , where k is a measure of radiochemical sensitivity. For cross-linking or reactions that might involve more than one absorption event, a quadratic function

might be more appropriate; however, a linear relation appears to be sufficient as a first approximation in the biological dose range.

It is more difficult to arrive at a satisfactory expression for  $R(x)$ , the number of defects removed by repair. However, if the Pettijohn-Hanawalt technique proves to be a suitable quantitative assay for repaired DNA (41), it may yet be possible to determine this function experimentally. A simple trial function can be justified on the basis of the following considerations: (a) the curve for  $R(x)$  must pass through the origin: obviously, no defects can be removed if none are there to begin with; (b) at low doses, it is reasonable to assume that the number of defects repaired increases in proportion to the number there, that is in proportion to the dose; (c) since cells appear to have only a finite capacity for repair,  $R(x)$  should reach a plateau at some suitably high dose. The simplest saturation function consistent with these criteria is  $(1 - e^{-\beta x})$ . Thus, we arrive at the expression,

$$-\ln S = kx - \alpha(1 - e^{-\beta x}) \quad (4)$$

where the parameters  $k$ ,  $\alpha$  and  $\beta$  characterize, respectively, the intrinsic inactivation probability per unit dose, the maximum number of potentially lethal hits which can be repaired, and the manner in which repair saturates with increasing dose.

The slope of the survival curve, obtained by differentiating equation 4, is  $(k - \alpha\beta e^{-\beta x})$ . This indicates that the curve has a shoulder with initial slope  $(k - \alpha\beta)$ , and this increases with dose to the asymptotic value  $k$ . Thus, despite the all-or-nothing character of the end-point, the dose-response curve need not be exponential, if a dose-dependent repair mechanism exists. The asymptote to the survival curve is given by the expression  $kx - \alpha$  and the intersections of this line on the abscissa and ordinate are  $\alpha/k$  and  $\alpha$ , respectively. The "extrapolation number" ( $\alpha$ ) associated with equation 4 is finite, in contrast to the infinite extrapolation number of the classical multi-hit equation (75); and it is equal to the maximum number of hits that are repaired, rather than the number of targets that must be inactivated (as in the classical, one-hit, multi-target equation shown in Fig. 6).

Equation 4 reduces to an exponential in two cases: 1) If no repair mechanism exists, or if none of the defects produced by a given agent can be repaired, then  $\alpha = 0$  and the survival curve is a simple exponential of slope  $k$ . 2) If  $\beta$  and  $x$  are such that  $\beta x \ll 1$ , then  $R(x) \approx \alpha\beta x$  and the curve remains exponential with slope  $(k - \alpha\beta)$  in the experimentally accessible dose-survival range. This shows that even though an exponential response is observed over several decades of survival, it is still possible for repair to be taking place (e.g., the X-ray survival curve is exponential for  $B/r$  as well as  $B_{s-1}$ ).

It is useful to define the efficiency of repair as the ratio of the number of hits actually repaired to the number initially produced by the radiation, that is,

$$\begin{aligned} \text{Efficiency} &= R(x)/F(x) \\ &= \frac{\alpha\beta}{k} (1 - \beta x/2 + \beta^2 x^2/6 - \dots) \end{aligned} \quad (5)$$

Clearly, the initial efficiency for  $\beta x \ll 1$  is approximately  $\alpha\beta/k$ ; and if  $\beta x$  remains small so that the observed survival is exponential, then over this range the efficiency of repair also remains constant. In equation 4 the magnitudes of  $k$ ,  $\alpha$  and  $\beta$  are adjustable, although in general,  $k \geq \alpha\beta$ ;  $k$  less than  $\alpha\beta$  would imply that survival is an initially increasing function of dose. In the case  $k = \alpha\beta$  the slope and efficiency of repair at the origin are zero and 100% respectively, and the number of adjustable parameters in the survival curve is reduced from three to two. Obviously 100% efficiency means that the repair mechanism works perfectly and all defects produced by the radiation are repairable.

An interesting theoretical question arises in the case  $k > \alpha\beta$ . Here, the survival curve has a non-zero initial slope and the efficiency of repair, even at the origin, is less than 100%. This can be interpreted in two ways, which are indistinguishable a priori: 1) Certain of the radiation-induced defects are intrinsically unrepairable; and 2) All the defects are repairable, but the repair mechanism itself is in some way defective. It would appear that this dilemma can be resolved in the case of cells whose survival curves for two different radiations are known to have non-zero and zero initial slopes. This is true of *E. coli* B/r: the initial slopes of its X-ray and UV survival curves are non-zero and zero respectively. Thus, since repair is apparently 100% efficient at low UV doses, it is unlikely that the mechanism is inherently defective and it seems reasonable to attribute the non-zero X-ray slope to the formation of unrepairable lesions.

A computer fit of equation 4 to typical UV survival points for *E. coli* B/r is shown in Fig. 6. Clearly a better fit can be obtained with this equation than with the classical multi-target expression, which is shown also for comparison. The values of the parameters used were:  $k = 1.292 \text{ sec}^{-1}$ ,  $\beta = 2.773 \times 10^{-3} \text{ sec}^{-1}$ ,  $\alpha = 465.9$ ; thus,  $k = \alpha\beta$ , and the initial slope is zero. At a UV dose rate of  $16.5 \text{ ergs/mm}^2/\text{sec}$ , the exposure required for 1 lethal hit ( $1/k$ ) was  $12.8 \text{ ergs/mm}^2$  as compared to a  $1/e$  dose of  $1.03 \text{ ergs/mm}^2$  obtained for *E. coli*  $B_{s-1}$  under similar experimental conditions. Certain practical difficulties were encountered in the computer program, and it is possible that another set of values with a slightly larger value of  $k$  would agree better with both the B/r and  $B_{s-1}$  data. However, in the light of the foregoing discussion, and the numerical values of these parameters for B/r, the following points can be made:

1) Since  $k = \alpha\beta$ , repair is initially 100% efficient. This suggests that no unrepairable defects are produced by low doses of UV. However, because even one unrepaired pyrimidine dimer is lethal, only a slight decline in repair efficiency at moderate doses would be expected to have a marked effect on viability. The efficiency of repair calculated from equation 5 declines very slowly: it is reduced to 95% at  $10^{-1}$  survival, 93% at  $10^{-2}$ , and 88% at  $10^{-6}$ . Thus, even at low survival substantial macromolecular repair may still be possible although it would have little effect on viability. If equation 5 is extrapolated to high doses beyond the "biological" range, it would appear that about  $14,000 \text{ ergs/mm}^2$  or  $2,537 \text{ Å}$  UV are required to reduce the efficiency of repair by  $1/e$ . This is comparable to the dose required for equivalent enzyme inactivation. However, until an action spectrum is available, the declining efficiency of repair may be attributed either to excessive DNA substrate damage or direct attack on the repair enzymes at high doses.

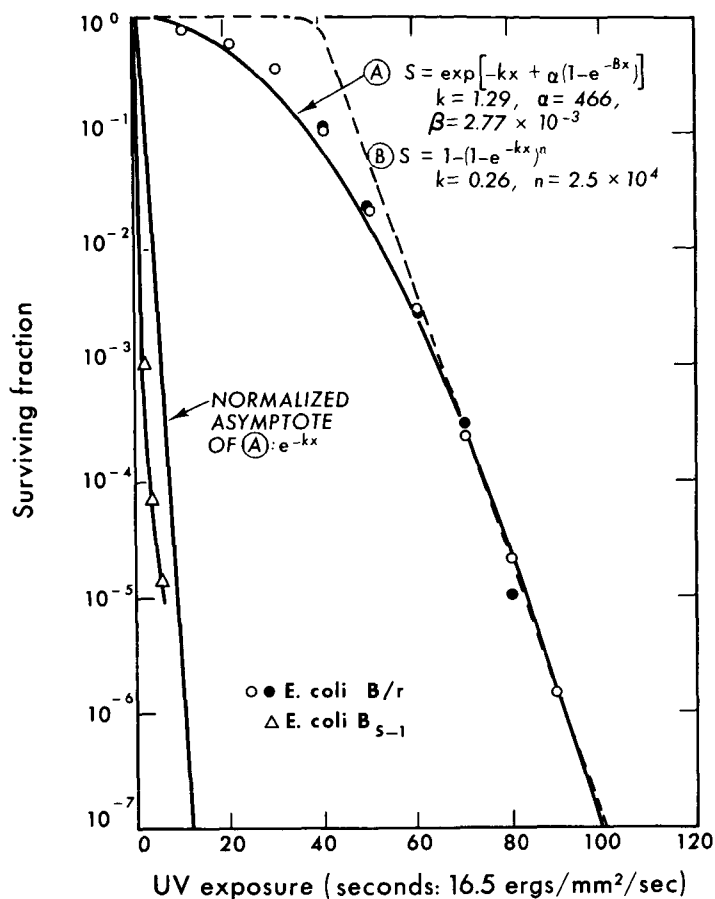


Figure 6. Curve A: the fitting of a typical set of UV survival points for *E. coli* B/r to a revised target-theoretical expression (equation 4), which includes the effect of a dose-dependent repair mechanism. Curve B: a fit to the classical one-hit, multi-target equation is shown for comparison. The asymptote of curve A is displaced to the left so it will pass through the origin; this is to be compared with the B<sub>s-1</sub> survival curve. MUB-10755

2) The asymptotic slope  $k$  is four times steeper than the apparent limiting slope even in the sixth decade of survival. However, considering the enormous extrapolation, the value of  $k$  is satisfyingly close to the slope of *E. coli* B<sub>s-1</sub> (cf. Fig. 6 where the asymptote is displaced to the origin for convenient comparison with the B<sub>s-1</sub> survival points).

To conclude, it would appear that the shoulders on many survival curves can be attributed to the existence of repair processes whose efficiency declines with dose. However, I do not wish to leave the impression that all shoulders can be interpreted in this way. There is no doubt that target multiplicity can contribute to shoulder formation independently of repair (76). Furthermore, the heat inactivation curves for *E. coli* B/r, B and B<sub>s-1</sub> are identical, indicating that thermal damage cannot be repaired by the dark reactivation mechanism, and yet they possess a broad shoulder that can only be interpreted as a multiplicity effect (1). The analysis of radiation dose-effect curves in terms of any particular model for cell lethality is at best a hazardous business. However, when coupled with independent studies of post-irradiation changes in macromolecular synthesis, it is of great heuristic value in synthesizing a general picture of the processes involved.



## REPAIR AND INTERACTIONS AMONG VARIOUS INACTIVATING AGENTS

Synergistic interactions among UV, X rays and HN2 have been observed in a number of organisms, and these effects seem to be correlated with the existence of reactivation or recovery mechanisms (23). No such effects have been observed in the nonreactivating mutants of *E. coli*; haploid yeast shows no dark recovery after X irradiation, nor do any interactions involving X rays occur in this organism (70). The synergistic UV-X-ray interaction in *E. coli* B/r has been described in detail elsewhere, and so only the main features relevant to this discussion will be summarized here (1,2). The UV survival curve for B/r has a broad shoulder (Fig. 2), whereas its X-ray curve is exponential. Sufficient preliminary UV exposure produces a threefold increase in the X-ray sensitivity of B/r, thereby making it equivalent in sensitivity to  $B_{s-1}$ . A substantial fraction of the UV-induced damage that sensitizes these cells to X rays is photoreactivable. On the other hand, preliminary X-ray exposure reduces the shoulder, but has no effect on the asymptotic slope of the UV survival curve. The total kill for any given pair of X-ray and UV exposures is independent of the order in which the radiations are given. This latter fact rules out the possibility that the effect arises at the level of the initial physico-chemical absorption processes, or that any of the defects produced by one radiation are directly "seen" by the other. Rather, it suggests that the synergism is based on the failure of some postirradiation process such as repair. Further evidence implicating repair is that the effect may be suppressed by the addition of acriflavin to the plating medium, and that no interaction occurs in cells containing 5-BU in their DNA (77).

We have seen how intracellular repair processes can determine both the exponential and sigmoidal shapes of many survival curves. A long-standing problem in this field concerns the interpretation of the peculiar inflected curve observed for the inactivation of *E. coli* B by both UV and HN2 (Figs. 2 and 3). The simplest interpretation is that the inflection reflects a population heterogeneity in B cultures. However, clones picked from the resistant "tail" region show the same UV response as the parental population, and so the heterogeneity must be regarded as being "phenotypic" rather than "genetic" in nature. Now is this phenotypic heterogeneity present as a physiological difference between two subpopulations in normal, unirradiated cultures, or is it actually induced by the radiation itself? Results of UV-X-ray interaction experiments tend to support the latter alternative (Fig. 7). The X-ray survival curve for our strain of *E. coli* B (ATCC #11303) is exponential with sensitivity approximately equal to that of B/r. If X-ray survival curves are measured after a graded series of preliminary UV exposures, the X-ray sensitivity is found first to decrease and then to increase (Fig. 7). This parallels the initially decreasing and subsequently increasing slope of the UV survival curve as it goes through the inflection. Clearly there is a correlation between the apparent X-ray and UV sensitivities of strain B, and yet no inflection is observed in the X-ray curve. This suggests that the resistant "tail" component of the B curve may be due to a UV-induced increase in the efficiency of repair, and that initially the B population is in fact homogeneous. However, it is difficult to see how the efficiency of repair could increase with dose except on the basis of an initially faulty coordination between the various steps in excision-repair.

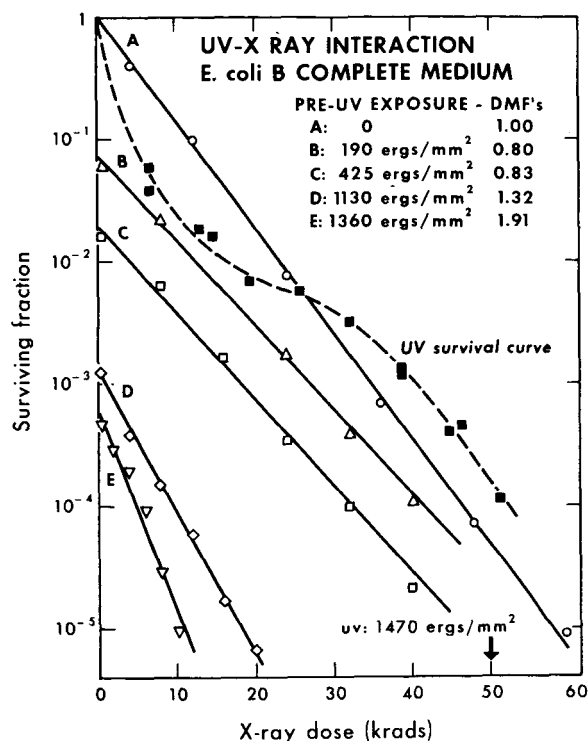


Figure 7. UV-X-ray interaction in *E. coli* B (strain ATCC #11303). Note that the X-ray sensitivity first decreases and then increases as the initial survival passes through the inflection of the UV survival curve for this strain.  
MUB-12204

## SUMMARY

1. Reproductive death in bacteria treated with X rays, ultraviolet light or nitrogen mustard arises primarily from the formation of structural defects in DNA serving to block normal DNA replication. In many cells, viability is enhanced through the action of certain enzymic processes that repair these defects before the onset of replication. Thus, in the analysis of dose-response curves, survival is determined jointly by the nature and distribution of the initial DNA defects and the probability of their subsequent repair. The apparent radio-sensitivity of cells can be increased by altering either the physico-chemical reactions involved in the formation of the defects or by interfering with the biochemical repair processes.

2. Sensitization by interference with repair appears to be involved in at least three well-known radiobiological effects: (a) the existence of "shoulders" on survival curves; (b) the synergistic interactions that occur among UV, X rays and nitrogen mustard; and (c) radio-sensitization by agents that either bind or are incorporated into DNA (e.g., acridine dyes and halogenated base analogs respectively). Since repair is an enzymic, energy-requiring process, it can be attenuated by excessive DNA substrate damage, by direct attack on the repair enzymes, or by blockage of its energy supply. In general, it is difficult to distinguish among these three alternatives.

3. Repair of UV damage in *E. coli* B/r is a multistep process involving nuclease excision of defective single-strand segments containing pyrimidine dimers, and a non-conservative mode of DNA replication which fills in the resulting gaps. Similarities in the

relative sensitivities of *E. coli* B/r, B and B<sub>s-1</sub> to UV and nitrogen mustard, the involvement of nucleases in repair, and the observation of repair replication after both UV and nitrogen mustard treatment lend strong support to the idea that it is not the damaged bases themselves that are recognized by the repair enzymes, but rather the associated secondary structural alternations in the phosphodiester backbone. Thus, repair might be of general biological significance in the maintenance of genetic stability by detecting and repairing a variety of possible distortions or defects in the Watson-Crick structure. The selective advantage arising from the possibility of repair inherent in the complementary structure of DNA might account for the ubiquity of double stranded nucleic acid molecules as the genetic material of living cells.

## ACKNOWLEDGMENTS

I wish to thank Dr. Byron Youtz, of Reed College, for his help with the calculations reported in this paper. I am also grateful for the research collaboration of Drs. J. T. Lyman, W. R. Inch, D. L. Dewey, and M. H. Patrick who have contributed much to the formulation of the ideas outlined here.

This work was supported by the U. S. Atomic Energy Commission and a grant from the National Institutes of Health, U. S. Public Health Service (GM-12667).

## REFERENCES

1. Haynes, R. H.; Photochem. Photobiol. 3:429-450, 1964.
2. Haynes, R. H.; in Physical Processes in Radiation Biology, edited by L. Augenstein, R. Mason and B. Rosenberg, New York, Academic Press, 1964, pp. 51-72.
3. Advances in Radiation Biology, Vol 2, edited by L. G. Augenstein, R. Mason and M. Zelle, New York, Academic Press, 1966, chpts. 1, 3, 4, 6.
4. Weiss, J. J.; in Progress in Nucleic Acid Research, Vol. 3, edited by J. N. Davidson and W. E. Cohn, New York, Academic Press, 1964.
5. Setlow, J. K.; in Current Topics in Radiation Research, Vol. 2, edited by M. Ebert and A. Howard, 1965.
6. Lea, D. E.; Haines, R. B., and Coulson, C. A.; Proc. Roy. Soc. (London) Ser. B120: 47-76, 1936.
7. Alper, T.; Phys. Med. Biol. 8:365-385, 1963.
8. Greer, S.; J. Gen. Microbiol. 22:618-634, 1960.
9. Djordjevic, B., and Szybalski, W.; J. Exptl. Med. 112:509-531, 1960.
10. Kaplan, H. S.; Smith, K. C., and Tomlin, P. A.; Radiation Res. 16:98-113, 1962.
11. Sauerbier, W.; Virology 15:465-472, 1961.
12. Szybalski, W., and Opara-Kubinska, Z.; in Cellular Radiation Biology, Baltimore, Williams and Wilkins, 1965, pp. 223-240.
13. Szybalski, W., and Lorkiewicz, Z.; Abhandl. Deut. Akad. Wiss. Berlin, Kl. Med. Nr. 1:63-71, 1962.
14. Stacey, K. A.; personal communication, 1965.
15. Kelner, A.; J. Bacteriol. 65:252-262, 1953.
16. Kaplan, H. S., and Moses, L. E.; Science 145:21-25, 1964.

17. Kaplan, H. S., and Zavarine, R.; *Biochem. Biophys. Res. Comm.* 8:432-436, 1962.
18. Swanson, C. P.; *J. Cell. Comp. Physiol.* (Suppl. 1):27-38, 1952.
19. Koller, P. C.; in *Progress in Biophysics and Biophysical Chemistry Vol. 4*, edited by J. A. V. Butler and J. T. Randall, London, Pergamon, 1954, pp. 195-243.
20. Wolff, S.; in *Mechanisms in Radiobiology*, edited by M. Errera and A. Forssberg, New York, Academic Press, 1961, pp. 419-476.
21. Hollaender, A., and Emmons, C. W.; *Cold Spring Harbor Symp. Quant. Biol.* 9:179-186, 1941.
22. Mortimer, R. K.; *Radiation Res.* 9:312-326, 1958.
23. Haynes, R. H., and Inch, W. R.; *Proc. Natl. Acad. Sci. U. S.* 50:839-846, 1963.
24. Bollum, F. J., and Setlow, R. B.; *Biochim. Biophys. Acta* 68:599-607, 1963.
25. Setlow, R. B.; Swenson, P. A., and Carrier, W. L.; *Science* 142:1464-1466, 1963.
26. Wulff, D. L., and Rupert, C. S.; *Biochem. Biophys. Res. Comm.* 7:237-240, 1962.
27. Setlow, J. K., and Setlow, R. B.; *Nature* 197:560-562, 1963.
28. Swenson, P. A., and Setlow, R. B.; *J. Mol. Biol.* 15:201-219, 1966.
29. Pollard, E. C.; *Science* 146:927-929, 1964.
30. Frampton, E. W., and Brinkley, B. R.; *J. Bacteriol.* 90:446-452, 1965.
31. Smith, K. C.; *Biochem. Biophys. Res. Comm.* 6:458-463, 1962.
32. Howard-Flanders, P.; Boyce, R. P., and Theriot, L.; *Nature* 195:51-54, 1962.
33. Aoki, S.; Boyce, R. P., and Howard-Flanders, P.; *Nature* 209:686-688, 1966.
34. Jagger, J.; Wise, W. C., and Stafford, R. S.; *Photochem. Photobiol.* 3:11-24, 1964.
35. Ginsberg, D. M., and Jagger, J.; *J. Gen. Microbiol.* 40:171-184, 1965.
36. Hanawalt, P. C.; *Photochem. Photobiol.* 5:1-12, 1966.
37. Lyman, J. T., and Haynes, R. H.; *Lawrence Radiation Laboratory Report UCRL-16613*, 1965.
38. Howard-Flanders, P.; Boyce, R. P.; Simson, E., and Theriot, L.; *Proc. Natl. Acad. Sci. U. S.* 48:2109-2115, 1962.
39. Setlow, R. B., and Carrier, W. L.; *Proc. Natl. Acad. Sci. U. S.* 51:226-231, 1964.
40. Boyce, R. P., and Howard-Flanders, P.; *Proc. Natl. Acad. Sci. U. S.* 51:293-300, 1964.
41. Pettijohn, D., and Hanawalt, P. C.; *J. Mol. Biol.* 9:395-410, 1964.
42. Setlow, R. B.; *J. Cell. Comp. Physiol.* 64 (Suppl. 1):51-68, 1964.
43. Howard-Flanders, P.; *Japan. J. Genetics* 40 (Suppl.):256-263, 1965.
44. Richardson, C. C.; Schildkraut, C. L., and Kornberg, A.; *Cold Spring Harbor Symp. Quant. Biol.* 28:9-20, 1964.
45. Brookes, P., and Lawley, P. D.; *Biochem. J.* 80:496-503, 1961.
46. Geiduschek, E. P.; *Proc. Natl. Acad. Sci. U. S.* 47:950-955, 1961.
47. Haynes, R. H.; Patrick, M. H., and Baptist, J. E.; *Radiation Research* 22:194, 1964.
48. Hanawalt, P. C., and Haynes, R. H.; *Biochem. Biophys. Res. Comm.* 19:462-467, 1965.
49. Papirmeister, B., and Davison, C. L.; *Biochem. Biophys. Res. Comm.* 17:608-617, 1964.
50. Kohn, K. W.; Steigbigel, N. H., and Spears, C. L.; *Proc. Natl. Acad. Sci. U. S.* 53:1154-1161, 1965.
51. Loveless, A.; Cook, J., and Wheatley, P.; *Nature* 205:980-983, 1965.

52. Lawley, P. D., and Brookes, P.; *Nature* 206:480-483, 1965.
53. Boyce, R. P., and Howard-Flanders, P.; *Z. Vererbungslhere* 95:345-350, 1964.
54. McGrath, R. A.; Williams, R. W., and Swartzendruber, C. S.; *Biophys. J.* 6:113-122, 1966.
55. Emmerson, P. T., Howard-Flanders, P.; *Biochem. Biophys. Res. Comm.* 18:24-29, 1965.
56. Bridges, B. A., Munson, R. J.; *Biochem. Biophys. Res. Comm.* 22:268-273, 1966.
57. Strauss, B. S.; *J. Gen. Microbiol.* 30:89-103, 1963.
58. Strauss, B. S., and Wahl, R.; *Biochim. Biophys. Acta* 80:116-126, 1964.
59. Searashi, T., and Strauss, B. S.; *Biochem. Biophys. Res. Comm.* 20:680-687, 1965.
60. Reiter, H., and Strauss, B. S.; *J. Mol. Biol.* 14:179-194, 1965.
61. Doerfler, W., and Hogness, D. S.; quoted in D. S. Hogness, *J. Gen. Physiol.*, 1966, in press.
62. Barendsen, G. W., and Walter, H. M. D.; *Radiation Res.* 21:314-329, 1964.
63. Todd, P. W.; Lawrence Radiation Laboratory Report UCRL-11614, 1964.
64. Alexander, P.; Lett, J. T.; Kopp, P., and Itzhaki, R.; *Radiation Res.* 14:363-373, 1961.
65. Guild, W. R.; *Radiation Res. Suppl.* 3:257-269, 1963.
66. Schambra, P. E., and Hutchinson, F.; *Radiation Res.* 23:514-526, 1964.
67. Inch, W. R., and Haynes, R. H.; *Radiation Res.* 27:546, 1966.
68. Moseley, B. E. B., and Laser, H.; *Proc. Roy. Soc. London B* 162:210-222, 1965.
69. Setlow, J. K.; *Photochem. Photobiol.* 3:405-414, 1964.
70. Patrick, M. H.; Haynes, R. H., and Uretz, R. B.; *Radiation Res.* 21:144-163, 1964.
71. Patrick, M. H., and Haynes, R. H.; *Radiation Res.* 23:564-579, 1964.
72. Zimmer, K. G.; *Studies on Quantitative Radiation Biology*, Edinburgh and London, Oliver and Boyd, 1961.
73. Hutchinson, F., and Pollard, E. C.; in *Mechanism in Radiobiology Vol. 1*, edited by M. Errera and A. Forssberg, New York, Academic Press, 1961, pp. 71-92.
74. Zirkle, R. E., and Tobias, C. A.; *Arch. Biochem. Biophys.* 47:282-306, 1953.
75. Fowler, J. F.; *Phys. Med. Biol.* 9:177-188, 1964.
76. Norman, A.; *J. Cell. Comp. Physiol.* 44:1-10, 1954.
77. Baptist, J. E.; Haynes, R. H., and Uretz, R. B.; *Radiation Res.* 27:544, 1966.

# Inactivation of Phage $\alpha$ by Single-Strand Breakage

David Freifelder

N67 15953

For most bacteriophages studied, sensitivity to inactivation by  $^{32}\text{P}$ -decay or X irradiation is related to their DNA content, (1). However, this is not so for bacteriophages S13,  $\phi\text{X174}$ , and  $\alpha$ , which are excessively sensitive. For coliphages S13 and  $\phi\text{X174}$  this is due to the fact that their DNA is single-stranded (2, 3) so that single-strand breaks, which are normally not lethal in double-stranded DNA (4), result in molecular cleavage and therefore inactivation. However, B. megaterium bacteriophage  $\alpha$  has the sensitivity to X rays and to  $^{32}\text{P}$ -suicide of a phage with single-stranded DNA, although its DNA is in fact double-stranded (5). Studies of inactivation of  $\alpha$  by  $^{32}\text{P}$ -decay have shown that the rate of production of lethal events is nearly equal to the rate of decay of the  $^{32}\text{P}$  atoms (to within a factor of 2) so that it is possible that  $\alpha$ , as contrasted with other known phages with double-stranded DNA, is inactivated by single-strand breaks. This idea can be tested directly by measuring the rate of production of single- and double-strand breaks in X-irradiated bacteriophage  $\alpha$ , at the level of one per molecule, and comparing this with the inactivation kinetics. In brief, the technique involves a measurement with the analytical ultracentrifuge of the percentage of the total number of DNA molecules broken by the X irradiation (4). Broken molecules are detected by the fact that they sediment more slowly than the initially, unbroken, homogeneous population of molecules. The result of this investigation indicates that phage  $\alpha$  is inactivated by single-strand breakage although not all breaks are lethal.

## MATERIALS AND METHODS

A clear mutant of phage  $\alpha$  propagated on B. megaterium, Parigi, was used. Both phage and host were obtained from the laboratory of Dr. E. P. Geiduscheck, University of Chicago, who originally received them from Prof. F. Graziosi, International Laboratory of Genetics, Naples. The phage was grown as described by Aurisicchio et al. (5) and purified by differential centrifugation. Viability was determined by plating on Difco nutrient agar plates and incubating for 16 hr at 30°C. The technique for measuring single- and double-strand breakage was that of Davison et al. (6) as modified for X-ray analysis (4, 7). Double-stranded DNA was isolated by heating the phage for 5 min at 70°C in a medium consisting of  $10^{-2}$  M Na phosphate, pH 7.8,  $10^{-3}$  M  $\ell$ -histidine, and 1 M NaCl. For isolation of single-stranded DNA, the phages were heated for 5 min at 70°C in  $10^{-2}$  M Na phosphate +  $10^{-3}$  M  $\ell$ -histidine, followed by addition of hot, neutralized 37% formaldehyde, heating for one minute more, and cooling quickly. Identical results were obtained for both irradiated and unirradiated DNA if the above time of heating in formaldehyde was extended to 5 min or if denaturation was accomplished by suspension of the phage in 0.2 M NaOH at room temperature. This

shows that the single-strand breaks detected are not sites of removal of bases from the DNA chain, as reported for inactivation by acridine orange and visible light (8).

The calculation of the percentage of strands receiving single-strand breaks is complicated by the presence of natural single-strand breaks in unirradiated DNA. For phage  $\alpha$ , 33% of the single-strands are broken. This differs from that previously reported (65%) by Davison *et al.* (6) since in the earlier experiments the effects of hydrodynamic shear on denatured DNA were not known. In the present experiments, shear degradation has been avoided (9). The existence of natural breaks is corrected for by assuming that initially broken and unbroken strands are equally susceptible to X-ray damage.

The conditions for X irradiation have already been described (4). The dose rate of the X-ray machine was 8,000 rads/min. Phages were suspended in  $10^{-3}$  M  $\ell$ -histidine buffered at pH 7.8 with  $10^{-2}$  M phosphate. The presence of histidine minimizes the indirect effects of the ionizations. The survival curve obtained under these conditions was the same as that for phage suspended in 1% Difco nutrient broth.

## RESULTS

Figure 1 gives the survival curve for irradiation of phage  $\alpha$  in buffered histidine by 150-kv X rays. The  $D_{37}$  dose is 27,300 rads, which differs only slightly from results by others (5, 10). The rate of DNA double-strand breakage is also shown in the figure. For coliphage T7 the ratio of the rate of phage inactivation to that of double-strand breakage is ca. 2.5 (4). If this were also the case for  $\alpha$ , the expected inactivation rate would be that shown in the figure. However,  $\alpha$  is about four times as sensitive as expected.

The survival of intact single-stranded molecules as a function of dose is given in Fig. 2. Using this curve and the one for double-strand breakage given in Fig. 1, one can calculate, as shown in Fig. 2, the survival of single strands broken by single-strand breaks that are not themselves components of double-strand breaks. Furthermore, a curve for the survival of phage inactivated neither by double-strand breakage nor base damage can be calculated by dividing the observed phage inactivation curve of Fig. 1 by the "expected inactivation" curve. This calculated curve is also shown in Fig. 2 and is nearly the same as the other curve for single-strand breaks not contained in double-strand breaks.

From the data of Figs. 1 and 2 it can be seen that: (a) the ratio of single- to double-strand breaks is the same as that observed for the DNA of both T7 and the *Pseudomonas aeruginosa* phage B3, irradiated under the same conditions (7), indicating that, as far as breakage is concerned, there is nothing extraordinary about  $\alpha$  DNA; (b) the rate of double-strand breakage is very low compared to the inactivation rate so that it can account for at most a small part of the inactivation; (c) the rate of breakage of single strands is very nearly equal to the rate of inactivation, suggesting that this type of damage is probably important in the mechanism of inactivation.

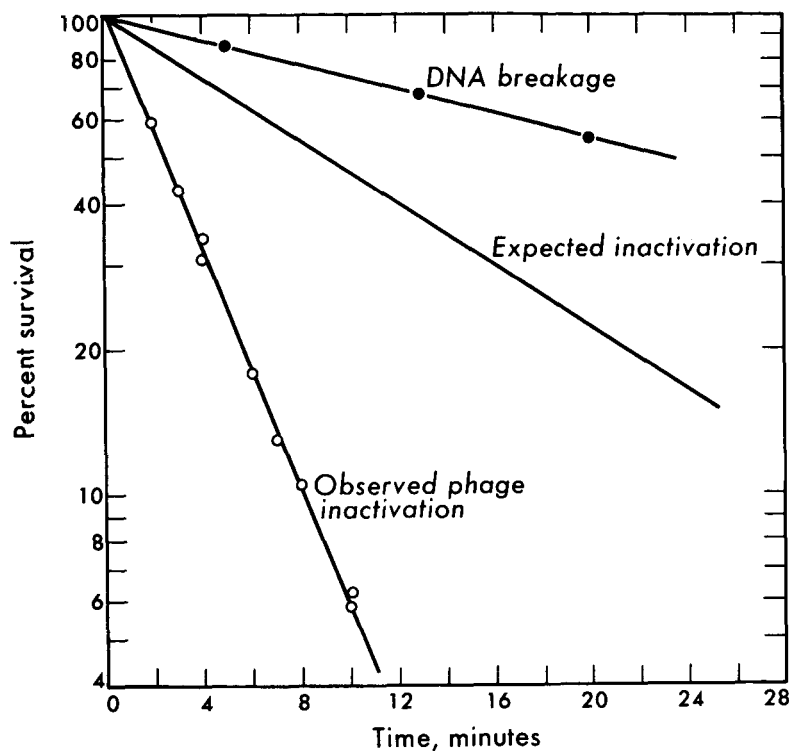
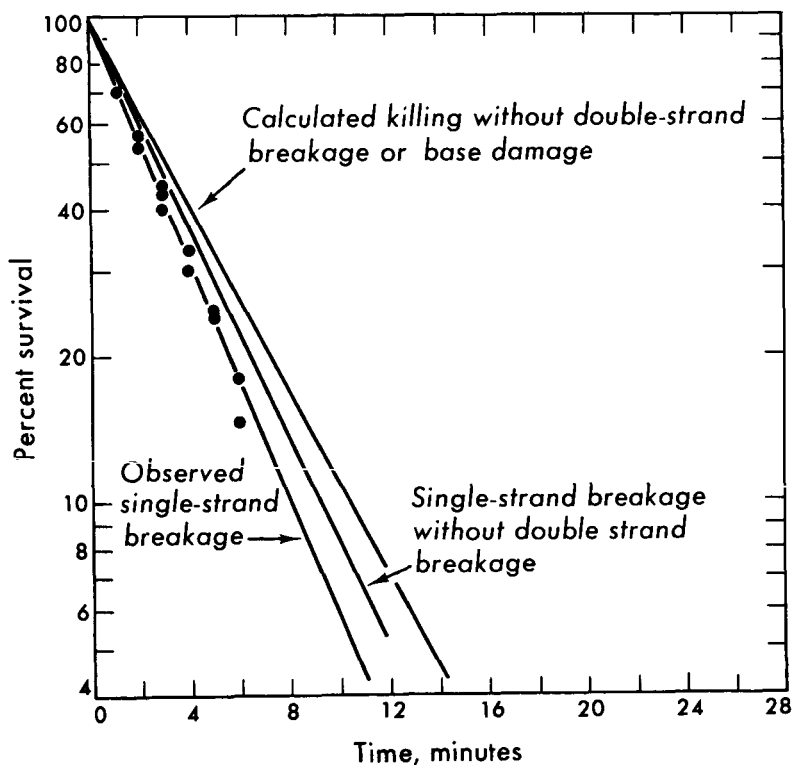


Figure 1. Inactivation of phage  $\alpha$  and breakage of  $\alpha$  DNA by X rays. "Observed phage inactivation" refers to loss of plaque-forming ability. "DNA breakage" refers to the percentage of DNA molecules extracted from irradiated phage that are still intact, i.e., no double-strand breaks. For coliphage T7 the rate of phage inactivation is circa two and a half times that for T7 DNA double-strand breakage. The curve "expected inactivation" is calculated from the  $\alpha$  DNA breakage curve by multiplying the breakage rate by 2.5. The X-ray dose rate was 8000 rads/min. MUB-10072

Figure 2. Rate of breakage of single strands of  $\alpha$  DNA by X rays. Percent survival refers to the percentage of single strands that in unirradiated phage contain no natural single-strand breaks and are still unbroken after X irradiation. "Single-strand breakage without double-strand breakage" is calculated from the "observed single-strand breakage" curve and the double-strand breakage curve of Fig. 1. "Calculated killing without double-strand breakage or base damage" is obtained by dividing the curve "observed phage inactivation" of Fig. 1 by the "expected inactivation" curve of Fig. 1. MUB-10073





## DISCUSSION

In previous experiments it has been shown that, in histidine, coliphage T7 is inactivated both by double-strand breakage and by base damage, each effect contributing essentially equally to the inactivation. Single-strand breaks were found to be ineffective, and it was assumed that this was either because they are tolerated in the DNA or that they are repaired. In the case of  $\alpha$ , however, it is clear that double-strand breakage is of minor importance. Also, since in general the X-ray sensitivity of most phages studied is simply related to the molecular weight of the DNA (1), it is unlikely that the high sensitivity of  $\alpha$  is primarily due to the base damage component since there is no evidence for anything extraordinary about the base composition of its DNA (5). Hence, in the following, the effect of single-strand breakage is considered.

On the assumption that the ratio of base damage to double-strand breakage is the same in  $\alpha$  as in T7, the "expected inactivation" curve of Fig. 1 was calculated. Since both double-strand breakage and base damage probably do account for part of the killing, the actual survival curve can be corrected by graphical division to yield the survival kinetics for damage other than base damage or double-strand breakage, as shown in Fig. 1. If this is compared to the rate of production of single-strand breaks that are not contained in double-strand breaks (Fig. 2), it is seen that these rates correlate closely, suggesting that indeed single-strand breaks are a major factor in the inactivation.

Evidence for the effectiveness of single-strand breaks comes also from the rate of inactivation of  $\alpha$  by  $^{32}\text{P}$ -decay. Whereas for most phages only 5 to 10% of the decays are lethal, in  $\alpha$  it has been shown that 50 to 100% of such decays are lethal (5). It has been postulated that each  $^{32}\text{P}$  decay leads to conversion of a phosphoester bond to a sulfoester bond, which presumably by hydrolysis leads to the appearance of a single-strand break (11).

Unless the inactivation event is a chemical alteration not detected in these experiments, it is likely that single-strand breakage is the major lethal process in phage  $\alpha$ . In the following the number of single-strand breaks per lethal event will be determined. The experiments with  $^{32}\text{P}$  enable one to count the number of decay per lethal event. Such data indicate that one or two breaks are sufficient for lethality, but it is not possible to be more precise. The experiments with the ultracentrifuge, on the other hand, indicate only the percentage of the strands receiving one or more breaks but not the number of broken strands per molecule required for lethality. This can be deduced by considering the following simple models for inactivation: (1) both strands must be broken, (2) either strand may be broken, (3) only one strand need be broken and this may be either strand but, in any given cell, the strand to be used is selected at random, and (4) a unique strand must be broken. Model 1 is immediately eliminated since it predicts two-hit kinetics of inactivation and exponential kinetics are observed. Figure 3 shows for the remaining models the theoretical relation between the surviving fraction of the phages inactivated by single-strand breaks only and the surviving fraction for single strands broken by single-strand breaks that are not paired in double-strand breaks. The experimental data (taken from Figs. 1 and 2) are also shown in the figure. It is

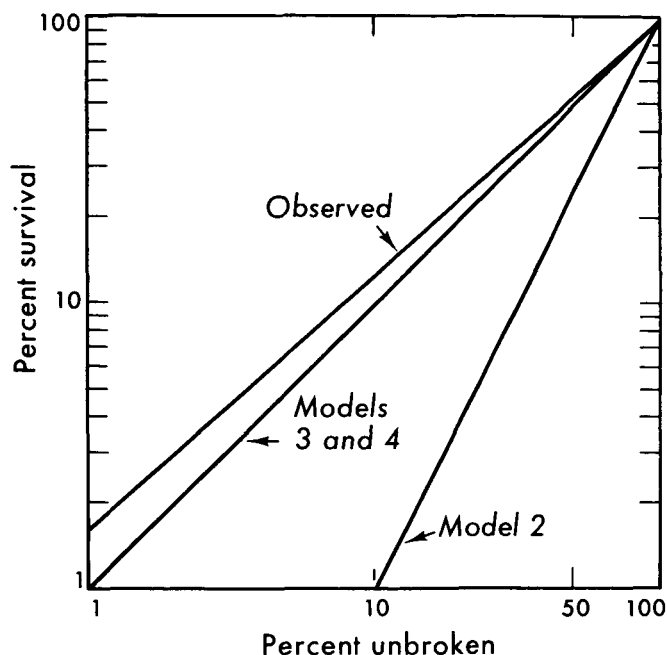


Figure 3. Theoretical relations between the percent survival of phages inactivated by damage other than both double-strand breakage and base damage and the percentage of single strands that have not been broken by single-strand breaks not contained in double-strand breaks. Three different models are considered. Model 2 (either strand may be broken) is calculated as follows: the probability of killing is the probability of breaking strand  $a(p_a)$  + the probability of breaking strand  $b(p_b) - p_a p_b = 2p - p^2$ , the term  $p_a p_b$  taking into account those broken strands paired with other broken strands. Models 3 and 4 (in a given phage, a break in only 1 strand can be lethal) is calculated as follows: the probability of killing =  $\frac{1}{2}(p_a + p_b) = p$ , since half of the time a break will be in an irrelevant strand.

MUB-10069

clear that model 2 is inconsistent with, and 3 and 4 are both consistent with, the data. The present experiments do not distinguish between models 3 and 4.

It is not clear why  $\alpha$  is inactivated by single-strand breaks and other phages are not. One possibility is that corrective systems which normally repair single-strand breaks are absent in the *B. megaterium* system. If so, this must be a phage defect rather than a property of the host cell since phage BM, which is active in the same host, does not show the excessive radiosensitivity (5). If it were true that damage must be in a unique strand (model 4), this might be explained by stating that repair does occur but that for some reason it is possible only in the other strand. Alternatively, an essential function can be ascribed to a particular strand.

It is known that following infection of the host bacterium by  $\alpha$ , the infected complex shows the normal sensitivity to X rays expected from the molecular weight of its DNA (10). The explanation is unclear but three simple possibilities are: (i) the essential function prevented by a single-strand break has occurred by the time the complexes are irradiated, (ii) a repair system is either activated immediately after infection and that this activation is not possible if the DNA contains a single-strand break, or (iii) the repair system is activated by irradiation of the complex. The question of repair is currently under investigation.

## SUMMARY

*B. megaterium* phage  $\alpha$  is more sensitive to X irradiation than a typical phage of its size containing double-stranded DNA. Double-strand breakage accounts for only a small part of the inactivation in contrast with many other phages. An ultracentrifuge assay has been used to measure single-strand breakage in the DNA of the X-irradiated phages. The

inactivating event is apparently a single-strand break. However, not all single-strand breaks are lethal. Two alternatives are possible: (1) a break is lethal only if it occurs in a particular strand or (2) only one strand can function in the cell, and this strand is selected at random. These alternatives cannot be distinguished by the present experiments.

## ACKNOWLEDGMENTS

I would like to thank Katherine LeBlanc and Kristin Chung for excellent technical help. I would also like to acknowledge a Career Development Award (#7617) from the Division of General Medical Sciences, U. S. Public Health Service.

## REFERENCES

1. Bertani, G.; *J. Bacteriol.* 79:387-393, 1960.
2. Tessman, I.; *Virology* 1:263-275, 1959.
3. Sinsheimer, R. L.; *J. Mol. Biol.* 1:43-53, 1959.
4. Freifelder, D.; *Proc. Nat. Acad. Sci.* 54:128-134, 1965.
5. Aurisicchio, S.; Coppo, A.; Frontali, C.; Graziosi, F., and Toschi, G.; *Nuovo Cimento* 25, Suppl. 35-40, 1962.
6. Davison, P. F.; Freifelder, D., and Holloway, B. W.; *J. Mol. Biol.* 8:1-10, 1964.
7. Freifelder, D.; DNA strand breakage by X-irradiation; *Radiation Res.*, 1966, in press.
8. Freifelder, D., and Uretz, R. B.; Mechanism of photoinactivation of coliphage T7 sensitized by acridine orange; *Virology*, 1966, in press.
9. Davison, P. F., and Freifelder, D.; *J. Mol. Biol.* 16:490-502, 1966.
10. Donini, P., and Epstein, H.; *Virology* 26:359-367, 1965.
11. Levinthal, C., and Davison, P. F.; *J. Mol. Biol.* 3:674-683, 1961.

# Replication of DNA During F'Lac Transfer

David Freifelder

N67 15954

F'Lac is a DNA-containing (1) episomal element, which can be transferred from a male donor strain of the bacterium *E. coli* to a female recipient by conjugation. The mechanism by which this transfer occurs is not known. Suggested models for transfer are of three types: those for which DNA synthesis is unnecessary, those for which DNA synthesis accompanies transfer, and those for which DNA synthesis precedes transfer. In most investigations, the nature of the DNA transferred under normal conditions of DNA synthesis has been examined. Herman and Forro (2) have shown that if radioactively labeled males are mated with females in nonradioactive medium, the transferred labeled DNA behaves as a single conserved unit during subsequent replication of the recipient cell, suggesting that the DNA is replicated in the nonradioactive medium prior to or during transfer. Ptashne (3) mated heavy-density-labeled males with light females in a light medium and showed that all transferred DNA was of a hybrid density, and reached a conclusion similar to that of Herman and Forro. An alternative explanation for both of these results is that replication occurs immediately after transfer, an idea proposed by Stouthamer, de Haan, and Bulten (4). Gross and Caro (5) studied chromosomal transfer in Hfr males using quantitative autoradiography and concluded that the DNA is replicated during transfer; substantial evidence was given for lack of replication in the female.

The nature of the transferred DNA can be studied in another way. If a thymine-requiring male transfers F'Lac in a medium containing 5-bromouracil deoxyriboside (BUDR) instead of thymine, the presence of BUDR in the transferred DNA can be detected by virtue of its sensitization to the effects of short or long wavelength ultraviolet irradiation (6, 7). DNA transferred without replication would be resolved as a fraction of F'Lac recipients relatively resistant to the irradiation. In the present paper, these experiments are described and it is shown that, in agreement with the results of others quoted above, the transferred DNA has been replicated prior to or during transfer.

## MATERIALS AND METHODS

Several strains of *E. coli* K-12 were used which have been designated DF18 (♂) and DF30 (♀). The history of these strains is given in Table 1. The growth medium was tris-glucose-0.1% casamino acids supplemented with 5 µg/ml thymine and 20 µg/ml hypoxanthine (H), which satisfies the purine requirement of DF30. All media transfers were by membrane filtration. Lactose fermentation was assayed on MacConkey agar plates (Difco) containing 100 µg/ml streptomycin.

Table 1.

Designation	Genotype*	Origin
200P	♂ F'Lac <sup>+</sup> /Lac-T-L-B1-Sm <sup>S</sup> T6 <sup>S</sup>	F. Jacob, Pasteur Inst.
CR34	♀ Lac-T-L-B1-Met-Sm <sup>S</sup> T6 <sup>S</sup> Thy-	M. Meselson, Harvard Univ.
DF3	Same as CR34, but Sm <sup>R</sup>	Ultraviolet mutation of CR34
DF30	Same as DF3, but Pur-	UV treatment of DF3
DF6	Same as CR34, but T6 <sup>R</sup>	Spontaneous mutant
DF18	♂ F'Lac <sup>+</sup> /Lac-T-L-B1-Sm <sup>S</sup> T6 <sup>R</sup> Thy-	200P × DF6

\* Abbreviations: Lac, ability to ferment lactose; F'Lac, male episomal particle carrying Lac gene; T, threonine; L, Leucine; B1, Vitamin B1; Met, methionine; Thy, thymine; Pur, purine; Sm<sup>R</sup>, streptomycin resistance; T6<sup>R</sup>, phage T6 resistance.

The cross was performed as follows: DF18 and DF30 were grown with aeration to  $2 \times 10^8$  ml. DF18 was transferred to iced -Thy-H medium. The DF30 females were transferred to +Thy-H medium, incubated at 37°C for 20 min with shaking and transferred again to iced -Thy-H medium. (Following this incubation period, DF30 will not incorporate C<sup>14</sup>-thymine into DNA unless hypoxanthine or adenine is added.) The DF18 males were then added at a ratio of 1 to 2 males/10 females and 2 µg/ml BUDR and 1 µg/ml thymine was added. (In such a BUDR-thy medium, cells will grow indefinitely without loss of viability.) The mating mixture was very gently shaken for 30 min at 37°C, diluted 100-fold into iced buffer and shaken on a Vortex mixer for 1 min to separate the mating pairs. The cells were then irradiated and plated. In a cross with thymine alone, ca. 50 to 100% of the DF18 males transfer F'Lac in 30 min. With the BUDR added, this is reduced to about 1 to 5%. In order to determine survival levels after irradiation with some accuracy, up to  $10^5$  cells are plated. The resolution of MacConkey agar is such that one red Lac<sup>+</sup> colony is easily detected against a background of  $10^4$ - $10^5$  pink Lac<sup>-</sup> colonies. At all times, cells containing BUDR were protected from inactivating wavelengths of visible light. Ultraviolet irradiation was accomplished with a 15-watt General Electric germicidal lamp. For visible light irradiation, the cells were iced and irradiated with an unfiltered General Electric 150-watt reflector spot lamp at a distance of 7 in. For both irradiations, the cells were suspended in 0.01 M phosphate, pH 7.5, 0.001 M MgSO<sub>4</sub>, 0.0001 M CaCl<sub>2</sub>.

## RESULTS AND DISCUSSION

In a control experiment, DF18 and hypoxanthine-starved DF30 were mated in the presence of 1 µg/ml thymine for 30 min, diluted 100-fold, and vortexed. Aliquots of the diluted suspension were irradiated with ultraviolet and visible light respectively and plated on MacConkey agar. Inactivation of Lac<sup>+</sup> and Lac<sup>-</sup> cells by ultraviolet proceeded at the same rate. There was little or no inactivation of either type by the visible light.

In a second experiment, the cells were mated in the BUDR-containing medium, diluted, vortexed, and irradiated. Figure 1 shows the result of ultraviolet irradiation. The

Lac<sup>+</sup> colonies are inactivated at a considerably greater rate than the Lac<sup>-</sup> colonies (which are inactivated at the same rate as those obtained from the thymine mating experiment). This is presumably a reflection of the sensitizing effect of the BUDR contained in the transferred DNA (6). The Lac<sup>+</sup> inactivation curve remains exponential for about two decades, implying that at least 99% of the transferred episomes have nearly the same BUDR content, i. e., there are few, if any, which contain only thymine.

The result of the irradiation with visible light is shown in Fig. 2. The Lac<sup>-</sup> cells are not inactivated, indicating that they have incorporated little, if any, BUDR. This should be compared with the rapid inactivation of DF30 grown for three generations in the BUDR medium. However, cells that have received the F'Lac are sensitive to visible light (the Lac<sup>+</sup> character is sensitive). Because of the low frequency of transfer in the BUDR medium, it is not possible to tell if the cell itself is killed or if only the F'Lac is inactivated, although the latter is the more likely.

The visible light inactivation differs from the UV case in that there is a resistant fraction of about 30%. It is possible that this represents transfer of F'Lac containing no BUDR, but this seems to be ruled out by the UV result. Fox and Meselson (8) have shown that only 50% of a population of phage  $\lambda$  that contains BUDR in only one strand of its DNA can be inactivated by visible light, from which they concluded that, for reasons still to be determined, damage in one of the two complementary strands is nonlethal. It is likely that a similar effect accounts for the resistant fraction encountered in the visible light experiment, although the inactivation is greater than 50%. Presumably, this is a result of a small fraction of episomes having replicated in the BUDR medium prior to the transfer process and therefore contain BUDR in both strands.

It might be asked why there is no resistant fraction in the UV experiment. This result agrees with other results for bifilarly labeled DNA (6) and is explained on the basis of BUDR inhibiting the systems that repair UV-irradiated DNA (9). This inhibition is presumably independent of the location of the BUDR.

The above experiments may be interpreted as follows: When male cells containing F'Lac are mated with female cells, the transferred F'Lac is replicated either prior to or during the transfer process. Some particles may replicate twice prior to transfer or once prior to and once during transfer. The percentage transferred without replication is probably less than 1%. Whether this is true of mating in thymine without BUDR and if this is also the case for Hfr transfer cannot be stated.

These results are consistent with those of Herman and Forro, Ptashne, and Gross and Caro, and with the replicon theory of Jacob, Brenner and Cuzin (10).

## ACKNOWLEDGMENTS

This work was supported by grants from the Atomic Energy Commission and a grant

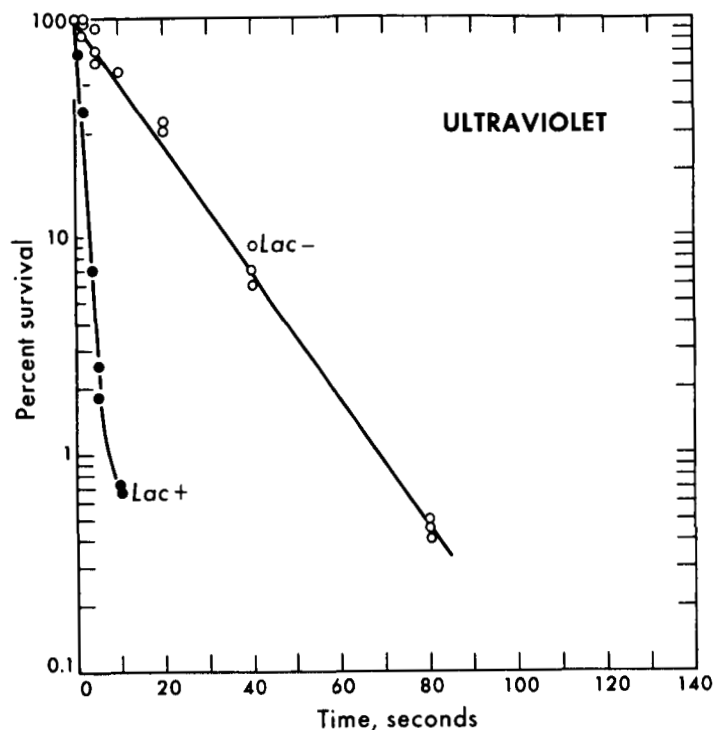
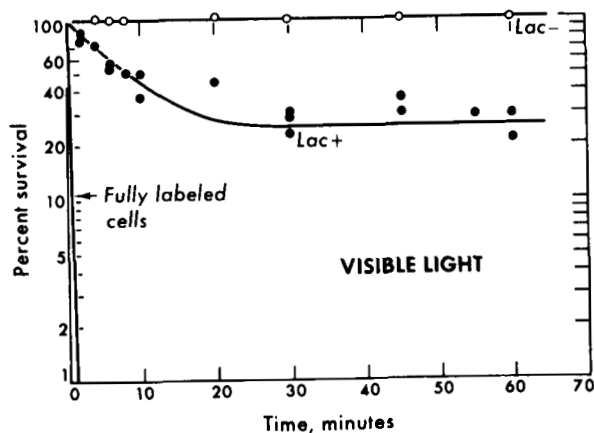


Figure 1. Inactivation by ultraviolet light of viability and the ability to ferment lactose in DF30 females that have received a BUDR-labeled F' Lac from DF18 males by bacterial conjugation. The curve labeled Lac- represents loss of viability of Lac- colonies. The curve labeled Lac+ represents loss of the Lac character. These latter cells presumably are not killed but rather are converted to Lac-. MUB-10070

Figure 2. Inactivation by visible light of viability and the ability to ferment lactose in DF30 females that have received a BUDR-labeled F' Lac from DF18 males by bacterial conjugation. The curve labeled Lac- represents the viability of Lac- colonies. The curve labeled Lac+ represents loss of the Lac character. These latter cells presumably are not killed but rather are converted to Lac-. The curve marked "fully labeled cells" represents loss of viability of cells whose chromosomes are extensively labeled in both strands with BUDR. MUB-10071



from the U. S. Public Health Service (#C-M-12667) awarded to Dr. Robert H. Haynes, to whom I am grateful. This work was performed while I was a recipient of a Career Development Award (#7617) from the National Institute of General Medical Sciences, U. S. Public Health Service. I would also like to thank Kristin Chung, who performed all of these experiments.

## REFERENCES

1. Silver, S.; J. Mol. Biol. 6: 349, 1963.
2. Herman and Forro, F., Biophys. J. 4: 335, 1964.
3. Ptashne, M., J. Mol. Biol. 11: 829, 1965.
4. Stouthamer, A. H.; de Haan, P. G., and Bulten, E. J.; Genet. Res., Cambridge, 4: 305, 1963.
5. Gross, J., and Caro, L.; Science 150: 1679, 1965.
6. Greer, S.; J. Gen. Microbiol. 22: 618, 1960.
7. Stahl, F. W.; Craseman, J. M.; Okun, L.; Fox, E., and Laird, C.; Virology 13: 98, 1961.
8. Fox, E., and Meselson, M.; J. Mol. Biol. 1: 583, 1963.
9. Howard-Flanders, P.; Boyce, R., and Theriot, L.; Nature 195: 51, 1962.
10. Jacob, F.; Brenner, S., and Cuzin, F.; Cold Spring Harbor Symp. Quant. Biol. 28: 329, 1963.



# Pleiotropy and Polymorphism

N67 15955

Jack Lester King

Recent work in theoretical population genetics has demonstrated, principally through the use of computer simulation of Mendelian populations, that genetic polymorphisms can be maintained through interactions between various factors that do not singly effect polymorphic balance. Thus neither linkage alone nor stabilizing selection alone leads to stable genetic diversity, but together these factors can maintain a polymorphic equilibrium (1). I have recently reviewed the interactions of stabilizing selection and mutation in this respect (2). Jain and Allard (3) have demonstrated triple interactions of linkage, epistasis and inbreeding in the maintenance of genetic diversity, and have admonished that multigenic systems cannot be dealt with by analyzing the isolated effect of any single variable. Other interacting variables must also be considered in turn: pleiotropy, temporal fluctuations in selection intensities, environmental clines, compensation, and more. It is the purpose of this paper to suggest that pleiotropy is potentially a potent factor toward the maintenance of genetic diversity, and to present a simple model demonstrating this in the interaction of pleiotropy and stabilizing selection.

Pleiotropy and stabilizing selection. Let there be two loci, A and B, and two developmental systems, X and Y. There are two alleles at each locus:  $A_1$  contributes a developmental value of +1 to X and +1 to Y;  $A_2$  contributes 0 to X and 0 to Y;  $B_1$  contributes +1 to X and 0 to Y;  $B_2$  contributes 0 to X and +1 to Y. Thus for the nine possible genotypes, the developmental values of X and Y are:

	X	Y
$A_1A_1B_1B_1$	4	2
$A_1A_1B_1B_2$	3	3
$A_1A_1B_2B_2$	2	4
$A_1A_2B_1B_1$	3	1
$A_1A_2B_1B_2$	2	2
$A_1A_2B_2B_2$	1	3
$A_2A_2B_1B_1$	2	0
$A_2A_2B_1B_2$	1	1
$A_2A_2B_2B_2$	0	2

If X and Y are subject to stabilizing selection such that the intermediate values 1, 2 and 3 are compatible with normal development, but the extreme values of 0 and 4 are deleterious in either system, the four doubly homozygous genotypes will be at a selective disadvantage to any of the five genotypes in which one or both loci are heterozygous. Selective losses

will be least frequent when there is a high frequency of heterozygosis at both loci, and a stable polymorphism at both loci will be maintained.

The model resembles the model for single locus heterosis, but selection is against double homozygotes only. At the most favorable gene frequencies, double homozygosis occurs in as few as 25% of all zygotes. In contrast, to maintain two alleles at one locus through simple heterosis at least 50% of all zygotes must be deleterious homozygotes.

## DISCUSSION

It is possible to make somewhat more complex models in which selection is solely against triple homozygotes. Selection against multiple homozygotes appears to have considerable empirical support, and the interaction of pleiotropy and stabilizing selection has been suggested as the underlying agency (4). While these two factors alone may not be sufficient to maintain polymorphism in any genetic systems beyond a drastically simplified model, in more complex interactions pleiotropy can be considered to be a potentially important factor contributing to the genetic diversity of real populations.

For a recent example of polygenes that are favorable in one component of fitness (rate of development) and unfavorable in another (fertility), see Spiess and Spiess (5).

## REFERENCES

1. Lewontin, R. C. ; Proc. 11th Intern. Congr. Genet. 3:517-525, 1964.
2. King, J. L. ; Genetics 53:403-413, 1966.
3. Jain, S. K., and Allard, R. W. ; Genetics 53:633-659, 1966.
4. Lerner, I. M. ; Genetic Homeostasis, New York, Wiley, 1954.
5. Spiess, B., and Spiess, L. D. ; Genetics 53:695-708, 1966.

# Increase in Plasma Growth-Hormone Level in the Monkey Following the Administration of Sheep Hypothalamic Extracts

N67 15956

- Joseph F. Garcia and Irving I. Geschwind

The control of anterior pituitary secretion is now generally accepted as being mediated by hypothalamic neurohumoral factors that are secreted into the primary plexus of the portal circulation to the anterior pituitary and that, upon arrival at the anterior pituitary, promote the release of most anterior pituitary hormones. Although much work has been done on the hypothalamic releasing factors for most of the anterior pituitary hormones, it has been only very recently that such studies have been directed to the search for a growth-hormone (GH) releasing factor. Both in vitro and in vivo studies have been carried out. In the in vitro studies the release of GH into a medium, in which pituitary fragments are incubated and to which hypothalamic extracts have been added, has been quantitated (1). The in vivo studies have been carried out by assaying for residual GH in the pituitaries of animals injected with hypothalamic extracts (2). In both cases the GH has been assayed by the tibia test (3). With the availability of sensitive radioimmunoassay techniques for GH (4, 5), it seemed worthwhile to explore the possibility of demonstrating the release of GH into the circulation after the administration of hypothalamic extracts.

The radioimmunoassay for human growth hormone has been shown to be useful in the measurement of the plasma concentration of other primate growth hormones (5). The method used in the present studies for the radioimmunoassay of GH has been modified from that of Hunter and Greenwood (5). Human growth hormone (HGH), supplied by Professor C. H. Li, University of California, Berkeley, was used to immunize rabbits. Some of this material was labeled with iodine 125 using the Chloramine T method of Hunter and Greenwood (6). The antibody-bound HGH-iodine-125 was precipitated, using a goat anti-rabbit gamma globulin serum.\* The percentage of the labeled HGH bound to the antibody was plotted against the logarithms of the concentrations of standard HGH.\*\* The concentrations of monkey plasma GH were read directly off such a curve and are therefore expressed in terms of the standard HGH preparation used.

The plasma GH level has been shown to respond to many factors; insulin-induced hypoglycemia, prolonged fasting, muscular exercise and the administration of certain amino

\*Obtained from Antibodies, Inc., Davis, Calif.

\*\*A gift from Professor A. E. Wilhelmi, Emory University, Atlanta, Ga. Lot No. HS503A had a specific activity of 1.7 IU/mg (standardized in terms of the bovine GH international standard).

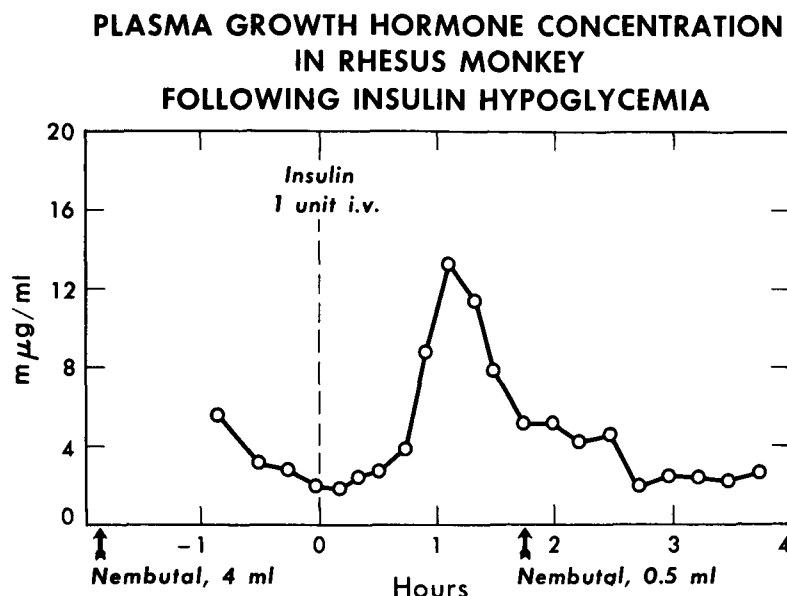


Figure 1. MUB-9722

acids will all result in high plasma GH levels (7-9). On the other hand, administration of glucose will depress the elevated plasma GH level of the hypoglycemic or fasting individual (7). In the normal human the response to insulin hypoglycemia is quite consistent.

Male Rhesus monkeys (*Macaca mulatta*), weighing between 10 and 20 pounds, were used throughout the course of this work. The animals were anesthetized with nembutal, and a polyethylene cannula was placed in a branch of the saphenous vein in the lower leg. At approximately one hour after the administration of the anesthetic, the collection of heparinized blood samples was begun and was continued over approximately a six-hour period. Additional nembutal was administered as needed to maintain the anesthetic state. After a one- to two-hour period, during which control blood samples were taken, the test material was injected intravenously using the cephalic vein in the forearm.

Initially studies were carried out, using insulin hypoglycemia as the stimulus for GH release. Figure 1 shows the results of one such study, in which one unit of glucagon-free insulin (Lilly) was injected. The plasma GH level begins to rise at approximately 40 min, reaching a high level by one hour. This response is not essentially different from that seen in the unanesthetized normal human. The importance of this response, however, is that it shows that the mechanisms responsible for the reflex release of GH are intact in the nembutalized monkey and that such a preparation can be used to study the release of GH. Many of the monkeys show a high GH level at the beginning of such a study. This is perhaps due to stress or to muscular exercise expended by the monkey attempting to evade capture and restraint prior to the injection of the nembutal.

Extracts of sheep hypothalami were prepared by extracting acetone powder representing 200 gland (stalk-median eminence plus adjacent areas) equivalents of sheep hypothalami by homogenization with ten milliliters of 0.1 N HCl. The homogenate was then diluted with an additional 40 ml of acid and stirred for 30 min. The material was centrifuged for 40 min at  $8,000 \times g$ , and the residue was reextracted with 30 ml of 0.1 N HCl for 30 min and then centrifuged as before. Up to this point all operations were carried out at  $4^{\circ}\text{C}$ . The supernatants were combined, heated to  $90^{\circ}\text{C}$  in a boiling water bath (approximately five minutes), chilled to  $15^{\circ}\text{C}$ , neutralized to pH 6.4 with 1 N NaOH and centrifuged for 20 min at  $35,000 \times g$  at  $4^{\circ}\text{C}$ . The supernatant was diluted to 100 ml with distilled water, distributed into ten vials and frozen. The final concentration was two gland equivalents per milliliter. Extracts of sheep cerebral tissue were also prepared in the same manner and were diluted to a final concentration representing a weight of tissue equivalent to that of the hypothalamic extract.

The response to the intravenous injection of sheep hypothalamic extracts has been studied in eight experiments. In seven of the eight experiments a release of GH was observed following the injection. Four such studies, in which 4.5 to 5.0 ml (9 to 10 sheep hypothalami) of the extract was administered, are presented in Fig. 2. There was a great variation in the magnitude of the response. The reasons for this great variation are not entirely clear, and at this point one can only speculate on their possible causes. It would seem possible that the state of the anterior pituitary before the administration of the extract may be a factor. The recent release of a large quantity of GH may make impossible a further large release in response to the administration of these extracts. Other influencing factors may be related to possible variations in the anterior pituitary portal blood flow or to the depth of the anesthetic state. Studies directed to minimizing the variations in the magnitude of these responses will be necessary before the monkey can be used as an assay animal for determining GH releasing factor levels.

The responses of the plasma GH level to the injection of hypothalamic extracts are all similar, however, in their time relationships. The GH level begins to rise between 20 and 30 min and reaches peak values between 45 and 60 min after the injection. At this time GH secretion may stop rather abruptly, for the GH levels decrease thereafter at a rate consistent with the half-life found in man for HGH (10). These temporal relationships are consistent with the type of response seen following the injection of insulin.

Since hypoglycemia appears to be a potent releaser of GH, plasma glucose determinations were made in most of these studies. In no case was a fall in plasma glucose observed; in fact, usually a slight rise in plasma glucose was observed after the injection of the hypothalamic extract. However, in order to rule out positively the possibility of a GH release mediated by changes in plasma glucose level, in two of the hypothalamic extract studies the animals were infused, as well, with glucose. Glucose infusion, at a rate of 75 mg per minute, was started one hour before the injection and continued for three hours. This brought the plasma-glucose level to approximately 300 mg per 100 ml at the time of the injection of the hypothalamic extract, and it remained between this value and 340 mg per 100 ml throughout

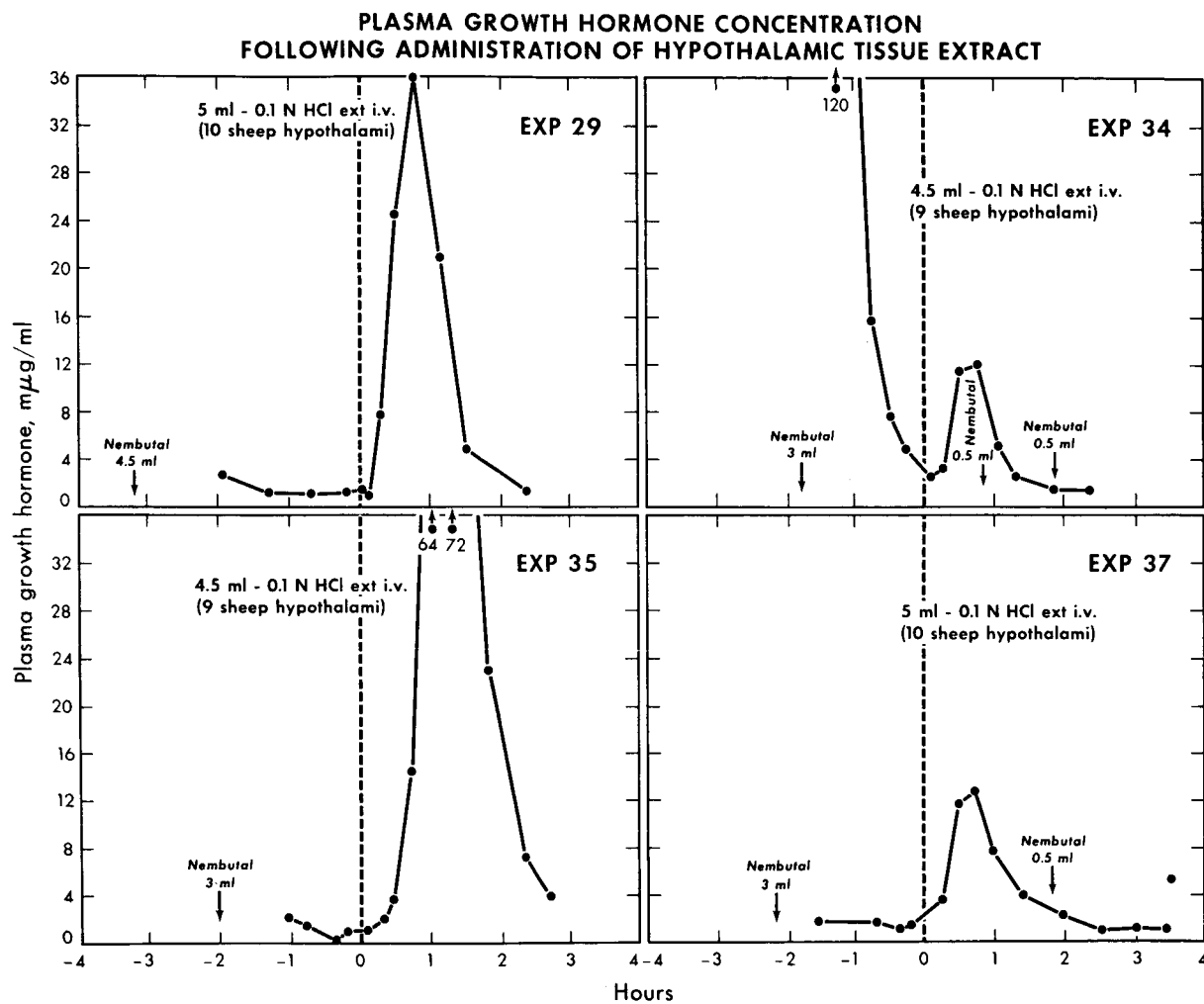


Figure 2. MUB-9724

the remaining glucose infusion period. In both of the glucose infusion experiments the hypothalamic extract caused a release of GH similar to those depicted in Fig. 2 (peak values of 12 and 36  $\mu\text{g}$  per milliliter).

As a control to the studies using hypothalamic extracts, extracts of cerebral tissue were injected. The results of four such experiments are depicted in Fig. 3. In two of the studies there was no change in the plasma GH level after the administration of the extracts. In the other two studies there was a GH release following the injection. This release, however, occurred much later than that following the injection of hypothalamic extracts, for a period of approximately two hours elapsed before rises in plasma GH levels were observed.

Although these late responses are disturbing, it must be emphasized that in all four of the cerebral extract studies no rise in plasma GH occurred during the period of time, in which responses to hypothalamic extract or to insulin hypoglycemia are evident. It is felt that these responses, although real, are not specific to a releasing factor but are reflex responses to other stimuli. In this connection, it is perhaps worthwhile to mention that an increase in plasma GH levels has been observed following the injection of certain amino acids (9). The depth of the anesthetic state and stress must also be considered as possible contributing factors in these late GH responses.

Although several recent studies in rats have failed to implicate vasopressin as a mediator of GH secretion (11, 12), the effect of vasopressin injection was studied in the present experiments. In our hypothalamic extract the concentration of vasopressin was 0.506 units per milliliter.\* Therefore, in the volume of hypothalamic extract injected, 2.28 or 2.53 units of vasopressin were present. Two animals were therefore each injected with five units of 'Pitressin', which resulted in a small, immediate increase in the plasma GH level. The first samples, taken about 15 min after the injection, were twice the basal level, and from this maximum the levels then decreased exponentially. Since the response to an amount of vasopressin twice that present in the hypothalamic extract was so minimal, the responses observed with the hypothalamic extract could not be due solely to its vasopressin content. The GH response to vasopressin injection is perhaps a non-specific response resulting from the well-known vasomotor effects of this hormone. In still another study the injection of five units of 'Pitocin' did not result in a release of GH.

In conclusion, we feel that the observations reported here support the concept that the secretion of anterior pituitary GH is mediated by a hypothalamic neurohumoral factor.

Since this paper was prepared, a report on similar experiments by E. Knobil has appeared (*The Physiologist* 9:25, 1966). This investigator found responses to the administration of porcine hypothalamic extract similar to those reported above. The results differ, however, in that the responses to the extract were more rapid than those we have observed, and

---

\*We are indebted to Professor R. Guillemin, Baylor University, Houston, Tex., for this assay.

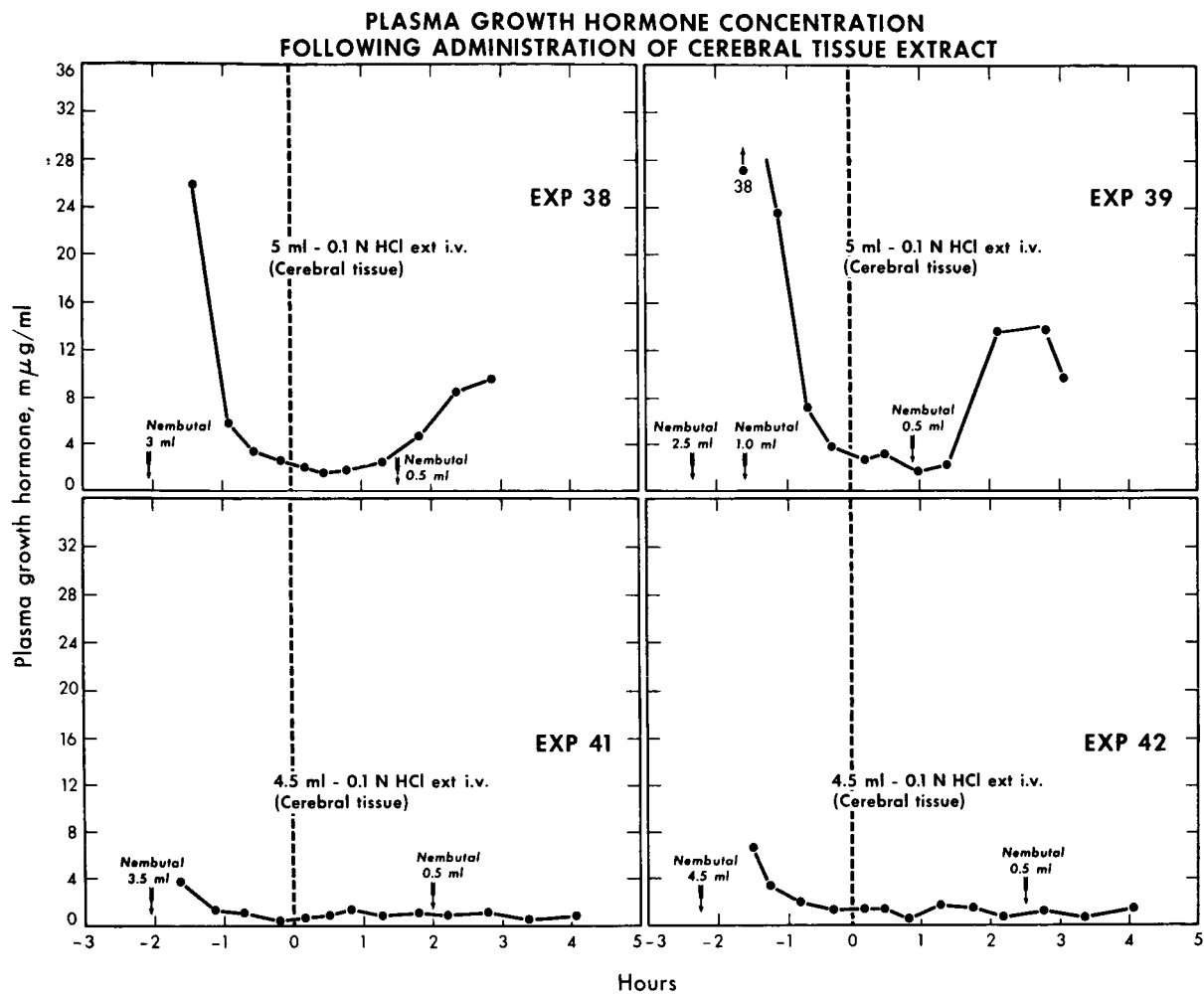


Figure 3. MUB-9723



the responses to the injection of vasopressin were more marked than ours--the greatest responses in any of their experiments having been obtained with vasopressin. The experiments differ in that in Knobil's experiments the monkeys were unanesthetized but restrained, the extract injected was equivalent to only two porcine hypothalami, and the antiserum utilized for the immunoassays was developed using a highly purified simian growth hormone as antigen. Whether these differences in procedure explain the differences in response to extract or vasopressin remains to be determined.

## ACKNOWLEDGMENTS

We should like to acknowledge the expert technical assistance of Patricia Smith and Robert Dewey, and the advice of Dr. John A. Linfoot.

This work was supported in part by the United States Atomic Energy Commission, by Cancer Research Funds of the University of California and by United States Public Health Service Grant HD-00394.

## REFERENCES

1. Deuben, R. R., and Meites, J.; *Endocrinology* 74:408, 1964.
2. Pecile, A.; Muller, E.; Falconi, G., and Martini, L.; *Endocrinology* 77:241, 1965.
3. Greenspan, F. S.; Li, C. H.; Simpson, M. E., and Evans, H. M.; *Endocrinology* 54:455, 1949.
4. Glick, S. M.; Roth, J.; Yalow, R. S., and Berson, S. A.; *Nature* 199:784, 1963.
5. Hunter, W. M., and Greenwood, F. C.; *Biochem. J.* 91:43, 1964.
6. Hunter, W. M., and Greenwood, F. C.; *Nature* 194:495, 1962.
7. Roth, J.; Glick, S. M.; Berson, S. A., and Yalow, R. S.; *Science* 140:987, 1963.
8. Hunter, W. M.; Fonseca, C. C., and Passmore, R.; *Quart. J. Exper. Physiol.* 50:406, 1965.
9. Knopf, R. F.; Conn, J. W.; Fajans, S. S.; Floyd, J. C.; Guntzsch, E. M., and Rull, J. A.; *J. Clin. Endocrinol. and Metabol.* 25:1140, 1965.
10. Glick, S. M.; Roth, J., and Lonergan, E. T.; *J. Clin. Endocrinol. and Metabol.* 24:501, 1964.
11. Müller, E.; Pecile, A., and Smirne, S.; *Endocrinology* 77:390, 1965.
12. Ishida, Y.; Kuroshima, A.; Bowers, C. Y., and Schally, A. V.; *Endocrinology* 77:759, 1965.

## STAFF PUBLICATIONS

- Bierman, E. L.; Hayes, T. L.; Hawkins, J. N.; Ewing, A. M., and Lindgren, F. T.: Particle-Size Distribution of Very Low Density Plasma Lipoproteins During Fat Absorption in Man, *J. Lipid Res.* 7:65-72, 1966.
- Davison, P. F., and Freifelder, D.: Lability of Single-Stranded Deoxyribonucleic Acid to Hydrodynamic Shear, *J. Mol. Biol.* 16:490-502, 1966.
- de Robichon-Szulmajster, H.; Surdin, Y., and Mortimer, R. K.: Genetic and Biochemical Studies of Genes Controlling the Synthesis of Threonine and Methionine in *Saccharomyces*, *Genetics* 53:606-619, 1966.
- Dobson, E. L.; Finkelstein, L. J.; Finney, C. R., and Kelly, L. S.: Particulate Chromic Phosphate: Colloid Characteristics Suitable for Measurement of Liver Circulation, in *Radioactive Pharmaceuticals*, edited by G. A. Andrews, Oak Ridge, Tenn., U. S. A. E. C., Div. of Technical Information, 1966, AEC Symposium series no. 6, CONF-651111, pp. 477-502.
- Fabricant, S. J.; Windsor, A. A., and Lindgren, F. T.: Ultracentrifuge Rotor Temperature Measurements and Control, *Rev. Sci. Instr.* 37:495-496, 1966.
- Freifelder, D.: Effect of NaClO<sub>4</sub> on Bacteriophage: Release of DNA and Evidence for Population Heterogeneity, *Virology* 28:742-750, 1966.
- Freifelder, D., and Freifelder, D. R.: Mechanism of X-ray Sensitization of Bacteriophage T7 by 5-Bromouracil, *Mutation Res.* 3:177-184, 1966.
- Freifelder, D.: Replication of DNA During F' Lac Transfer, *Biochem. Biophys. Res. Commun.* 23:576-582, 1966.
- Garcia, J. F., and Schooley, J. C.: Dose-Response Relationships for Erythropoietin Given in Serum or in Saline, *Proc. Soc. Exptl. Biol. Med.* 120:614-616, 1965.
- Glaeser, R. M.; Hayes, T.; Mel, H., and Tobias, C.: Membrane Structure of OsO<sub>4</sub>-Fixed Erythrocytes Viewed "Face On" by Electron Microscope Techniques, *Exptl. Cell Res.* 42:467-477, 1966.
- Glaeser, R. M., and Mel, H. C.: Microelectrophoretic and Enzymic Studies Concerning the Carbohydrate at the Surface of Rat Erythrocytes, *Arch. Biochem. Biophys.* 113:77-82, 1966.
- Goldman, M.; Rosenberg, L. L.; La Roche, G., and Srebnik, H. H.: Iodine Metabolism in Intact and Hypophysectomized Rats of a Colony Maintained on a Low-Iodine Diet, *Endocrinology* 78:889-892, 1966.
- Hayes, T. L.; Freeman, N. K.; Lindgren, F. T.; Nichols, A. V., and Bierman, E. L.: Some Physical and Chemical Aspects of the Structure of the Very Low-Density Serum Lipoproteins, in *Protides of the Biological Fluids Colloquium*, 13th, April 29-May 2, 1965, Bruges, Proceedings, edited by H. Peeters, Elsevier, Amsterdam, 1966, Sec. B. Lipoproteins, pp. 273-279.
- Henriksen, T.: Effect of the Irradiation Temperature on the Production of Free Radicals in Solid Biological Compounds Exposed to Various Ionizing Radiations, *Radiation Res.* 27:694-709, 1966.

- Henriksen, T.: Production of Free Radicals in Solid Biological Substances by Heavy Ions, *Radiation Res.* 27:676-693, 1966.
- King, J. L.: The Gene Interaction Component of the Genetic Load, *Genetics* 53:403-413, 1966.
- Lawrence, J. H.; Tobias, C. A.; Born, J. L.; Linfoot, J. A., and D'Angio, G. J.: Heavy Particles in Experimental Medicine and Therapy, *J. Am. Med. Assoc.* 196:166-170, 1966.
- Linfoot, J. A., and Greenwood, F. C.: Growth Hormone in Acromegaly: Effect of Heavy Particle Pituitary Irradiation, *J. Clin. Endocrinol. Metab.* 25:1515-1518, 1965.
- Maccabee, H. D., and Raju, M. R.: Fluctuations of Energy Loss by Heavy Charged Particles in Silicon Detectors: Preliminary Measurements, *Nucl. Instr. Methods* 37:176-178, 1965.
- Maccabee, H. D.; Raju, M. R., and Tobias, C. A.: Fluctuations of Energy Loss in Semiconductor Detectors, presented at 10th Scintillation and Semiconductor Counter Symposium, 1966, Washington, D. C., *IEEE Trans. Nucl. Sci.* NS-13:176-177, 1966.
- McDonald, L. W.; King, G. A., and Tobias, C. A.: Radiosensitivity of the Vestibular Apparatus of the Rabbit, in Symposium on the Role of the Vestibular Organs in the Exploration of Space, U. S. Naval School of Aviation Medicine, Pensacola, Fla., Jan. 20-22, 1965, National Aeronautics and Space Administration report no. NASA SP-77, 1965.
- Mel, H. C., and Schooley, J. C.: Stable-Flow Free Boundary Fractionation of Spleen-Colony-Forming Cells from Mouse Bone Marrow, in Centre National de Recherche Scientifique, Colloques Internationaux no. 147 on La Greffe des Cellules Hématopoïétique Allogéniques, Paris, Sept. 1964, Centre National de Recherche Scientifique, Paris, 1965, pp. 221-223.
- Mortimer, R. K., and Hawthorne, D. C.: Genetic Mapping in *Saccharomyces*, *Genetics* 53:165-173, 1966.
- Mortimer, R.; Brustad, T., and Cormack, D. V.: Influence of Linear Energy Transfer and Oxygen Tension on the Effectiveness of Ionizing Radiations for Induction of Mutations and Lethality in *Saccharomyces cerevisiae*, *Radiation Res.* 26:465-482, 1965.
- Nichols, A. V., and Coggiola, E. L.: Lipid Transfer Between Human Serum High Density Lipoproteins and Egg Yolk Lipoproteins in Incubation Mixtures, *J. Lipid Res.* 7:215-220, 1966.
- Nobel, P. S., and Mel, H. C.: Electrophoretic Studies of Light-Induced Charge in Spinach Chloroplasts, *Arch. Biochem. Biophys.* 113:695-702, 1966.
- Packer, L.; Nobel, P. S.; Gross, E. L., and Mel, H. C.: Fractionation of Spinach Chloroplasts by Flow Sedimentation-Electrophoresis, *J. Cell Biol.* 28:443-448, 1966.
- Pease, R. F. W., and Hayes, T. L.: Scanning Electron Microscopy of Biological Material, *Nature* 210:1049, 1966.
- Raju, M. R.; Aceto, H., and Richman, C.: Pion Studies with Silicon Detectors, *Nucl. Instr. Methods* 37:152-158, 1965.
- Rescigno, A., and Richardson, I. W.: On the Competitive Exclusion Principle, *Bull. Math. Biophys.* 27 Special Issue:85-89, 1965.
- Richman, C.; Aceto, H.; Raju, M. R., and Schwartz, B.: The Radiotherapeutic Possibilities of Negative Pions, preliminary physical experiments, *Am. J. Roentgenol. Radium Therapy Nucl. Med.* 96:777-790, 1966.
- Rooth, G.: Acid-base, Electrolyte and Water Changes During Tissue Hypoxia in Rats, *Clin. Sci.* 30:417-424, 1966.